# SUPPORTING INFORMATION

## Assessing the Flexibility of the Prochlorosin 2.8 Scaffold for Bioengineering Applications

*Julian D. Hegemann,[a,b] Silvia C. Bobeica,[a,b] Mark C. Walker,[a,b] Ian R. Bothwell,[a,b] and Wilfred A. van der Donk[a,b,†]*

*[a]Howard Hughes Medical Institute and [b]Department of Chemistry, University of Illinois at Urbana-Champaign, 600 S. Mathews Ave, Urbana, Illinois 61801, United States.* †Corresponding author: vddonk@illinois.edu

**Table S1.** Overview of all ProcA2.8(G−1K) variants co-expressed with ProcM in this study. Core peptide sequences, observed dehydration states, numbers of NEM adducts, and ring topologies as determined by tandem MS experiments are shown.

| name | core peptide sequence | dehydration state | NEM added | ring topology |
|---|---|---|---|---|
| WT | AA CHNHAPS MPP SYWEGEC | −2 $H_2O$ | 0 | Cys3-Ser9, Ser13-Cys19 |
| H4A | AA C**A**NHAPS MPP SYWEGEC | −2 $H_2O$ | 0 | Cys3-Ser9, Ser13-Cys19 |
| N5A | AA CH**A**HAPS MPP SYWEGEC | −2 $H_2O$ | 0 | Cys3-Ser9, Ser13-Cys19 |
| H6A | AA CHN**A**APS MPP SYWEGEC | −2 $H_2O$ | 0 | Cys3-Ser9, Ser13-Cys19 |
| P8A | AA CHNHA**A**S MPP SYWEGEC | −2 $H_2O$ | 0 | Cys3-Ser9, Ser13-Cys19 |
| M10A/P11A/P12A | AA CHNHAPS **AAA** SYWEGEC | −2 $H_2O$ | 0 | Cys3-Ser9, Ser13-Cys19 |
| ΔP11 | AA CHNHAPS MP_ SYWEGEC | −2 $H_2O$ | 0 | Cys3-Ser9, Ser12-Cys18 |
| ΔP11P12 | AA CHNHAPS M__ SYWEGEC | −2 $H_2O$ | 0 | Cys3-Ser9, Ser11-Cys17 |
| linker +1 aa | AA CHNHAPS**A**MPP SYWEGEC | −2 $H_2O$ | 0 | Cys3-Ser9, Ser14-Cys20 |
| linker +2 aa | AA CHNHAPS**A**MPP**A**SYWEGEC | (unmodified/−1)[a]/ −2 $H_2O$ | 0 | Cys3-Ser9, Ser15-Cys21 |
| Y14A | AA CHNHAPS MPP S**A**WEGEC | −2 $H_2O$ | 0 | Cys3-Ser9, Ser13-Cys19 |
| W15A | AA CHNHAPS MPP SY**A**EGEC | −2 $H_2O$ | 0 | Cys3-Ser9, Ser13-Cys19 |
| E16A | AA CHNHAPS MPP SYW**A**GEC | −2 $H_2O$ | 0 | Cys3-Ser9, Ser13-Cys19 |
| G17A | AA CHNHAPS MPP SYWE**A**EC | −2 $H_2O$ | 0 | Cys3-Ser9, Ser13-Cys19 |
| E18A | AA CHNHAPS MPP SYWEG**A**C | −2 $H_2O$ | 0 | Cys3-Ser9, Ser13-Cys19 |
| ring1 −1 aa (ΔH6) | AA CHN_APS MPP SYWEGEC | −2 $H_2O$ | 0 | Cys3-Ser8, Ser12-Cys18 |
| ring1 −2 aa (ΔH6A7) | AA CHN__PS MPP SYWEGEC | −2 $H_2O$ | 0 | Cys3-Ser7, Ser11-Cys17 |
| ring1 +1 aa | AA CH**A**NHAPS MPP SYWEGEC | −2 $H_2O$ | 0 | Cys3-Ser10, Ser14-Cys20 |
| ring1 +2 aa | AA CH**A**N**A**HAPS MPP SYWEGEC | −2 $H_2O$ | 0 | Cys3-Ser11, Ser15-Cys21 |
| ring1 +3 aa | AA CH**A**N**A**HAP**A**S MPP SYWEGEC | −2 $H_2O$ | 0 | Cys3-Ser12, Ser16-Cys22 |
| ring2 −1 aa (ΔW15) | AA CHNHAPS MPP SY_EGEC | −2 $H_2O$ | 0 | Cys3-Ser9, Ser13-Cys18 |
| ring2 −2 aa (ΔW15E16) | AA CHNHAPS MPP SY__GEC | −2 $H_2O$ | 0 | Cys3-Ser9, Ser13-Cys17 |
| ring2 +1 aa | AA CHNHAPS MPP SY**A**WEGEC | −1/−2 $H_2O$ | 1/0 | Cys3-Ser13 / Cys3-Ser9, Ser13-Cys20 |
| ring2 +2 aa | AA CHNHAPS MPP SY**A**W**A**EGEC | −1/−2 $H_2O$ | 1/0 | Cys3-Ser13 / Cys3-Ser9, Ser13-Cys21 |
| C3S S9C | AA **S**HNHAP**C** MPP SYWEGEC | −2 $H_2O$ | 0 | Ser3-Cys9, Ser13-Cys19 |
| S13C/C19S | AA CHNHAPS MPP **C**YWEGE**S** | −1 $H_2O$ | 1 | Cys3-Ser9 |
| S13C/C19S-A | AA CHNHAPS MPP **C**YWEGE**SA** | unmodified | 2 | none |
| S13C/C19S-AA | AA CHNHAPS MPP **C**YWEGE**SAA** | unmodified/−1 $H_2O$ | 2/1 | none / Cys3-Ser9 |
| H4P | AA C**P**NHAPS MPP SYWEGEC | (−1$H_2O$)[a]/−2 $H_2O$ | (1)/0 | (n.d.[*])/Cys3-Ser9, Ser13-Cys19 |
| H6P | AA CHN**P**APS MPP SYWEGEC | (−1$H_2O$)[a]/−2 $H_2O$ | (1)/0 | (n.d.[*])/Cys3-Ser9, Ser13-Cys19 |
| H4P/H6P | AA C**P**N**P**APS MPP SYWEGEC | unmodified | 2 | none |
| Y14P/E16P | AA CHNHAPS MPP S**P**W**P**GEC | unmodified | 2 | none |
| Y14P/E18P | AA CHNHAPS MPP S**P**WEG**P**C | −1 $H_2O$ | 1 | n. d.[b] |
| E16P/E18P | AA CHNHAPS MPP SYW**P**G**P**C | −2 $H_2O$ | 0 | n. d.[b] |
| Y14P/E16P/E18P | AA CHNHAPS MPP S**P**W**P**G**P**C | −1 $H_2O$ | 1 | n. d.[b] |
| 5RGD | AA CH**RGD**PS MPP SYWEGEC | −1/−2 $H_2O$ | 1/0 | Ser13-Cys19 / Cys3-Ser9, Ser13-Cys19 |
| 15RGD | AA CHNHAPS MPP SY**RGD**EC | −2 $H_2O$ | 0 | Cys3-Ser9, Ser13-Cys19 |
| 16RGD | AA CHNHAPS MPP SYW**RGD**C | −2 $H_2O$ | 0 | Cys3-Ser9, Ser13-Cys19 |

[a] parentheses emphasize that only trace amounts of this species were observed
[b] n.d. = not determined because of low yields

**Table S2a.** Oligonucleotide primers used for mutating residues in ring 1 of ProcA2.8. SLIM overhangs are underlined and mutated residues are highlighted in bold.

| name | sequence |
|---|---|
| FP_ProcA2.8-Ring1 | CCT CCA TCC TAT TGG GAG GGT GAG TGC TAA G |
| RP_ProcA2.8-Ring1 | GGC CGC TTT CCC AGC CAC ACC TTC CAG |
| FPtail_ProcA2.8-H4A | TGT **GCG** AAC CAT GCT CCA TCT ATG CCT CCA TCC TAT TGG GAG GGT GAG TGC TAA G |
| RPtail_ProcA2.8-H4A | CAT AGA TGG AGC ATG GTT **CGC** ACA GGC CGC TTT CCC AGC CAC ACC TTC CAG |
| FPtail_ProcA2.8-N5A | TGT CAT **GCG** CAT GCT CCA TCT ATG CCT CCA TCC TAT TGG GAG GGT GAG TGC TAA G |
| RPtail_ProcA2.8-N5A | CAT AGA TGG AGC ATG **CGC** ATG ACA GGC CGC TTT CCC AGC CAC ACC TTC CAG |
| FPtail_ProcA2.8-H6A | TGT CAT AAC **GCG** GCT CCA TCT ATG CCT CCA TCC TAT TGG GAG GGT GAG TGC TAA G |
| RPtail_ProcA2.8-H6A | CAT AGA TGG AGC **CGC** GTT ATG ACA GGC CGC TTT CCC AGC CAC ACC TTC CAG |
| FPtail_ProcA2.8-P8A | TGT CAT AAC CAT GCT **GCG** TCT ATG CCT CCA TCC TAT TGG GAG GGT GAG TGC TAA G |
| RPtail_ProcA2.8-P8A | CAT AGA **CGC** AGC ATG GTT ATG ACA GGC CGC TTT CCC AGC CAC ACC TTC CAG |
| FPtail_ProcA2.8-R1−1aa | TGT CAT AAC GCT CCA TCT ATG CCT CCA TCC TAT TGG GAG GGT GAG TGC TAA G |
| RPtail_ProcA2.8-R1−1aa | CAT AGA TGG AGC GTT ATG ACA GGC CGC TTT CCC AGC CAC ACC TTC CAG |
| FPtail_ProcA2.8-R1−2aa | TGT CAT AAC CCA TCT ATG CCT CCA TCC TAT TGG GAG GGT GAG TGC TAA G |
| RPtail_ProcA2.8-R1−2aa | CAT AGA TGG GTT ATG ACA GGC CGC TTT CCC AGC CAC ACC TTC CAG |
| FPtail_ProcA2.8-R1+1aa | TGT CAT **GCG** AAC CAT GCT CCA TCT ATG CCT CCA TCC TAT TGG GAG GGT GAG TGC TAA G |
| RPtail_ProcA2.8-R1+1aa | CAT AGA TGG AGC ATG GTT **CGC** ATG ACA GGC CGC TTT CCC AGC CAC ACC TTC CAG |
| FPtail_ProcA2.8-R1+2aa | TGT CAT **GCG** AAC **GCC** CAT GCT CCA TCT ATG CCT CCA TCC TAT TGG GAG GGT GAG TGC TAA G |
| RPtail_ProcA2.8-R1+2aa | CAT AGA TGG AGC ATG GGC GTT CGC ATG ACA GGC CGC TTT CCC AGC CAC ACC TTC CAG |
| FPtail_ProcA2.8-R1+3aa | TGT CAT **GCG** AAC **GCC** CAT GCT CCA **GCG** TCT ATG CCT CCA TCC TAT TGG GAG GGT GAG TGC TAA G |
| RPtail_ProcA2.8-R1+3aa | CAT AGA **CGC** TGG AGC ATG **GGC** GTT **CGC** ATG ACA GGC CGC TTT CCC AGC CAC ACC TTC CAG |
| FPtail_ProcA2.8-C3S_S9C | **AGC** CAT AAC CAT GCT CCA **TGC** ATG CCT CCA TCC TAT TGG GAG GGT GAG TGC TAA G |
| RPtail_ProcA2.8- C3S_S9C | CAT **GCA** TGG AGC ATG GTT ATG **GCT** GGC CGC TTT CCC AGC CAC ACC TTC CAG |
| FPtail_Proc2.8-H4P | TGT **CCG** AAC CAT GCT CCA TCT ATG CCT CCA TCC TAT TGG GAG GGT GAG TGC TAA G |
| RPtail_Proc2.8-H4P | CAT AGA TGG AGC ATG GTT **CGG** ACA GGC CGC TTT CCC AGC CAC ACC TTC CAG |
| FPtail_Proc2.8-H6P | TGT CAT AAC **CCG** GCT CCA TCT ATG CCT CCA TCC TAT TGG GAG GGT GAG TGC TAA G |
| RPtail_Proc2.8-H6P | CAT AGA TGG AGC **CGG** GTT ATG ACA GGC CGC TTT CCC AGC CAC ACC TTC CAG |
| FPtail_Proc2.8-H4P-H6P | TGT **CCG** AAC **CCG** GCT CCA TCT ATG CCT CCA TCC TAT TGG GAG GGT GAG TGC TAA G |
| RPtail_Proc2.8-H4P-H6P | CAT AGA TGG AGC **CGG** GTT **CGG** ACA GGC CGC TTT CCC AGC CAC ACC TTC CAG |
| FPtail_ProcA2.8-R5G6D7 | TGT CAT **CGT GGC GAT** CCA TCT ATG CCT CCA TCC TAT TGG GAG GGT GAG TGC TAA G |
| RPtail_ProcA2.8-R5G6D7 | CAT AGA TGG **ATC GCC ACG** ATG ACA GGC CGC TTT CCC AGC CAC ACC TTC CAG |

**Table S2b.** Oligonucleotide primers used for mutating residues in the linker region between rings 1 and 2 of ProcA2.8. SLIM overhangs are underlined and mutated residues are highlighted in bold.

| name | sequence |
|---|---|
| FP_ProcA2.8-Linker | TGG GAG GGT GAG TGC TAA GCG GCC G |
| RP_ProcA2.8- Linker | ATG GTT ATG ACA GGC CGC TTT CCC AGC CAC |
| FPtail_ProcA2.8-MPPtoAAA | GCT CCA TCT **GCC GCG GCA** TCC TAT TGG GAG GGT GAG TGC TAA GCG GCC G |
| RPtail_ProcA2.8-MPPtoAAA | ATA GGA **TGC CGC GGC** AGA TGG AGC ATG GTT ATG ACA GGC CGC TTT CCC AGC CAC |
| FPtail_ProcA2.8-DeltaP11 | GCT CCA TCT ATG CCA TCC TAT TGG GAG GGT GAG TGC TAA GCG GCC G |
| RPtail_ProcA2.8-DeltaP11 | ATA GGA TGG CAT AGA TGG AGC ATG GTT ATG ACA GGC CGC TTT CCC AGC CAC |
| FPtail_ProcA2.8-DeltaP11P12 | GCT CCA TCT ATG TCC TAT TGG GAG GGT GAG TGC TAA GCG GCC G |
| RPtail_ProcA2.8-DeltaP11P12 | ATA GGA CAT AGA TGG AGC ATG GTT ATG ACA GGC CGC TTT CCC AGC CAC |
| FPtail_ProcA2.8-linker+1aa | GCT CCA TCT **GCG** ATG CCT CCA TCC TAT TGG GAG GGT GAG TGC TAA GCG GCC G |
| RPtail_ProcA2.8- linker+1aa | ATA GGA TGG AGG CAT **CGC** AGA TGG AGC ATG GTT ATG ACA GGC CGC TTT CCC AGC CAC |
| FPtail_ProcA2.8-linker+2aa | GCT CCA TCT **GCG** ATG CCT CCA **GCA** TCC TAT TGG GAG GGT GAG TGC TAA GCG GCC G |
| RPtail_ProcA2.8- linker+2aa | ATA GGA **TGC** TGG AGG CAT **CGC** AGA TGG AGC ATG GTT ATG ACA GGC CGC TTT CCC AGC CAC |

**Table S2c.** Oligonucleotide primers used for mutating residues in ring 2 of ProcA2.8. SLIM overhangs are underlined and mutated residues are highlighted in bold.

| name | sequence |
|---|---|
| FP_ProcA2.8-Ring2 | GCG GCC GCA TAA TGC TTA AGT CGA ACA G |
| RP_ProcA2.8-Ring2 | TGG AGG CAT AGA TGG AGC ATG GTT ATG ACA GG |
| FPtail_ProcA2.8-Y14A | TCC **GCG** TGG GAG GGT GAG TGC TAA GCG GCC GCA TAA TGC TTA AGT CGA ACA G |
| RPtail_ProcA2.8-Y14A | TTA GCA CTC ACC CTC CCA **CGC** GGA TGG AGG CAT AGA TGG AGC ATG GTT ATG ACA GG |
| FPtail_ProcA2.8-W15A | TCC TAT **GCG** GAG GGT GAG TGC TAA GCG GCC GCA TAA TGC TTA AGT CGA ACA G |
| RPtail_ProcA2.8-R2_W15A | TTA GCA CTC ACC CTC **CGC** ATA GGA TGG AGG CAT AGA TGG AGC ATG GTT ATG ACA GG |
| FPtail_ProcA2.8-E16A | TCC TAT TGG **GCG** GGT GAG TGC TAA GCG GCC GCA TAA TGC TTA AGT CGA ACA G |
| RPtail_ProcA2.8-E16A | TTA GCA CTC ACC **CGC** CCA ATA GGA TGG AGG CAT AGA TGG AGC ATG GTT ATG ACA GG |
| FPtail_ProcA2.8-G17A | TCC TAT TGG GAG **GCG** GAG TGC TAA GCG GCC GCA TAA TGC TTA AGT CGA ACA G |
| RPtail_ProcA2.8- G17A | TTA GCA CTC **CGC** CTC CCA ATA GGA TGG AGG CAT AGA TGG AGC ATG GTT ATG ACA GG |
| FPtail_ProcA2.8-E18A | TCC TAT TGG GAG GGT **GCG** TGC TAA GCG GCC GCA TAA TGC TTA AGT CGA ACA G |
| RPtail_ProcA2.8-E18A | TTA **CGC** CTC ACC CTC CCA ATA GGA TGG AGG CAT AGA TGG AGC ATG GTT ATG ACA GG |
| FPtail_ProcA2.8-R2−1aa | TCC TAT GAG GGT GAG TGC TAA GCG GCC GCA TAA TGC TTA AGT CGA ACA G |
| RPtail_ProcA2.8-R2−1aa | TTA GCA CTC ACC CTC ATA GGA TGG AGG CAT AGA TGG AGC ATG GTT ATG ACA GG |
| FPtail_ProcA2.8-R2−2aa | TCC TAT GGT GAG TGC TAA GCG GCC GCA TAA TGC TTA AGT CGA ACA G |
| RPtail_ProcA2.8-R2−2aa | TTA GCA CTC ACC ATA GGA TGG AGG CAT AGA TGG AGC ATG GTT ATG ACA GG |
| FPtail_ProcA2.8-R2+1aa | TCC TAT **GCG** TGG GAG GGT GAG TGC TAA GCG GCC GCA TAA TGC TTA AGT CGA ACA G |
| RPtail_ProcA2.8-R2+1aa | TTA GCA CTC ACC CTC CCA **CGC** ATA GGA TGG AGG CAT AGA TGG AGC ATG GTT ATG ACA GG |
| FPtail_ProcA2.8-R2+2aa | TCC TAT **GCG** TGG **GCC** GAG GGT GAG TGC TAA GCG GCC GCA TAA TGC TTA AGT CGA ACA G |
| RPtail_ProcA2.8-R2+2aa | TTA GCA CTC ACC CTC **GGC** CCA **CGC** ATA GGA TGG AGG CAT AGA TGG AGC ATG GTT ATG ACA GG |
| FPtail_ProcA2.8-S13C_C19S | **TGC** TAT TGG GAG GGT GAG **AGC** TAA GCG GCC GCA TAA TGC TTA AGT CGA ACA G |
| RPtail_ProcA2.8- S13C_C19S | TTA **GCT** CTC ACC CTC CCA ATA **GCA** TGG AGG CAT AGA TGG AGC ATG GTT ATG ACA GG |
| FPtail_ProcA2.8-S13C-C19S-A | **TGC** TAT TGG GAG GGT GAG **AGC GCG** TAA GCG GCC GCA TAA TGC TTA AGT CGA ACA G |
| RPtail_ProcA2.8-S13C-C19S-A | TTA **CGC GCT** CTC ACC CTC CCA ATA **GCA** TGG AGG CAT AGA TGG AGC ATG GTT ATG ACA GG |
| FPtail_ProcA2.8-S13C-C19S-AA | **TGC** TAT TGG GAG GGT GAG **AGC GCG GCC** TAA GCG GCC GCA TAA TGC TTA AGT CGA ACA G |
| RPtail_ProcA2.8-S13C-C19S-AA | TTA **GGC CGC GCT** CTC ACC CTC CCA ATA **GCA** TGG AGG CAT AGA TGG AGC ATG GTT ATG ACA GG |
| FPtail_Proc2.8-Y14P-E16P | TCC **CCG** TGG **CCA** GGT GAG TGC TAA GCG GCC GCA TAA TGC TTA AGT CGA ACA G |
| RPtail_Proc2.8-Y14P-E16P | TTA GCA CTC ACC **TGG** CCA **CGG** GGA TGG AGG CAT AGA TGG AGC ATG GTT ATG ACA GG |
| FPtail_Proc2.8-E16P-E18P | TCC TAT TGG **CCG** GGT **CCA** TGC TAA GCG GCC GCA TAA TGC TTA AGT CGA ACA G |
| RPtail_Proc2.8-E16P-E18P | TTA GCA **TGG** ACC **CGG** CCA ATA GGA TGG AGG CAT AGA TGG AGC ATG GTT ATG ACA GG |
| FPtail_Proc2.8-Y14P-E18P | TCC **CCG** TGG GAG GGT **CCA** TGC TAA GCG GCC GCA TAA TGC TTA AGT CGA ACA G |
| RPtail_Proc2.8-Y14P-E18P | TTA GCA **TGG** ACC CTC CCA **CGG** GGA TGG AGG CAT AGA TGG AGC ATG GTT ATG ACA GG |
| FPtail_Proc2.8-Y14E16E18PPP | TCC **CCG** TGG **CCA** GGT **CCG** TGC TAA GCG GCC GCA TAA TGC TTA AGT CGA ACA G |
| RPtail_Proc2.8-Y14E16E18PPP | TTA GCA **CGG** ACC **TGG** CCA **CGG** GGA TGG AGG CAT AGA TGG AGC ATG GTT ATG ACA GG |
| FPtail_ProcA2.8-R15G16D17 | TCC TAT **CGT GGC GAT** GAG TGC TAA GCG GCC GCA TAA TGC TTA AGT CGA ACA G |
| RPtail_ProcA2.8- R15G16D17 | TTA GCA CTC **ATC GCC ACG** ATA GGA TGG AGG CAT AGA TGG AGC ATG GTT ATG ACA GG |
| FPtail_ProcA2.8-R16G17D18 | TCC TAT TGG **CGT** GGT **GAT** TGC TAA GCG GCC GCA TAA TGC TTA AGT CGA ACA G |
| RPtail_ProcA2.8- R16G17D18 | TTA GCA **ATC** ACC **ACG** CCA ATA GGA TGG AGG CAT AGA TGG AGC ATG GTT ATG ACA GG |

**Table S2d.** Oligonucleotide primers used for deleting the *procM* gene from the *procA2.8*:*procM* pRSF Duet co-expression plasmids, allowing expression of linear Pcn2.8(WT) and Pcn2.8(16RGD). SLIM overhangs are underlined .

| name | sequence |
|---|---|
| FP_DeltaProcM | TCT GGT AAA GAA ACC GCT GCT GCG AAA TTT G |
| RP_DeltaProcM | CTC CCA ATA GGA TGG AGG CAT AGA TGG AGC ATG |
| FPTail_DeltaProcM | GGTGAGTGCTAAGGTACCCTCGAG TCT GGT AAA GAA ACC GCT GCT GCG AAA TTT G |
| RPTail_DeltaProcM | CTCGAGGGTACCTTAGCACTCACC CTC CCA ATA GGA TGG AGG CAT AGA TGG AGC ATG |
| JDH_FP_DeltaProcM16RGD | TCT GGT AAA GAA ACC GCT GCT GCG AAA TTT G |
| JDH_RP_DeltaProcM16RGD | ACG CCA ATA GGA TGG AGG CAT AGA TGG AGC ATG |
| JDH_FPTail_DeltaProcM16RGD | GGTGATTGCTAAGGTACCCTCGAG TCT GGT AAA GAA ACC GCT GCT GCG AAA TTT G |
| JDH_RPTail_DeltaProcM16RGD | CTCGAGGGTACCTTAGCAATCACC ACG CCA ATA GGA TGG AGG CAT AGA TGG AGC ATG |

**Table S3a.** Data of the fluorescence polarization competition assays with Pcn2.8(15RGD).

| conc. (Pcn2.8(15RGD)) / μM | replicate 1 | replicate 2 | replicate 3 | mean | standard deviation |
|---|---|---|---|---|---|
| 1000 | 112.02 | 107.63 | 113.52 | 111.06 | 3.06 |
| 500 | 112.05 | 106.32 | 110.59 | 109.65 | 2.98 |
| 250 | 106.41 | 107.15 | 110.15 | 107.90 | 1.98 |
| 125 | 105.09 | 104.87 | 108.12 | 106.03 | 1.81 |
| 62.5 | 108.93 | 106.85 | 110.89 | 108.89 | 2.02 |
| 31.25 | 117.19 | 109.26 | 115.46 | 113.97 | 4.17 |
| 15.625 | 118.34 | 118.77 | 120.15 | 119.08 | 0.95 |
| 7.8125 | 130.26 | 120.75 | 130.31 | 127.11 | 5.50 |
| 3.9063 | 131.15 | 135.35 | 137.26 | 134.59 | 3.13 |
| 1.9531 | 146.17 | 141.80 | 144.23 | 144.06 | 2.19 |
| 0.9766 | 153.78 | 148.55 | 154.62 | 152.31 | 3.29 |
| 0.4883 | 157.49 | 150.76 | 157.91 | 155.38 | 4.01 |
| 0.2441 | 163.92 | 156.72 | 161.68 | 160.77 | 3.68 |
| 0.1221 | 161.36 | 157.53 | 162.19 | 160.36 | 2.49 |
| 0.0610 | 166.53 | 157.02 | 164.80 | 162.79 | 5.06 |
| 0.0305 | 164.11 | 156.24 | 166.76 | 162.37 | 5.47 |

**Table S3b.** Data of the fluorescence polarization competition assays with Pcn2.8(16RGD).

| conc. (Pcn2.8(16RGD)) / μM | replicate 1 | replicate 2 | replicate 3 | mean | standard deviation |
|---|---|---|---|---|---|
| 5 | 101.28 | 96.92 | 99.51 | 99.24 | 2.19 |
| 2.5 | 105.69 | 100.40 | 104.65 | 103.58 | 2.81 |
| 1.25 | 106.41 | 103.01 | 108.21 | 105.88 | 2.64 |
| 0.625 | 107.27 | 104.18 | 107.94 | 106.46 | 2.01 |
| 0.3125 | 109.43 | 108.46 | 107.22 | 108.37 | 1.11 |
| 0.1563 | 110.09 | 108.31 | 114.28 | 110.89 | 3.06 |
| 0.0781 | 117.08 | 112.54 | 116.79 | 115.47 | 2.54 |
| 0.0391 | 124.69 | 118.57 | 124.44 | 122.57 | 3.46 |
| 0.0195 | 130.26 | 127.53 | 130.42 | 129.40 | 1.63 |
| 0.0098 | 138.58 | 142.75 | 138.80 | 140.04 | 2.35 |
| 0.0049 | 150.59 | 149.95 | 146.64 | 149.06 | 2.12 |
| 0.0024 | 153.71 | 150.10 | 152.09 | 151.96 | 1.81 |
| 0.0012 | 156.68 | 157.83 | 155.55 | 156.69 | 1.14 |
| 0.0006 | 161.00 | 160.59 | 156.96 | 159.52 | 2.23 |
| 0.0003 | 159.91 | 160.96 | 158.42 | 159.76 | 1.28 |
| 0.0002 | 160.92 | 159.30 | 157.60 | 159.27 | 1.66 |

**Table S3c.** Data of the fluorescence polarization competition assays with Pcn2.8(5RGD).

| conc. (Pcn2.8(5RGD)) / μM | data |
|---|---|
| 100 | 123.90 |
| 50 | 133.58 |
| 25 | 141.46 |
| 12.5 | 149.40 |
| 6.25 | 159.54 |
| 3.125 | 155.33 |
| 1.5625 | 152.49 |
| 0.7813 | 154.38 |
| 0.3906 | 157.56 |
| 0.1953 | 163.72 |
| 0.0977 | 160.08 |
| 0.0488 | 162.09 |
| 0.0244 | 156.88 |
| 0.0122 | 158.63 |
| 0.0061 | 158.19 |

**Table S3d.** Data of the fluorescence polarization competition assays with linear Pcn2.8(16RGD) core peptide.

| conc. (linear Pcn2.8(16RGD)) / μM | replicate 1 | replicate 2 | replicate 3 | mean | standard deviation |
|---|---|---|---|---|---|
| 36.2 | 103.19 | 106.03 | 109.71 | 106.31 | 3.27 |
| 18.1 | 102.34 | 108.39 | 109.32 | 106.68 | 3.79 |
| 9.04 | 107.41 | 109.15 | 110.33 | 108.96 | 1.47 |
| 4.52 | 109.86 | 110.34 | 112.21 | 110.80 | 1.24 |
| 2.26 | 112.27 | 114.27 | 116.16 | 114.23 | 1.95 |
| 1.13 | 121.09 | 119.86 | 120.57 | 120.51 | 0.62 |
| 0.5648 | 131.21 | 131.72 | 130.61 | 131.18 | 0.56 |
| 0.2824 | 144.13 | 144.65 | 144.02 | 144.27 | 0.33 |
| 0.1412 | 157.65 | 159.81 | 157.58 | 158.35 | 1.27 |
| 0.0706 | 174.14 | 174.16 | 171.98 | 173.42 | 1.25 |
| 0.0353 | 181.37 | 189.18 | 184.29 | 184.95 | 3.95 |
| 0.0177 | 191.16 | 192.94 | 191.50 | 191.87 | 0.94 |
| 0.0088 | 191.50 | 195.58 | 194.79 | 193.96 | 2.16 |
| 0.0044 | 194.62 | 195.57 | 194.59 | 194.93 | 0.56 |
| 0.0022 | 193.52 | 190.78 | 194.44 | 192.91 | 1.90 |
| 0.0011 | 194.23 | 195.15 | 196.25 | 195.21 | 1.01 |

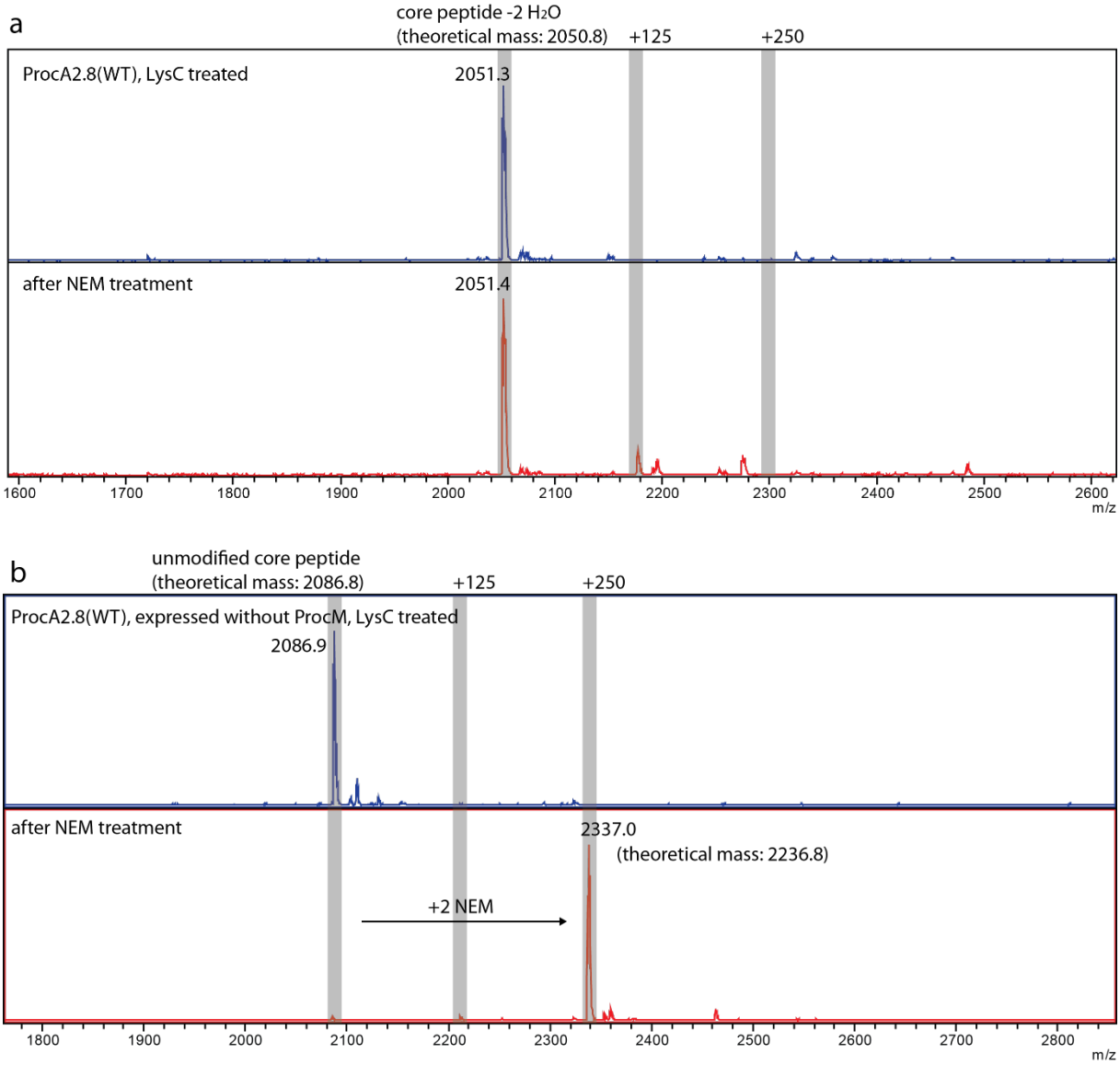


**Figure S1.** a.) MALDI-TOF-MS analysis of LysC treated ProcA2.8(WT) (co-expressed with ProcM) before (blue) and after NEM treatment (red). Every mass region that corresponds to core peptide or NEM adducts thereof is highlighted in a gray box. b.) MALDI-TOF-MS analysis of a LysC treated ProcA2.8(WT) control (not co-expressed with ProcM) before (blue) and after NEM treatment (red). Every mass region that corresponds to core peptide or NEM adducts thereof is highlighted in a gray box.

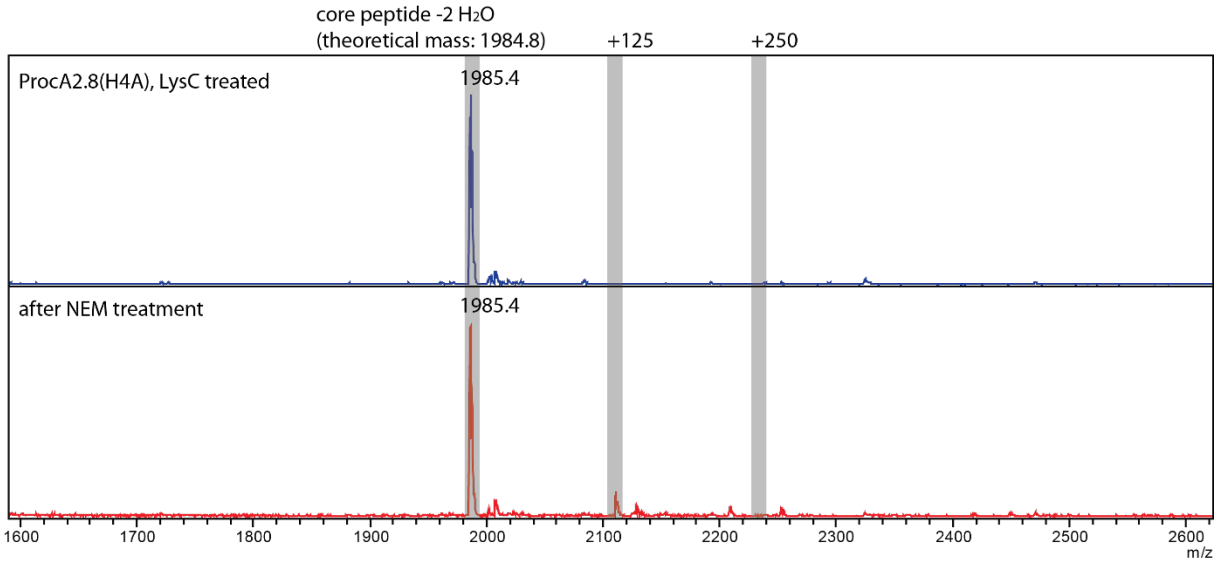


**Figure S2.** MALDI-TOF-MS analysis of LysC treated ProcA2.8(H4A) before (blue) and after NEM treatment (red). Every mass region that corresponds to core peptide or NEM adducts thereof is highlighted in a gray box.

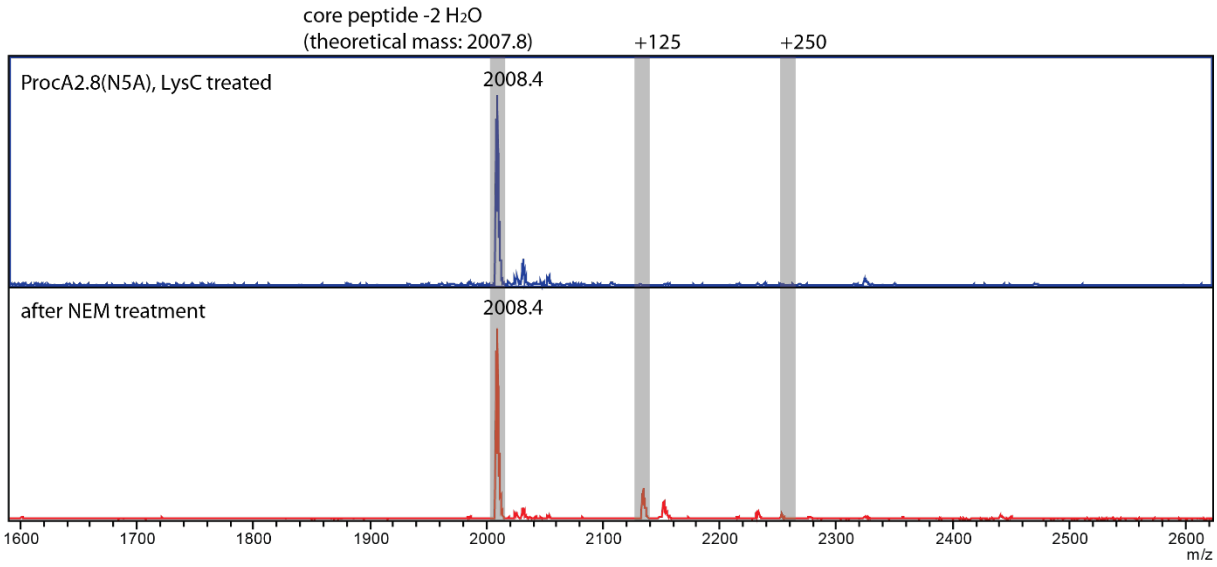


**Figure S3.** MALDI-TOF-MS analysis of LysC treated ProcA2.8(N5A) before (blue) and after NEM treatment (red). Every mass region that corresponds to core peptide or NEM adducts thereof is highlighted in a gray box.

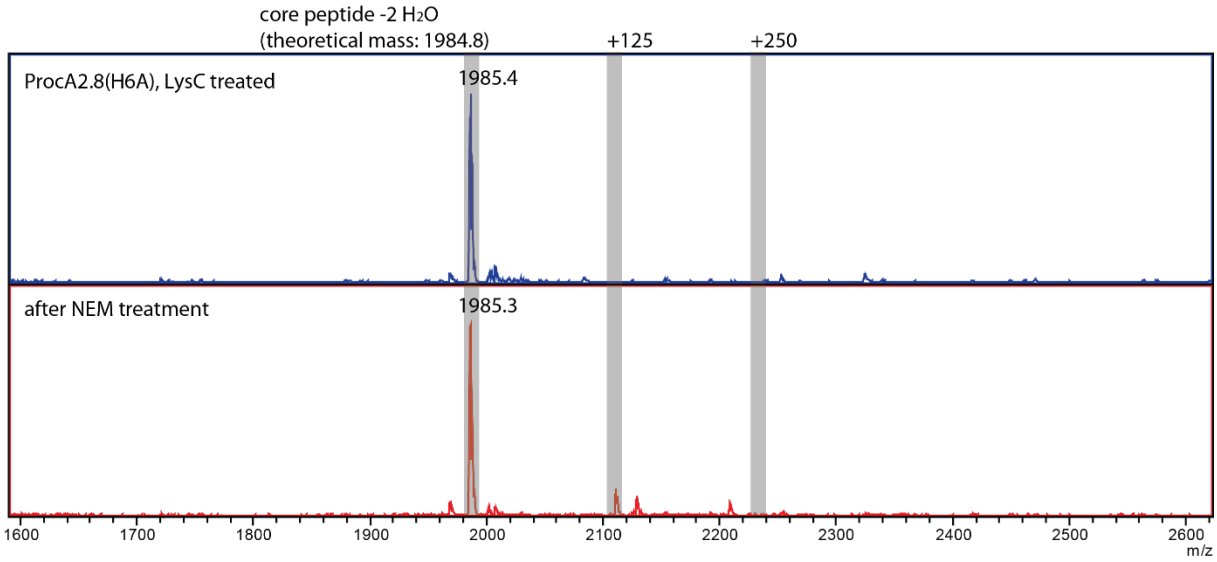


**Figure S4.** MALDI-TOF-MS analysis of LysC treated ProcA2.8(H6A) before (blue) and after NEM treatment (red). Every mass region that corresponds to core peptide or NEM adducts thereof is highlighted in a gray box.

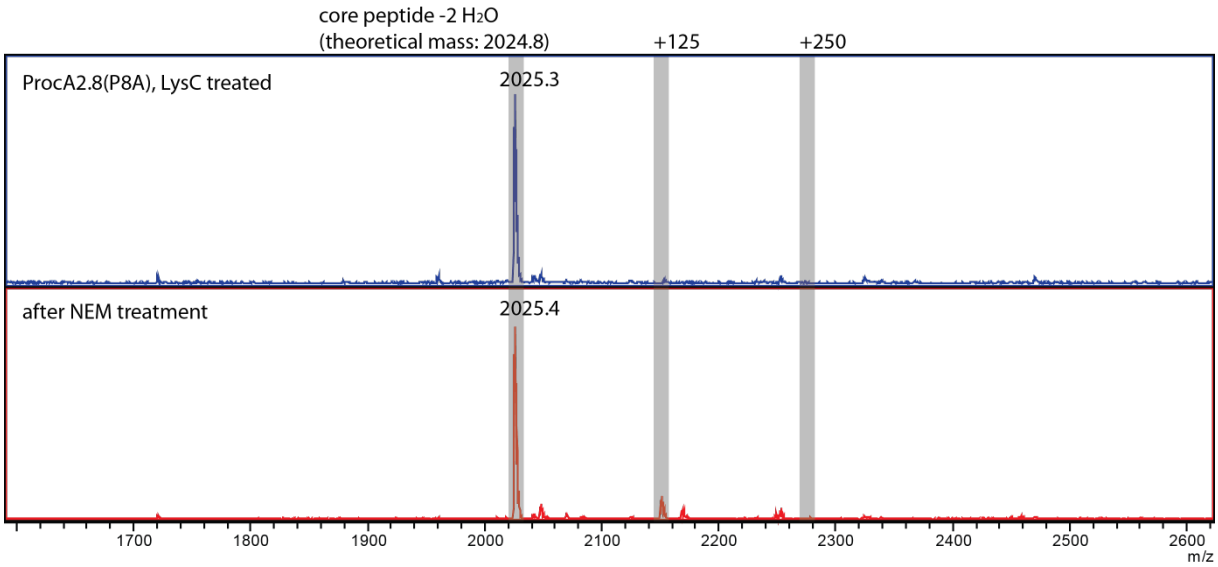


**Figure S5.** MALDI-TOF-MS analysis of LysC treated ProcA2.8(P8A) before (blue) and after NEM treatment (red). Every mass region that corresponds to core peptide or NEM adducts thereof is highlighted in a gray box.

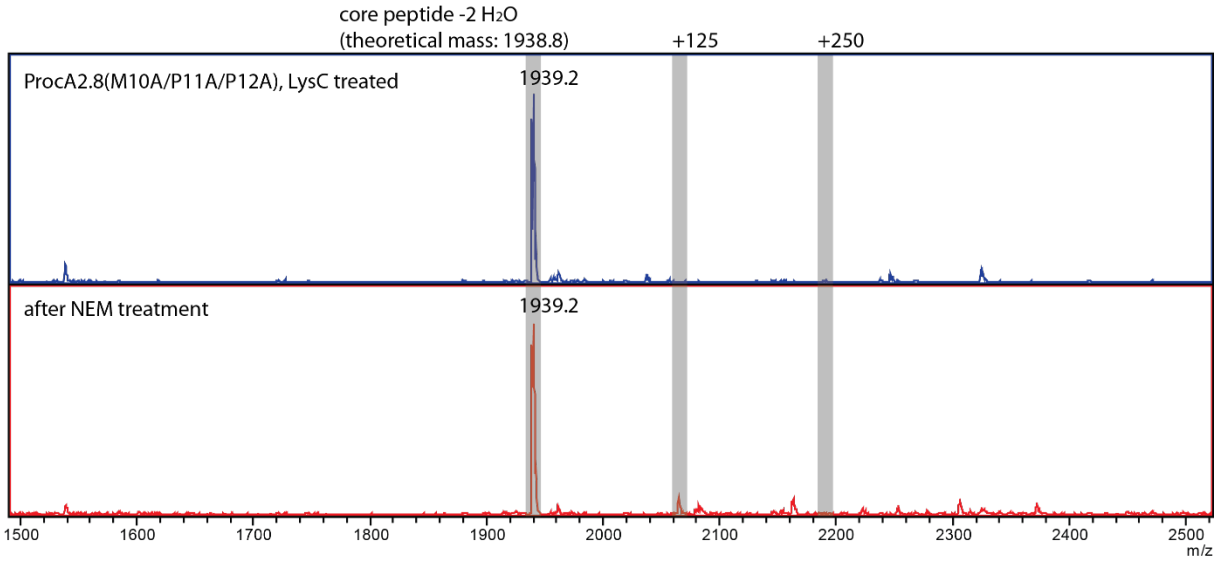


**Figure S6.** MALDI-TOF-MS analysis of LysC treated ProcA2.8(M10A/P11A/P12A) before (blue) and after NEM treatment (red). Every mass region that corresponds to core peptide or NEM adducts thereof is highlighted in a gray box.

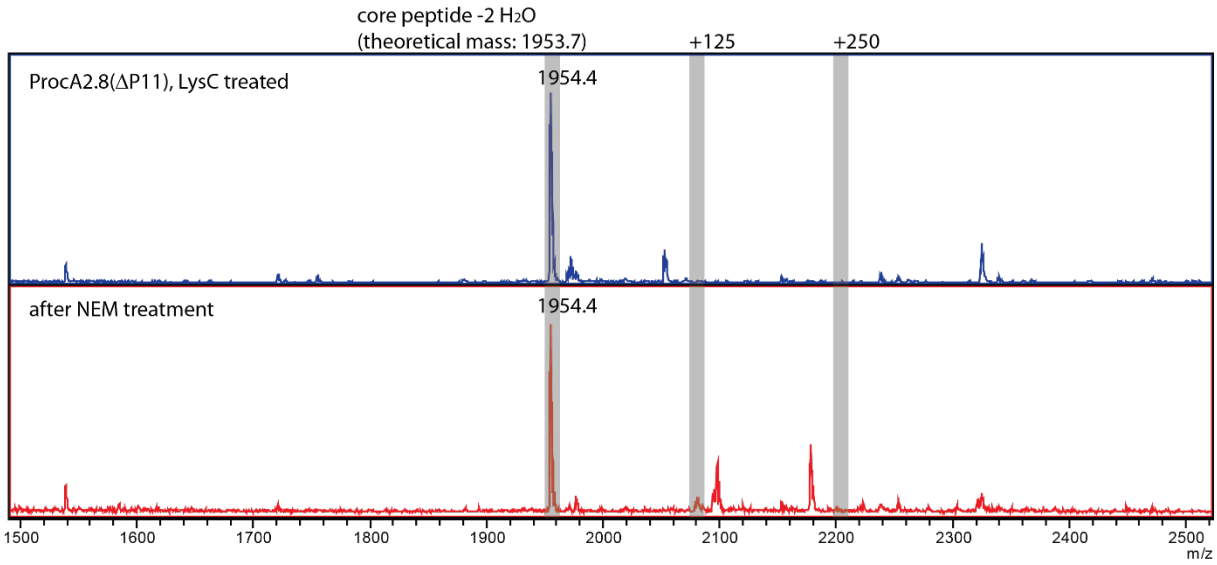


**Figure S7.** MALDI-TOF-MS analysis of LysC treated ProcA2.8(ΔP11) before (blue) and after NEM treatment (red). Every mass region that corresponds to core peptide or NEM adducts thereof is highlighted in a gray box.

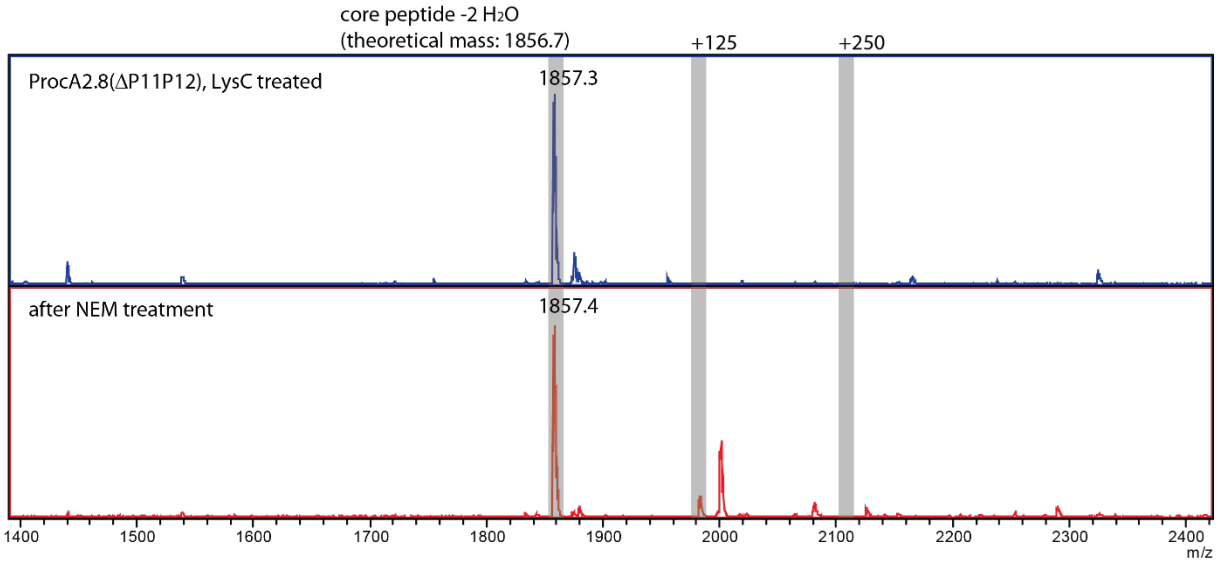


**Figure S8.** MALDI-TOF-MS analysis of LysC treated ProcA2.8(ΔP11P12) before (blue) and after NEM treatment (red). Every mass region that corresponds to core peptide or NEM adducts thereof is highlighted in a gray box.

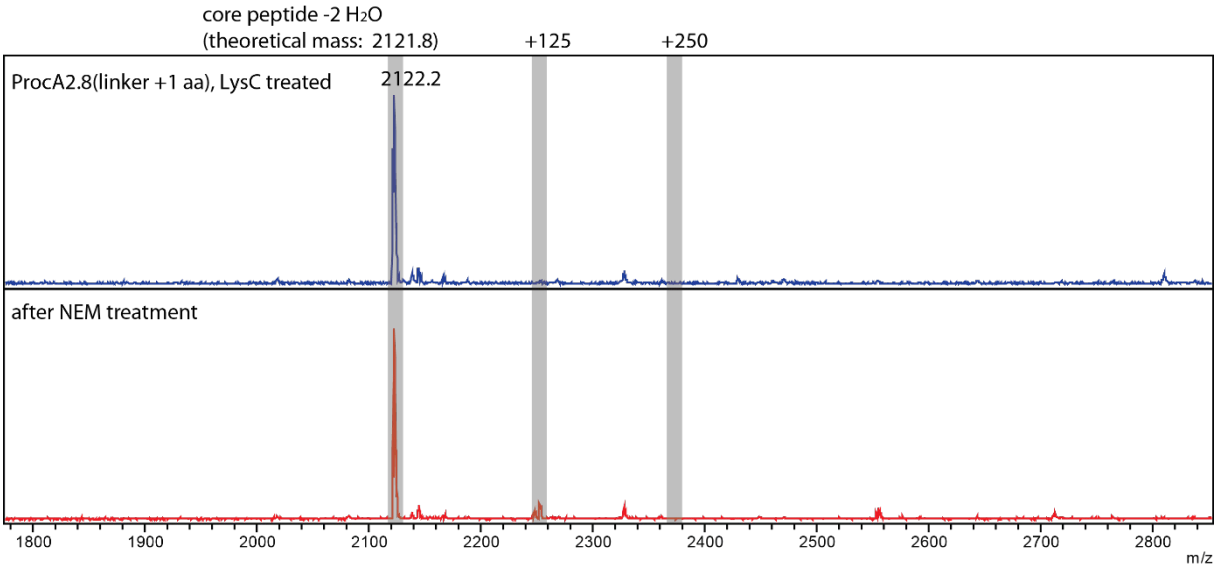


**Figure S9.** MALDI-TOF-MS analysis of LysC treated ProcA2.8(linker +1 aa) before (blue) and after NEM treatment (red). Every mass region that corresponds to core peptide or NEM adducts thereof is highlighted in a gray box.

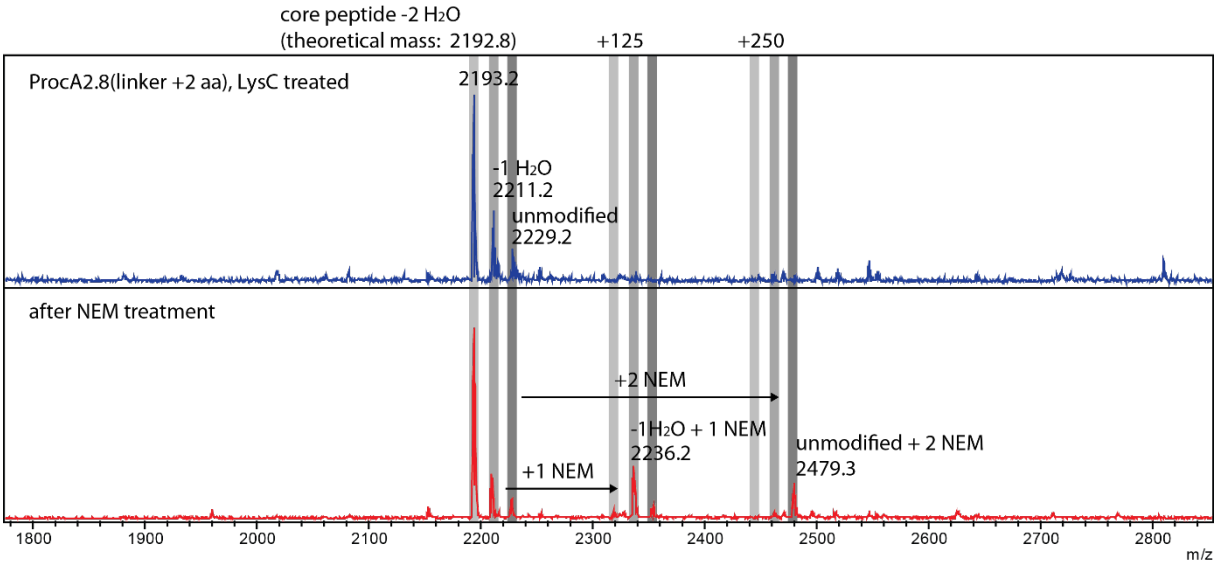


**Figure S10.** MALDI-TOF-MS analysis of LysC treated ProcA2.8(linker +2 aa) before (blue) and after NEM treatment (red). Every mass region that corresponds to core peptide or NEM adducts thereof is highlighted in a gray box.

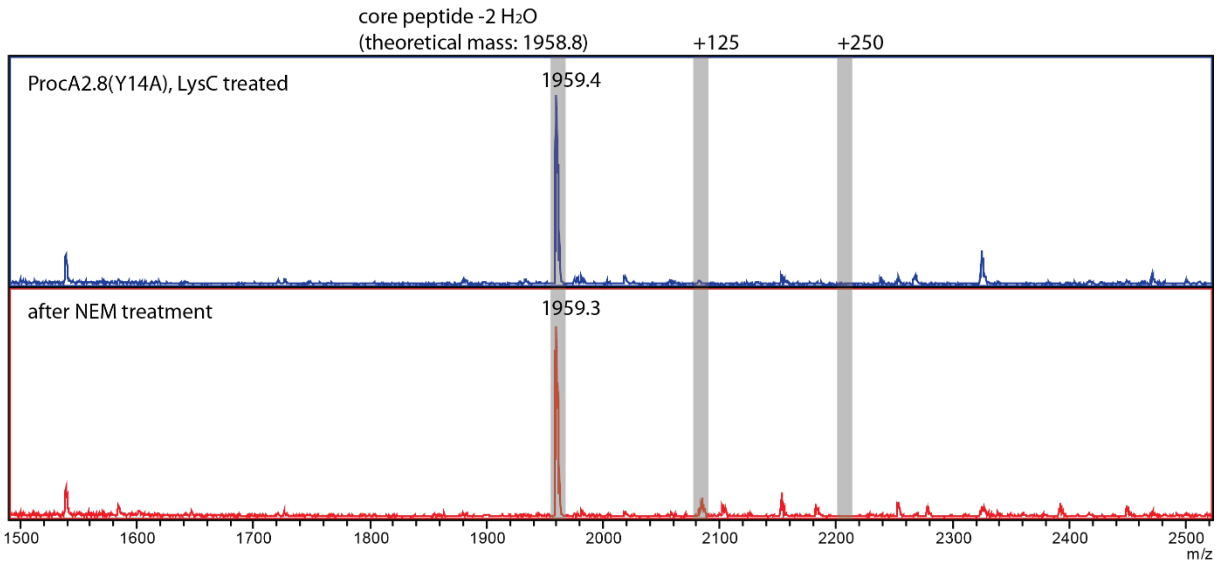


**Figure S11.** MALDI-TOF-MS analysis of LysC treated ProcA2.8(Y14A) before (blue) and after NEM treatment (red). Every mass region that corresponds to core peptide or NEM adducts thereof is highlighted in a gray box.

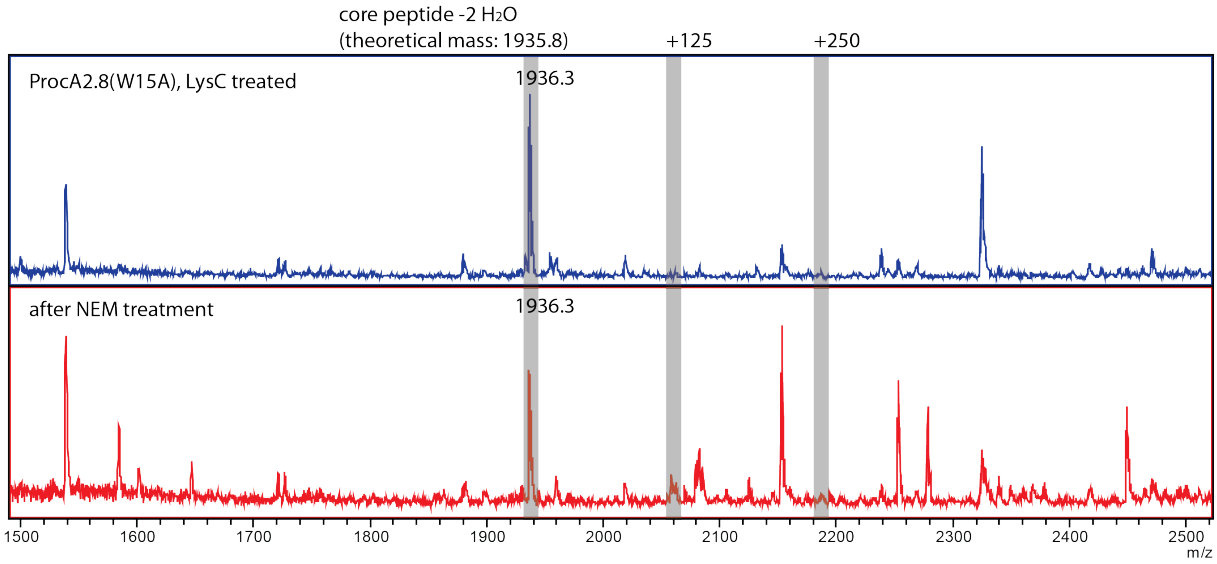


**Figure S12.** MALDI-TOF-MS analysis of LysC treated ProcA2.8(W15A) before (blue) and after NEM treatment (red). Every mass region that corresponds to core peptide or NEM adducts thereof is highlighted in a gray box.

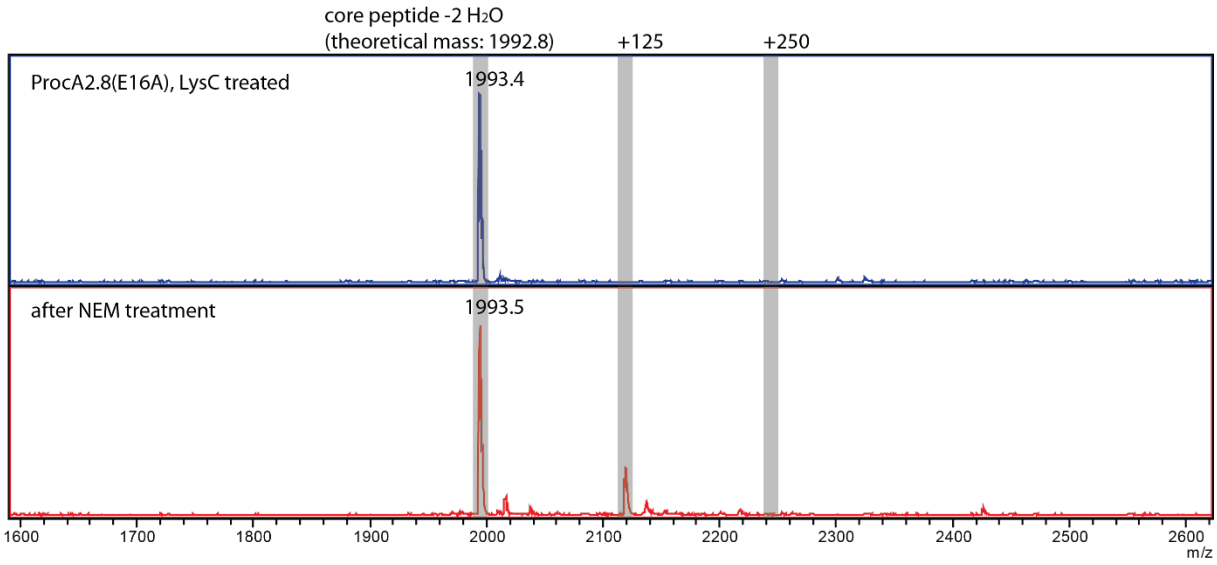


**Figure S13.** MALDI-TOF-MS analysis of LysC treated ProcA2.8(E16A) before (blue) and after NEM treatment (red). Every mass region that corresponds to core peptide or NEM adducts thereof is highlighted in a gray box.

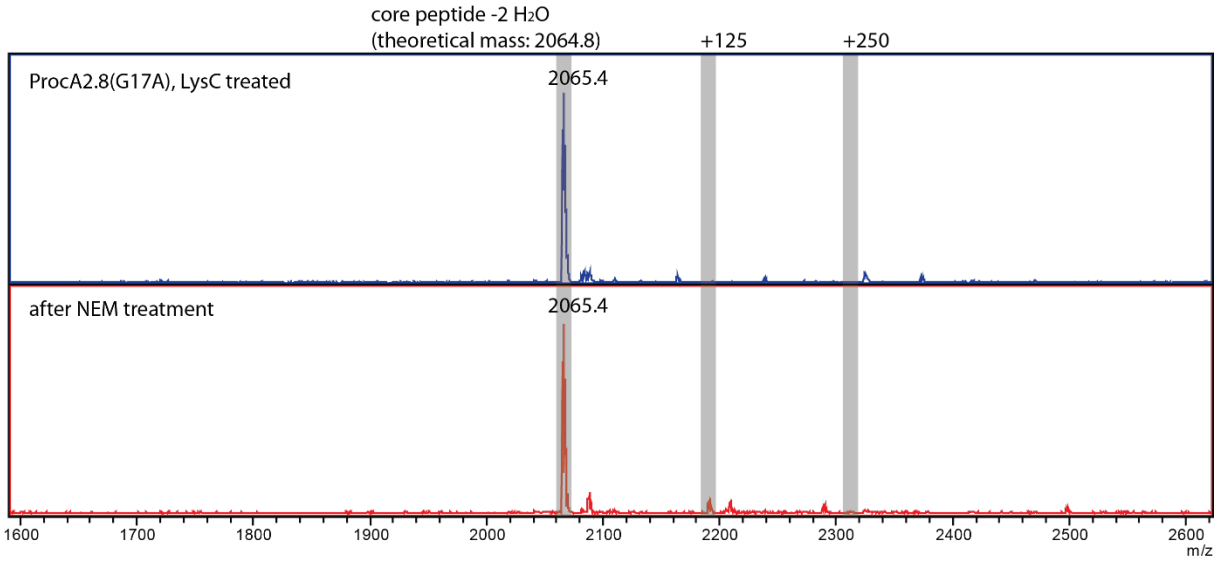


**Figure S14.** MALDI-TOF-MS analysis of LysC treated ProcA2.8(G17A) before (blue) and after NEM treatment (red). Every mass region that corresponds to core peptide or NEM adducts thereof is highlighted in a gray box.

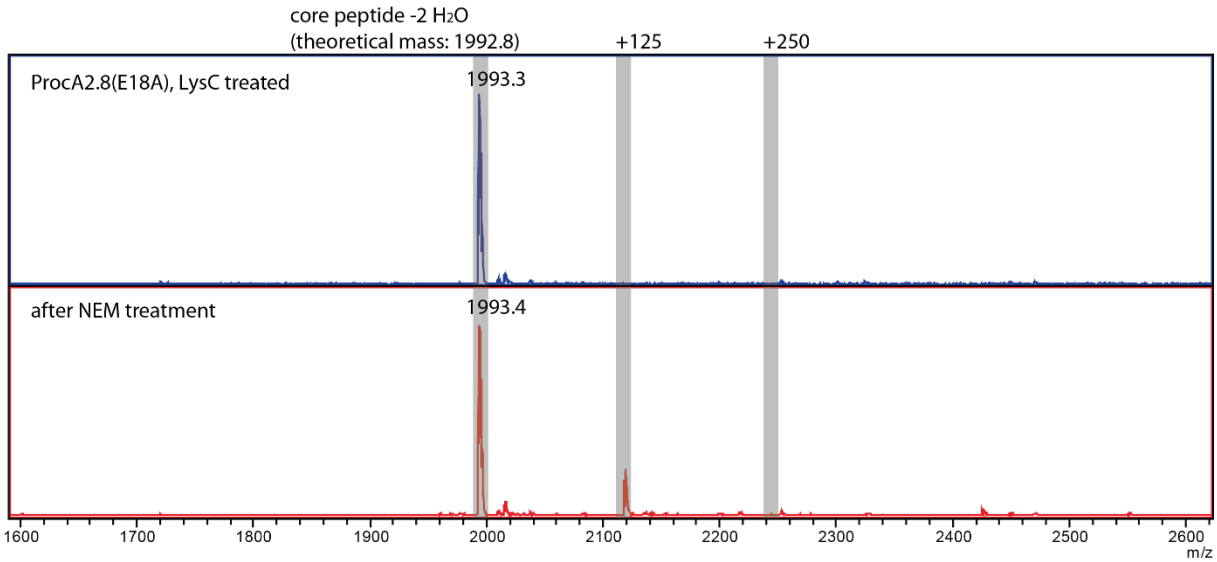


**Figure S15.** MALDI-TOF-MS analysis of LysC treated ProcA2.8(E18A) before (blue) and after NEM treatment (red). Every mass region that corresponds to core peptide or NEM adducts thereof is highlighted in a gray box.

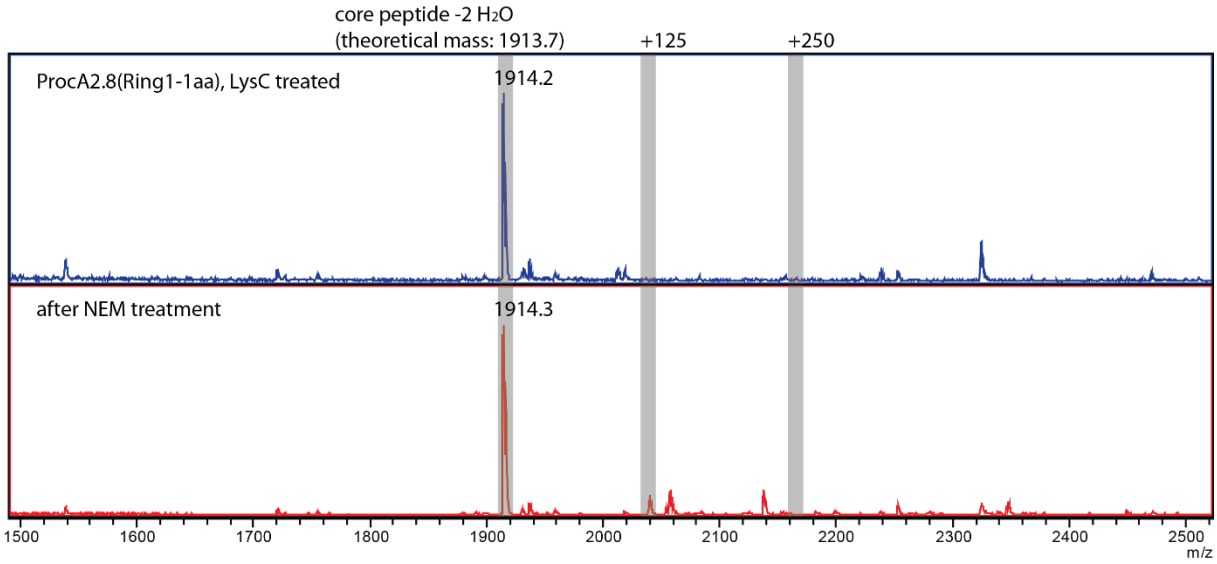


**Figure S16.** MALDI-TOF-MS analysis of LysC treated ProcA2.8(Ring1−1aa) before (blue) and after NEM treatment (red). Every mass region that corresponds to core peptide or NEM adducts thereof is highlighted in a gray box.

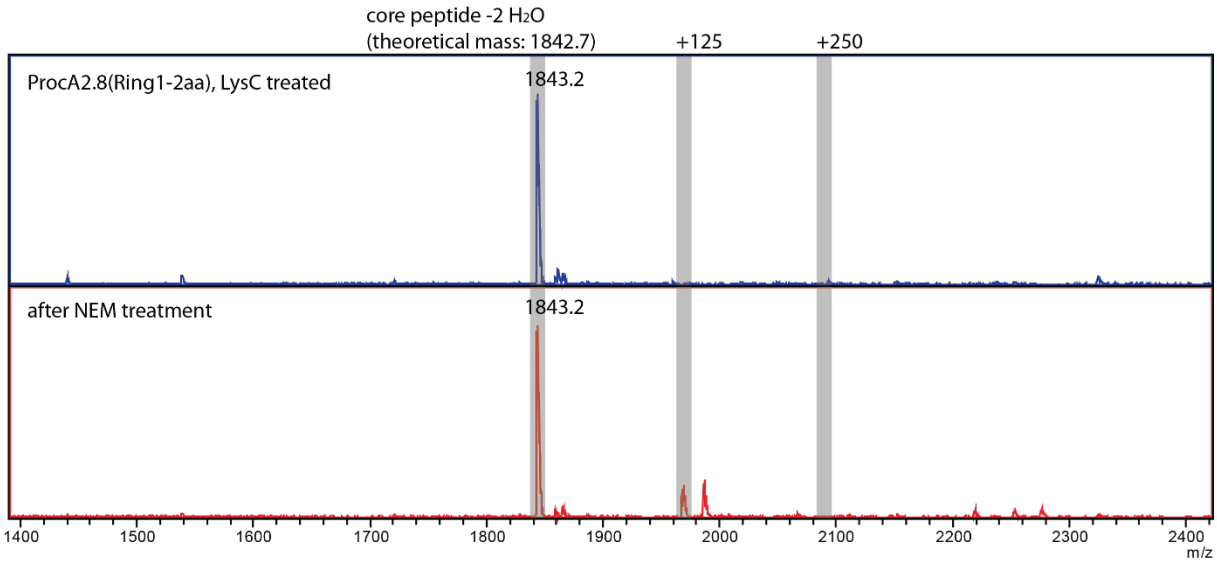


**Figure S17.** MALDI-TOF-MS analysis of LysC treated ProcA2.8(Ring1−2aa) before (blue) and after NEM treatment (red). Every mass region that corresponds to core peptide or NEM adducts thereof is highlighted in a gray box.

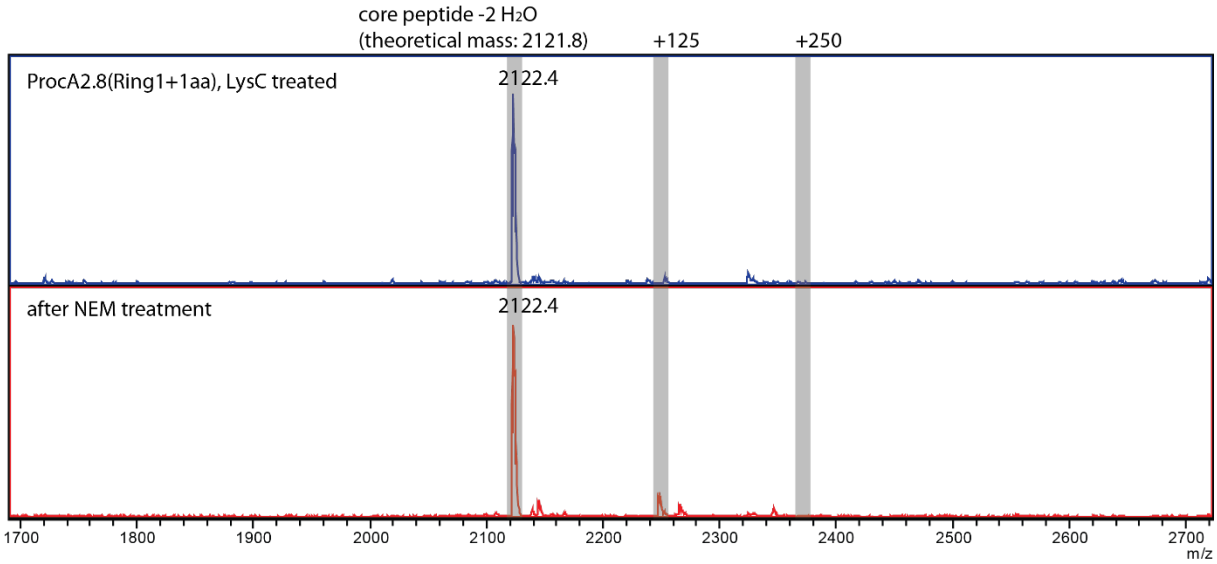


**Figure S18.** MALDI-TOF-MS analysis of LysC treated ProcA2.8(Ring1+1aa) before (blue) and after NEM treatment (red). Every mass region that corresponds to core peptide or NEM adducts thereof is highlighted in a gray box.

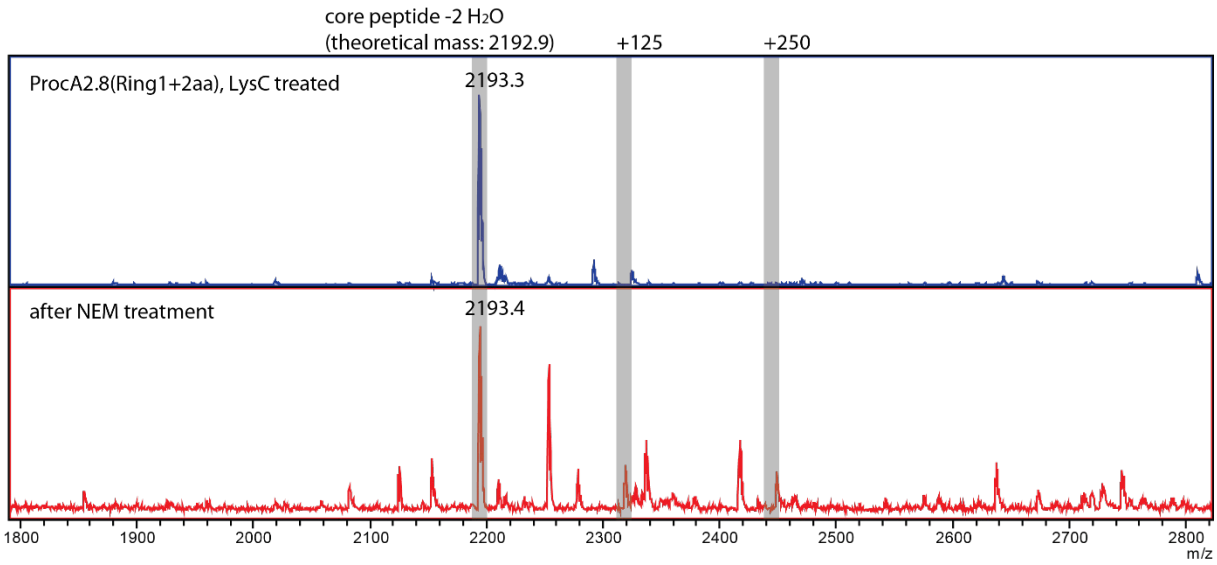


**Figure S19.** MALDI-TOF-MS analysis of LysC treated ProcA2.8(Ring1+2aa) before (blue) and after NEM treatment (red). Every mass region that corresponds to core peptide or NEM adducts thereof is highlighted in a gray box.

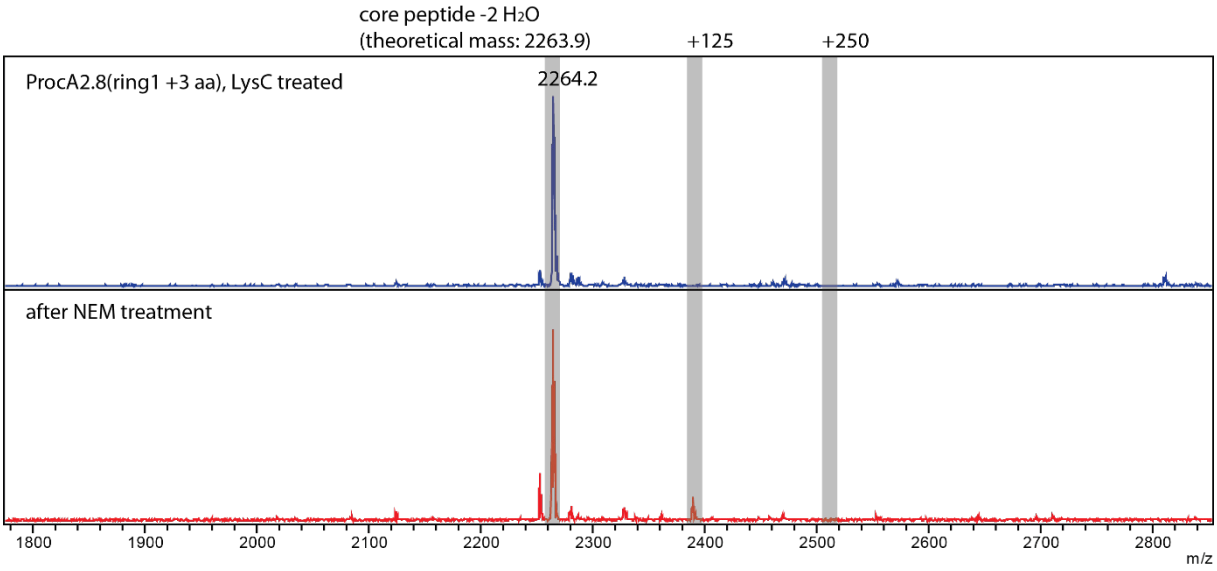


**Figure S20.** MALDI-TOF-MS analysis of LysC treated ProcA2.8(Ring1+3aa) before (blue) and after NEM treatment (red). Every mass region that corresponds to core peptide or NEM adducts thereof is highlighted in a gray box.

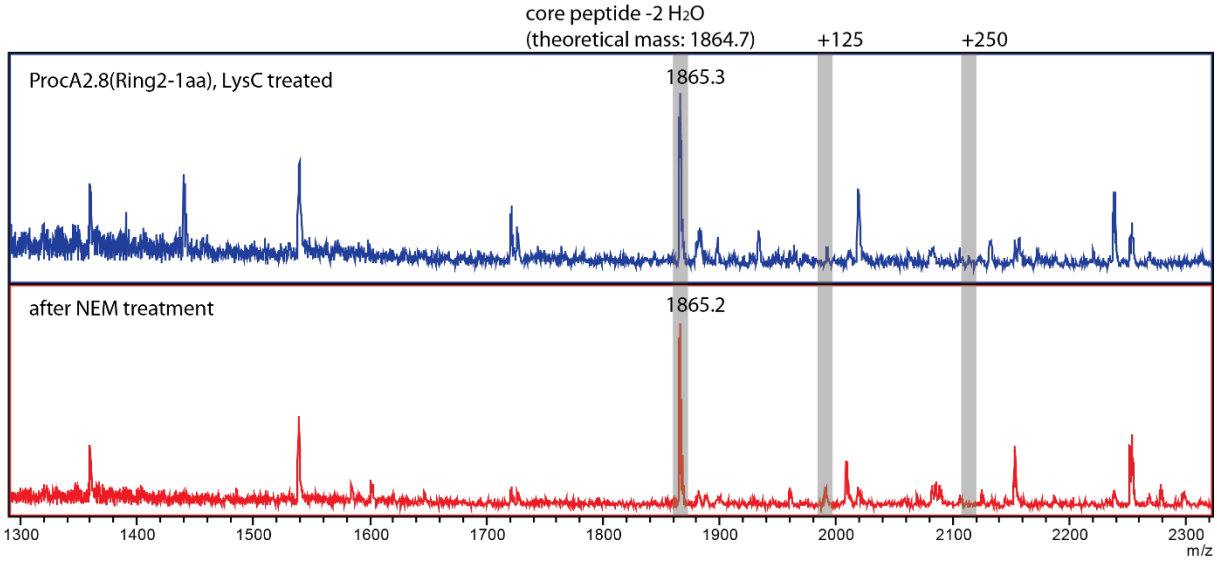


**Figure S21.** MALDI-TOF-MS analysis of LysC treated ProcA2.8(Ring2−1aa) before (blue) and after NEM treatment (red). Every mass region that corresponds to core peptide or NEM adducts thereof is highlighted in a gray box.

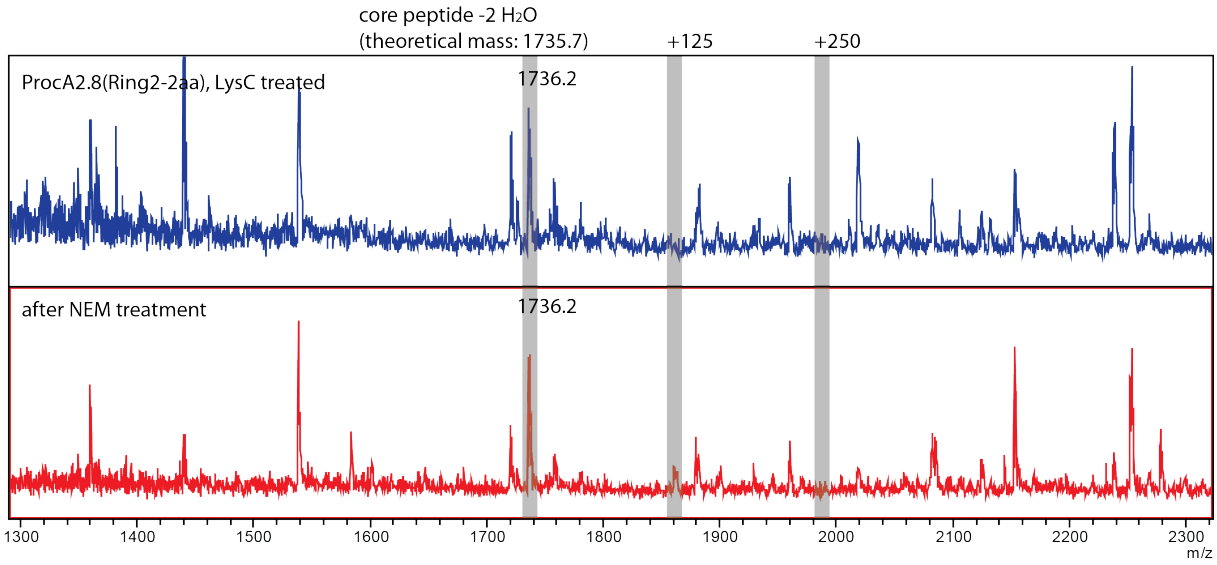


**Figure S22.** MALDI-TOF-MS analysis of LysC treated ProcA2.8(Ring2−2aa) before (blue) and after NEM treatment (red). Every mass region that corresponds to core peptide or NEM adducts thereof is highlighted in a gray box.

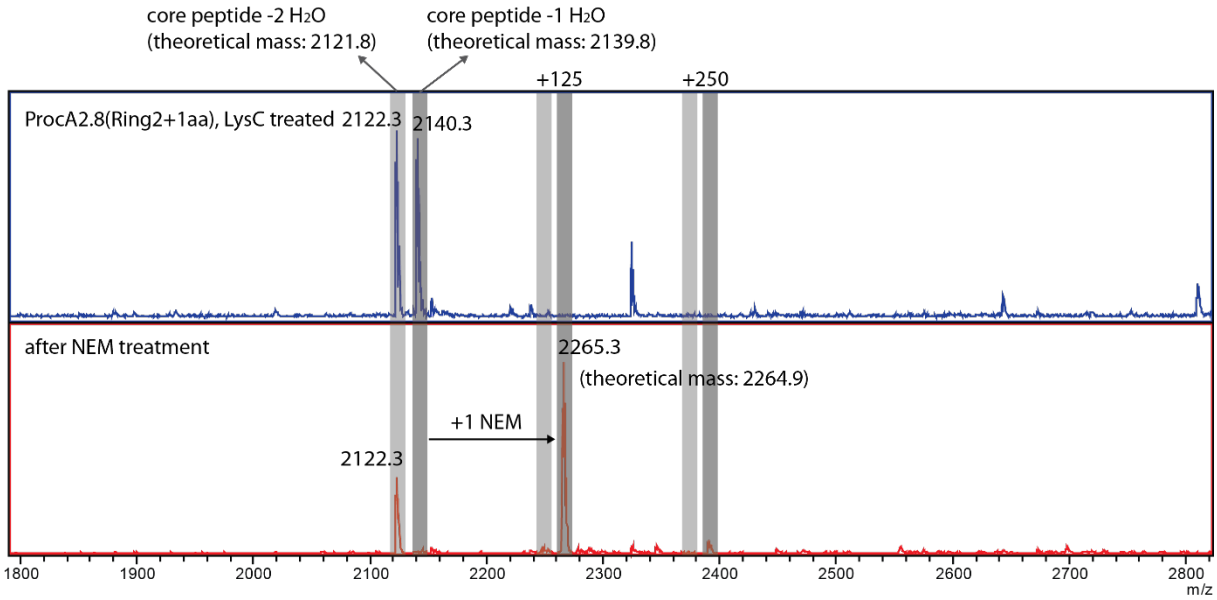


**Figure S23.** MALDI-TOF-MS analysis of LysC treated ProcA2.8(Ring2+1aa) before (blue) and after NEM treatment (red). Every mass region that corresponds to core peptide or NEM adducts thereof is highlighted in a gray box.

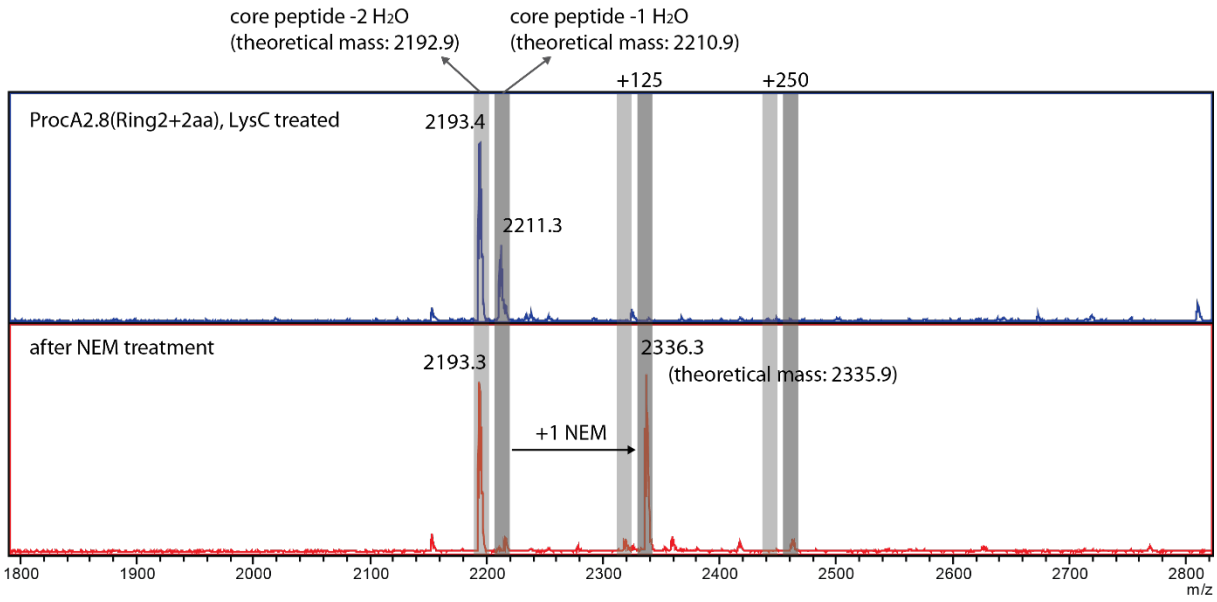


**Figure S24.** MALDI-TOF-MS analysis of LysC treated ProcA2.8(Ring2+2aa) before (blue) and after NEM treatment (red). Every mass region that corresponds to core peptide or NEM adducts thereof is highlighted in a gray box.

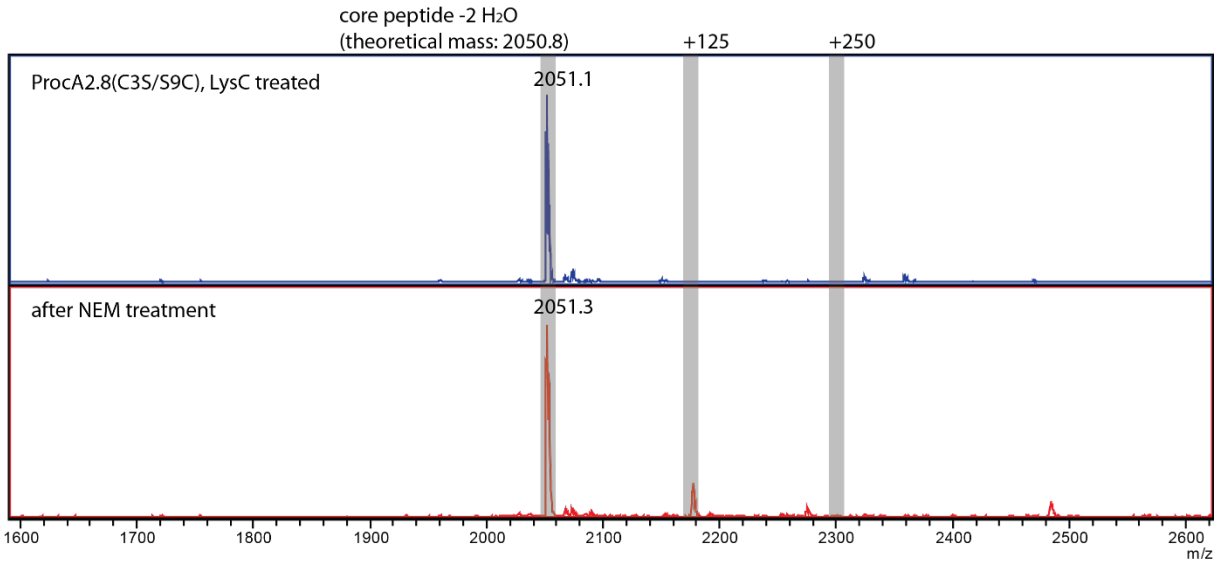


**Figure S25.** MALDI-TOF-MS analysis of LysC treated ProcA2.8(C3S/S9C) before (blue) and after NEM treatment (red). Every mass region that corresponds to core peptide or NEM adducts thereof is highlighted in a gray box.

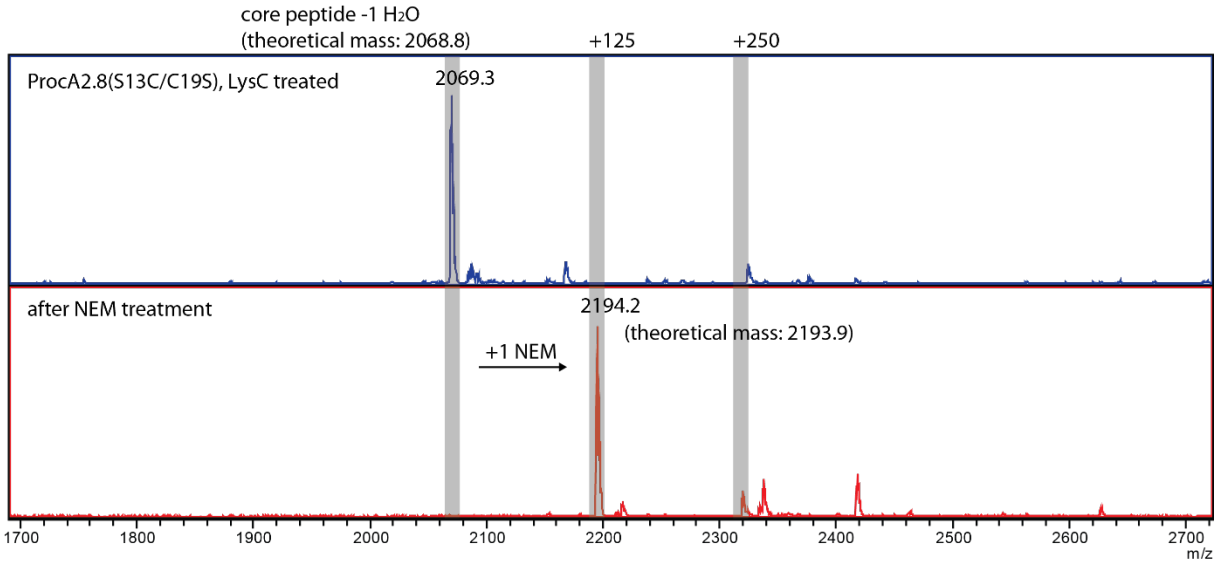


**Figure S26.** MALDI-TOF-MS analysis of LysC treated ProcA2.8(S13C/C19S) before (blue) and after NEM treatment (red). Every mass region that corresponds to core peptide or NEM adducts thereof is highlighted in a gray box.

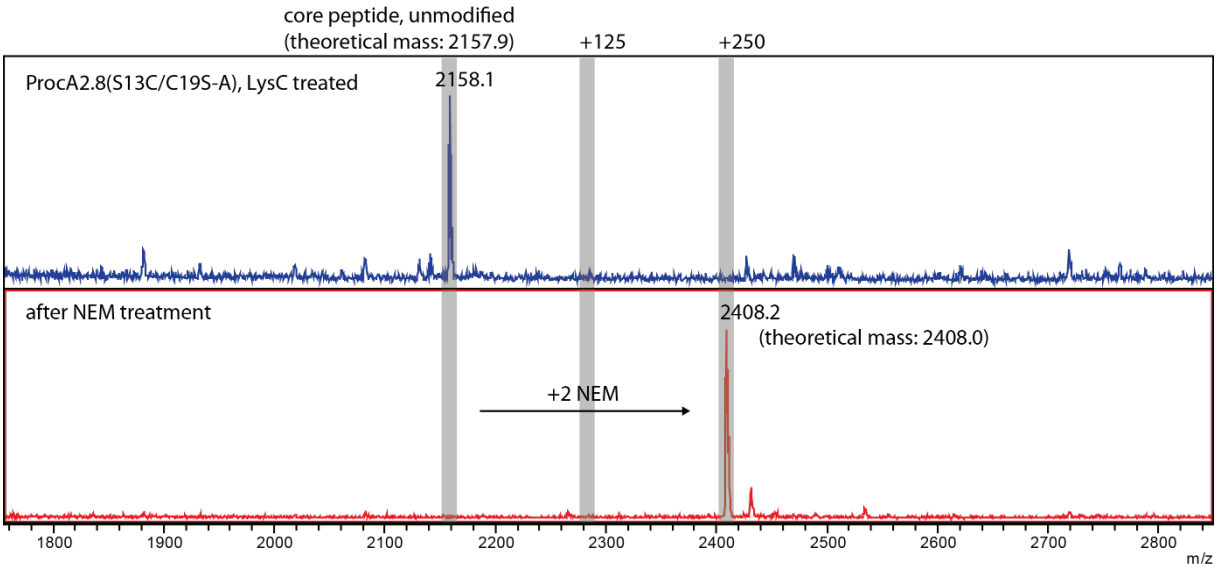


**Figure S27.** MALDI-TOF-MS analysis of LysC treated ProcA2.8(S13C/C19S-A) before (blue) and after NEM treatment (red). Every mass region that corresponds to core peptide or NEM adducts thereof is highlighted in a gray box.

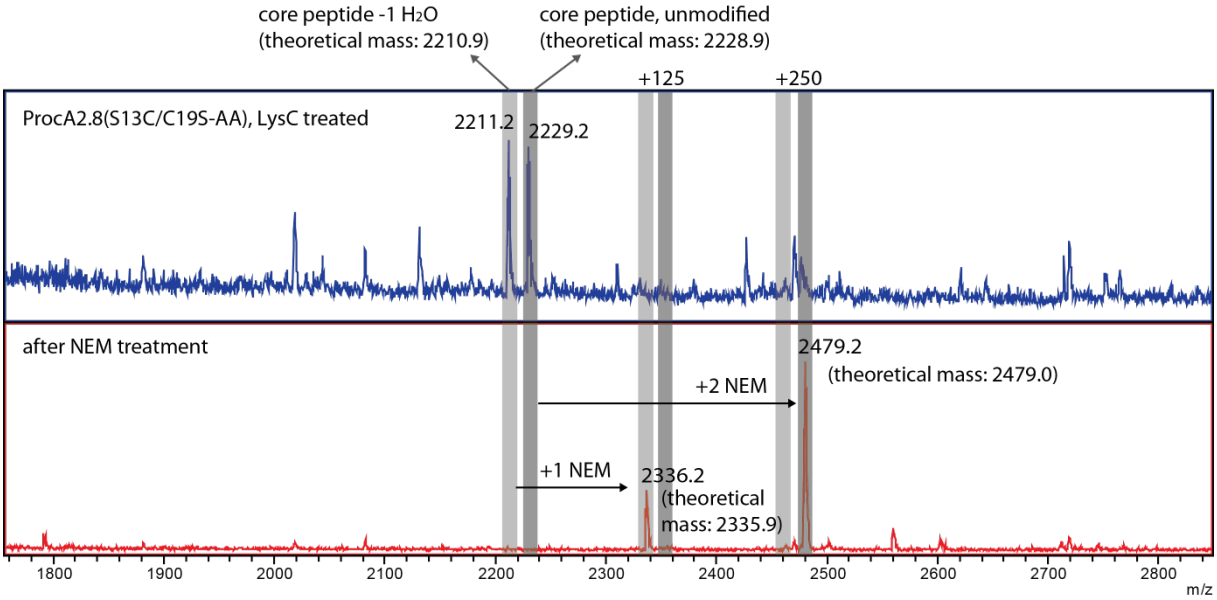


**Figure S28.** MALDI-TOF-MS analysis of LysC treated ProcA2.8(S13C/C19S-AA) before (blue) and after NEM treatment (red). Every mass region that corresponds to core peptide or NEM adducts thereof is highlighted in a gray box.

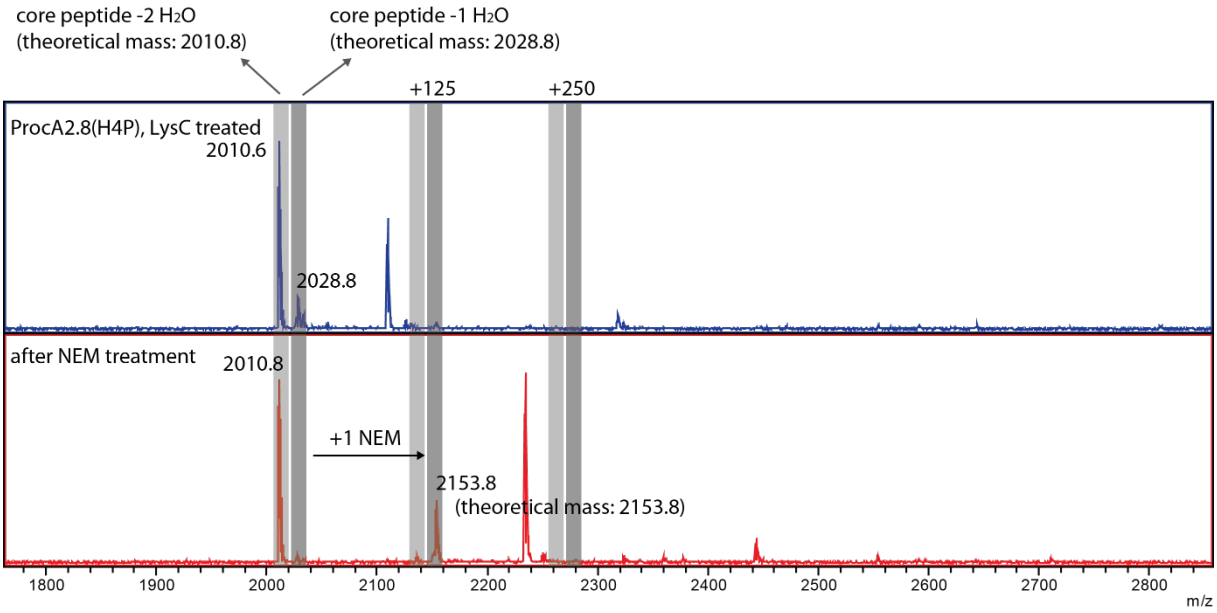


**Figure S29.** MALDI-TOF-MS analysis of LysC treated ProcA2.8(H4P) before (blue) and after NEM treatment (red). Every mass region that corresponds to core peptide or NEM adducts thereof is highlighted in a gray box.

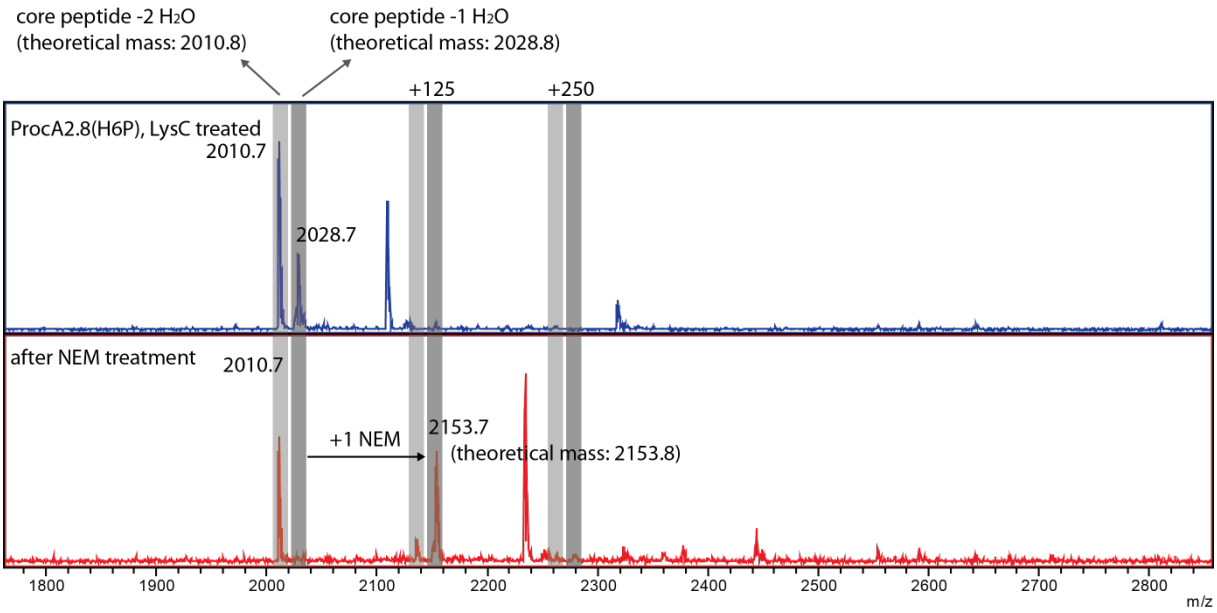


**Figure S30.** MALDI-TOF-MS analysis of LysC treated ProcA2.8(H6P) before (blue) and after NEM treatment (red). Every mass region that corresponds to core peptide or NEM adducts thereof is highlighted in a gray box.

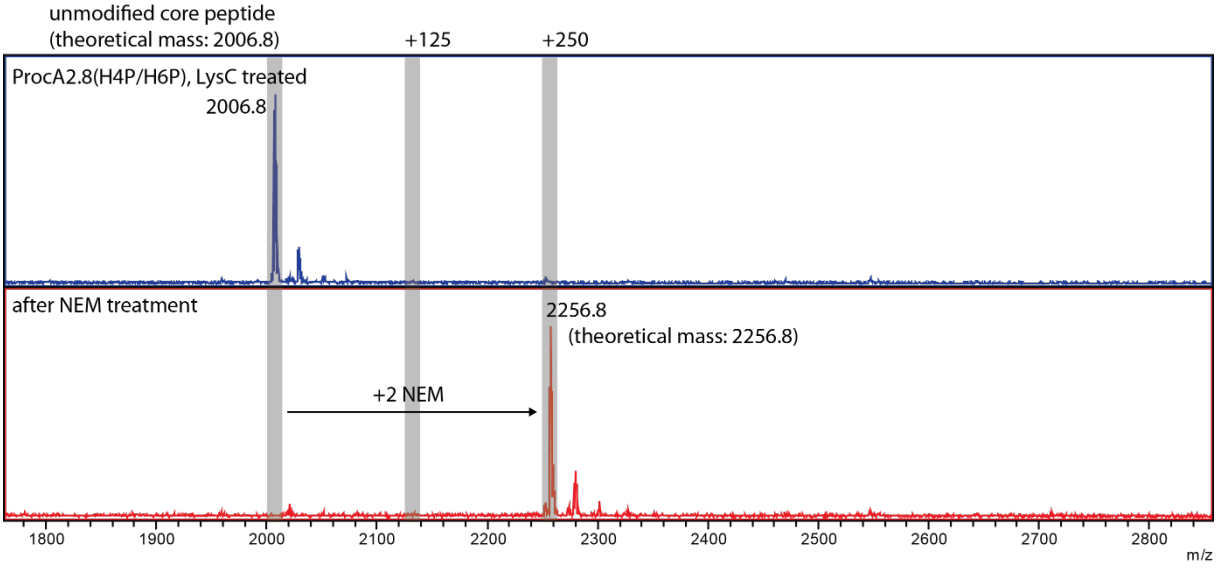


**Figure S31.** MALDI-TOF-MS analysis of LysC treated ProcA2.8(H4P/H6P) before (blue) and after NEM treatment (red). Every mass region that corresponds to core peptide or NEM adducts thereof is highlighted in a gray box.

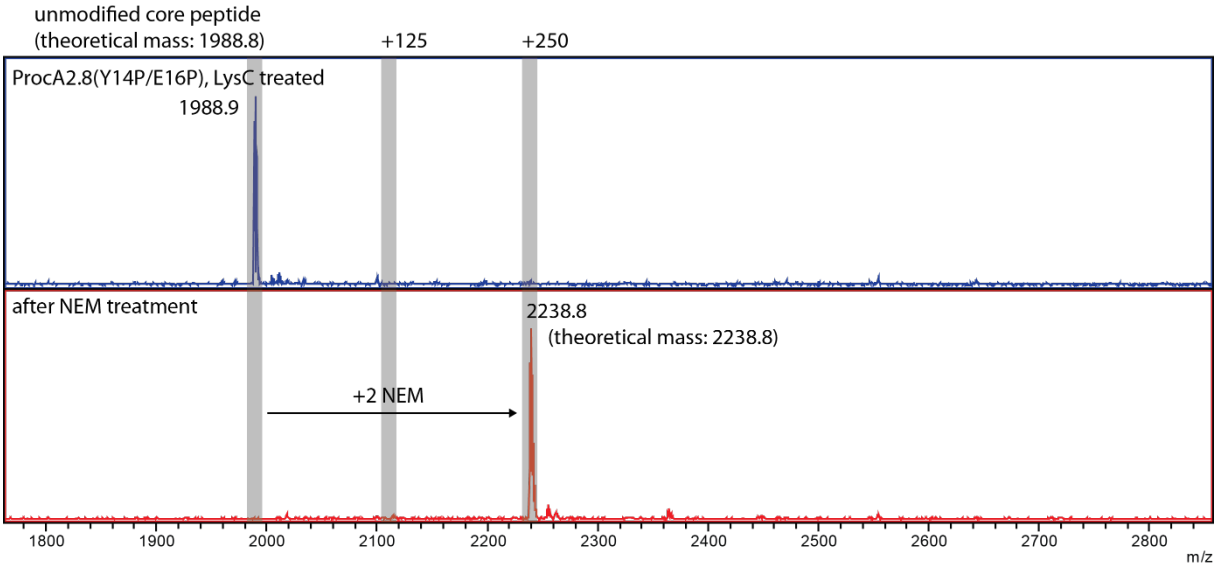


**Figure S32.** MALDI-TOF-MS analysis of LysC treated ProcA2.8(Y14P/E16P) before (blue) and after NEM treatment (red). Every mass region that corresponds to core peptide or NEM adducts thereof is highlighted in a gray box.

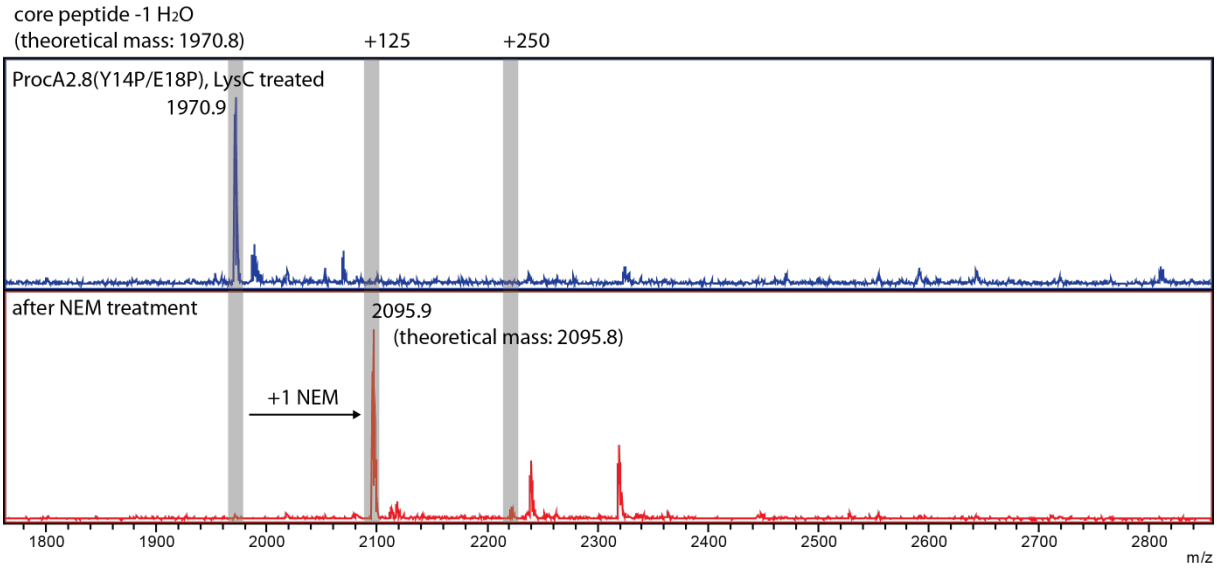


**Figure S33.** MALDI-TOF-MS analysis of LysC treated ProcA2.8(Y14P/E18P) before (blue) and after NEM treatment (red). Every mass region that corresponds to core peptide or NEM adducts thereof is highlighted in a gray box.

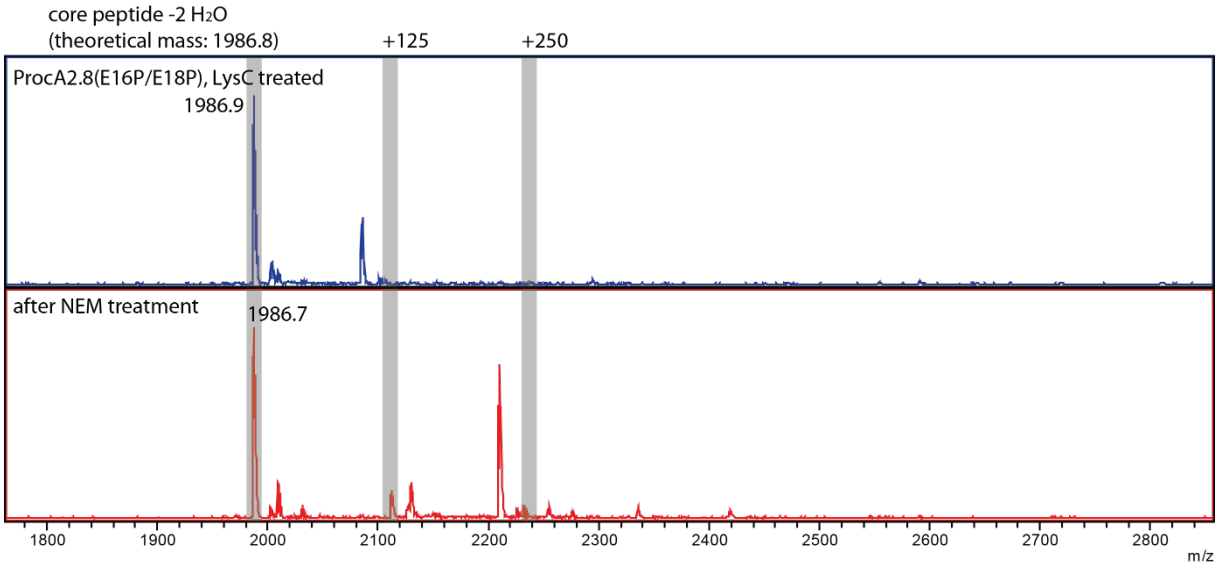


**Figure S34.** MALDI-TOF-MS analysis of LysC treated ProcA2.8(E16P/E18P) before (blue) and after NEM treatment (red). Every mass region that corresponds to core peptide or NEM adducts thereof is highlighted in a gray box.

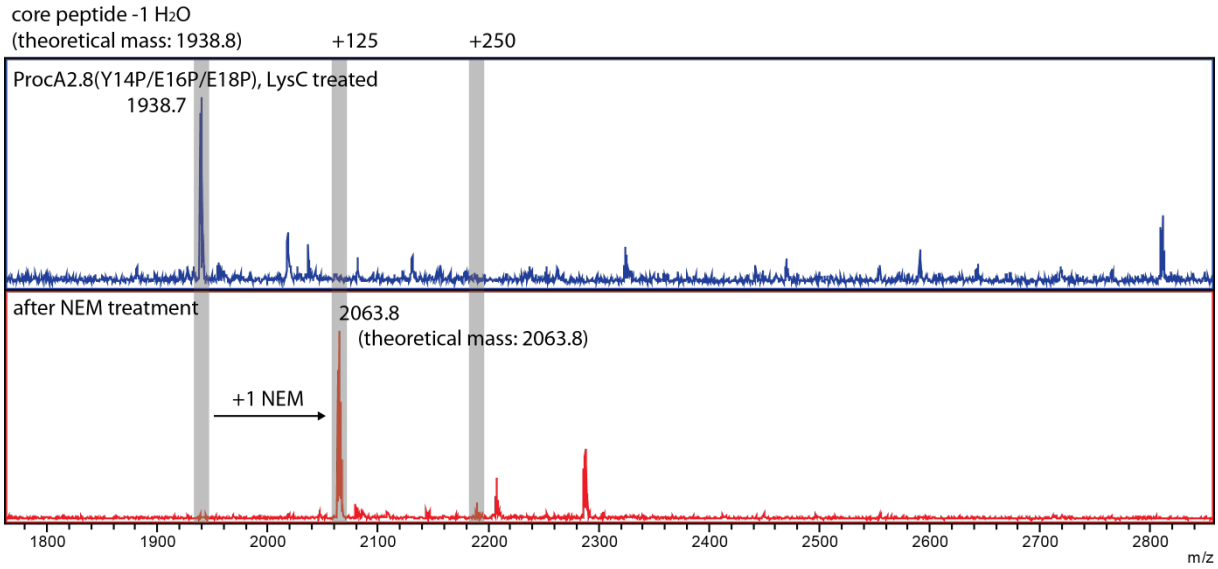


**Figure S35.** MALDI-TOF-MS analysis of LysC treated ProcA2.8(Y14P/E16P/E18P) before (blue) and after NEM treatment (red). Every mass region that corresponds to core peptide or NEM adducts thereof is highlighted in a gray box.

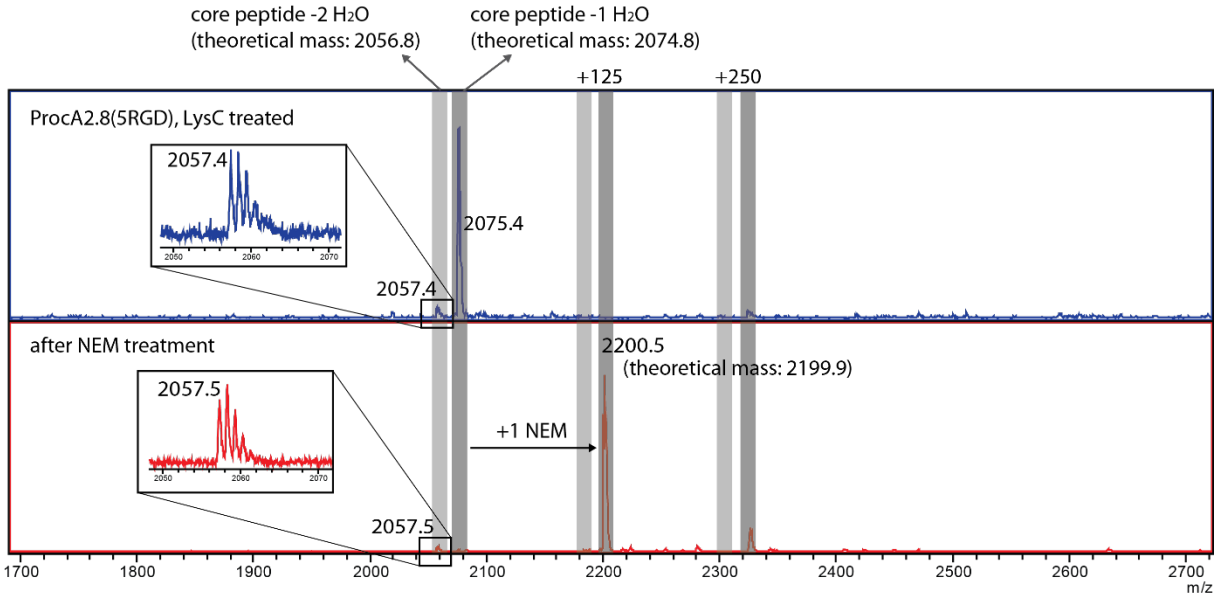


**Figure S36.** MALDI-TOF-MS analysis of LysC treated ProcA2.8(5RGD) before (blue) and after NEM treatment (red). Every mass region that corresponds to core peptide or NEM adducts thereof is highlighted in a gray box.

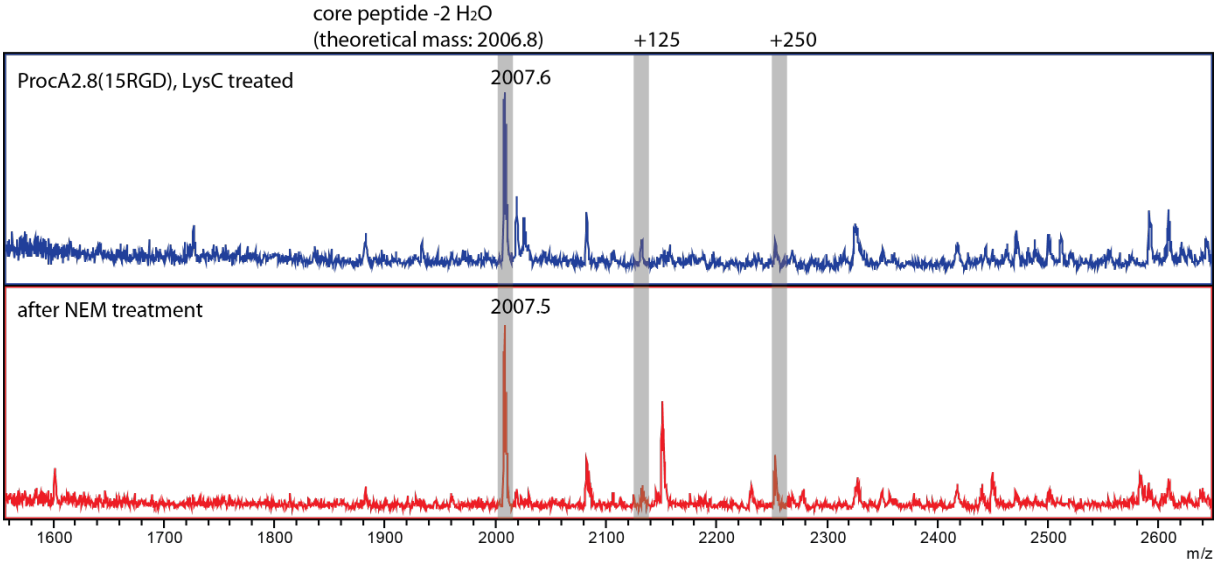


**Figure S37.** MALDI-TOF-MS analysis of LysC treated ProcA2.8(15RGD) before (blue) and after NEM treatment (red). Every mass region that corresponds to core peptide or NEM adducts thereof is highlighted in a gray box.

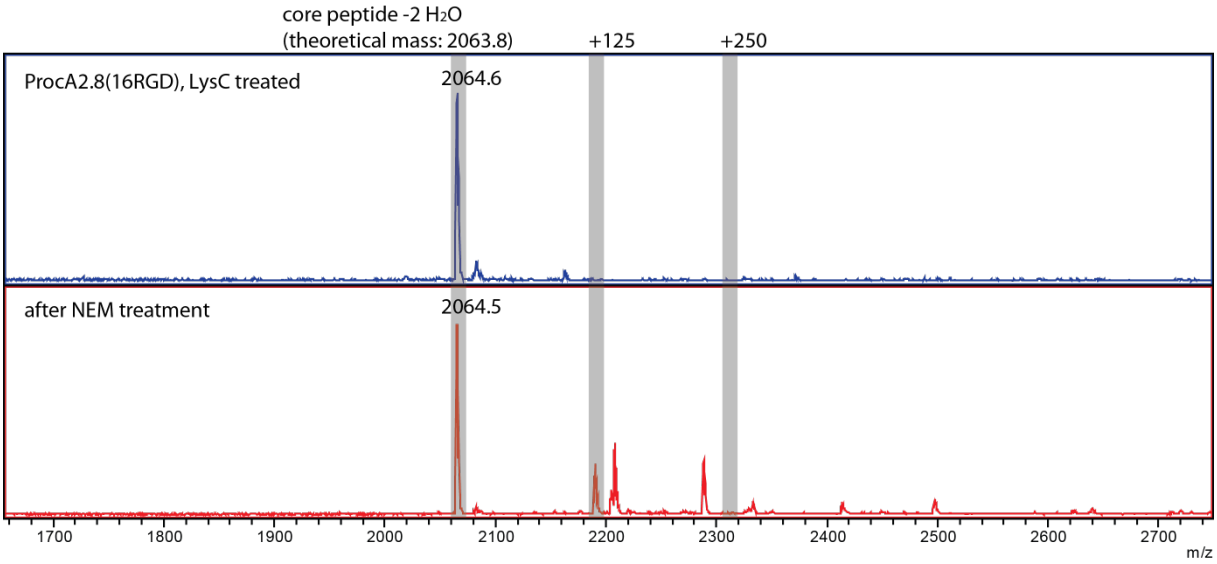


**Figure S38.** MALDI-TOF-MS analysis of LysC treated ProcA2.8(16RGD) before (blue) and after NEM treatment (red). Every mass region that corresponds to core peptide or NEM adducts thereof is highlighted in a gray box.

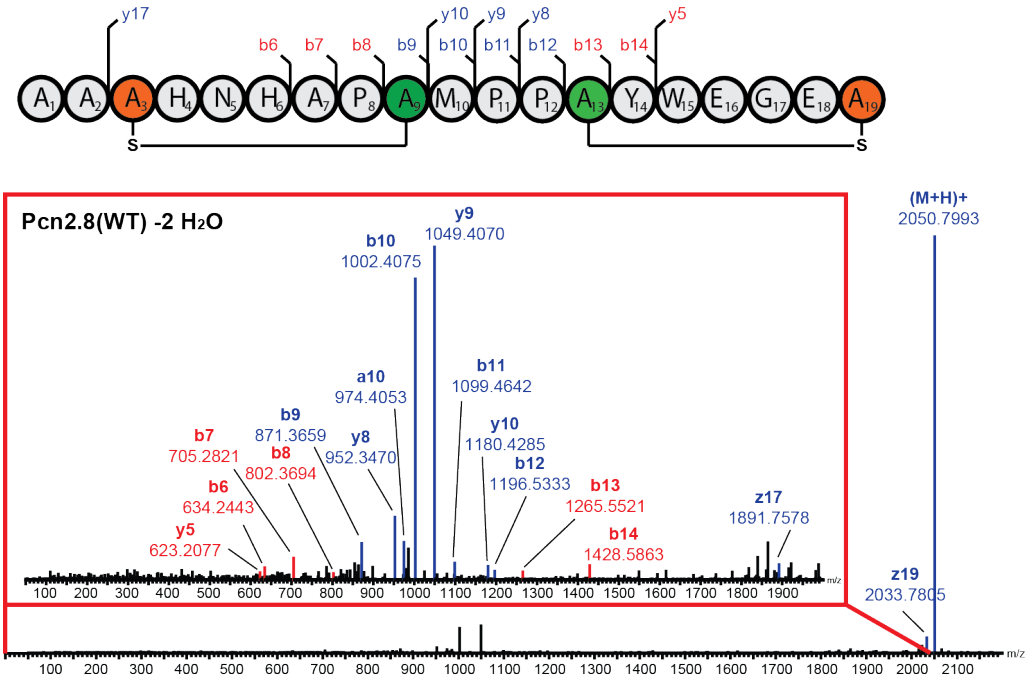


**Figure S39a.** MS$^2$ spectra of Pcn2.8(WT) −2 $H_2O$. The red insert is a magnification of the indicated part of the spectrum shown at the bottom. Identified fragment ions are highlighted: Fragment ions resulting from fragmentation outside of lanthionine rings are colored in blue. Minor fragment ions that likely arise from the presence of trace amounts of non- or partially cyclized peptides are highlighted in red.

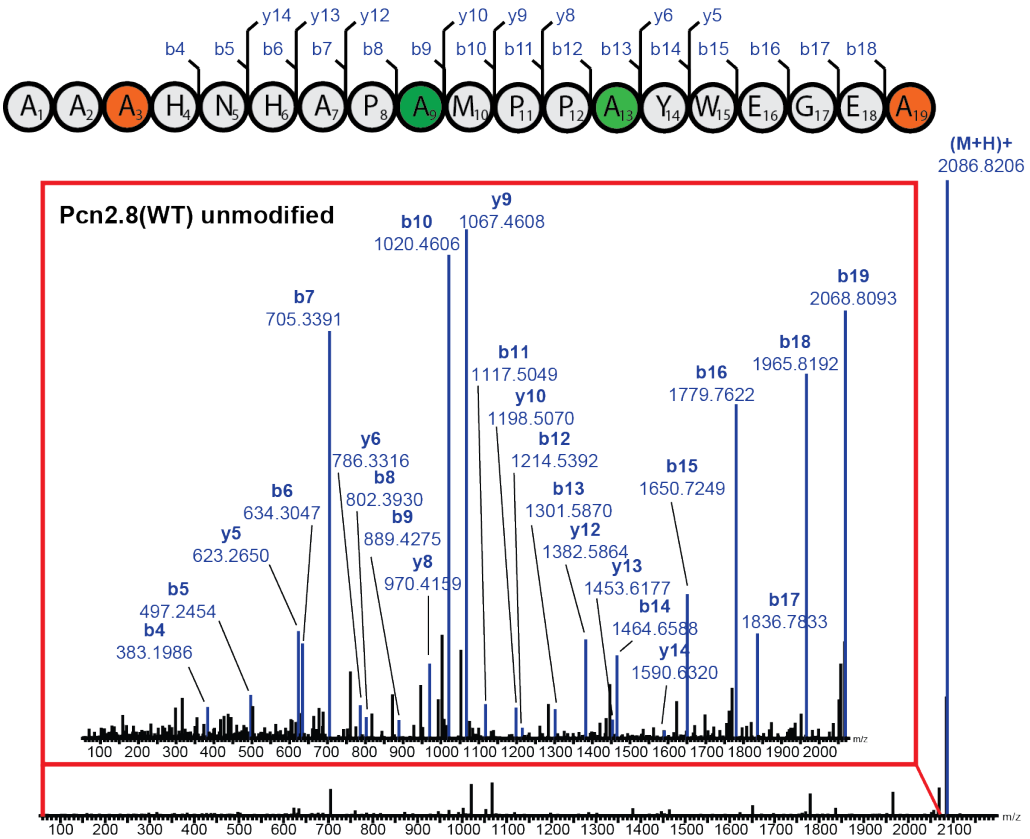


**Figure S39b.** MS$^2$ spectra of an unmodified Pcn2.8(WT) control. The red insert is a magnification of the indicated part of the spectrum shown at the bottom. Identified fragment ions are highlighted in blue.

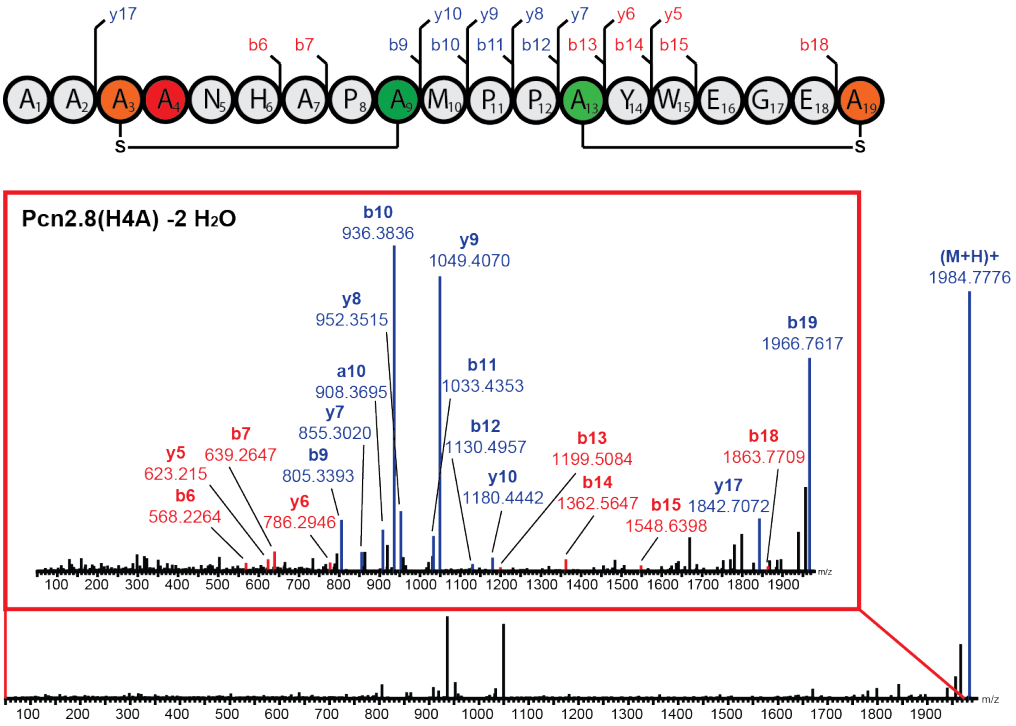


**Figure S40.** MS$^2$ spectra of Pcn2.8(H4A) −2 $H_2O$. The red insert is a magnification of the indicated part of the spectrum shown at the bottom. Identified fragment ions are highlighted: Fragment ions resulting from fragmentation outside of lanthionine rings are colored in blue. Minor fragment ions that likely arise from the presence of trace amounts of non- or partially cyclized peptides are highlighted in red.

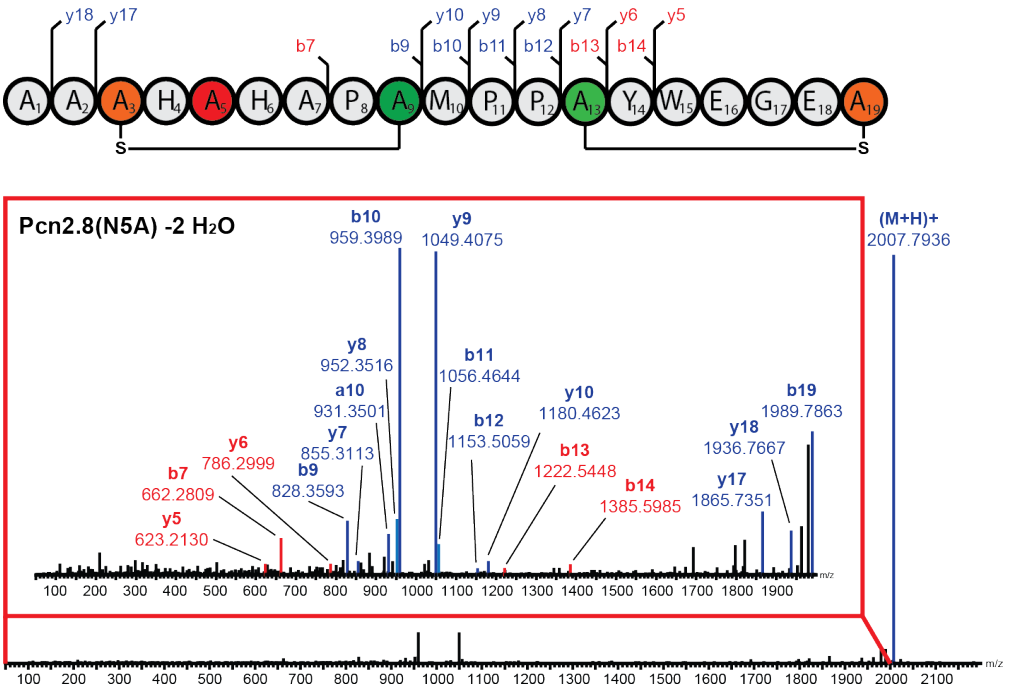


**Figure S41.** MS$^2$ spectra of Pcn2.8(N5A) −2 $H_2O$. The red insert is a magnification of the indicated part of the spectrum shown at the bottom. Identified fragment ions are highlighted: Fragment ions resulting from fragmentation outside of lanthionine rings are colored in blue. Minor fragment ions that likely arise from the presence of trace amounts of non- or partially cyclized peptides are highlighted in red.

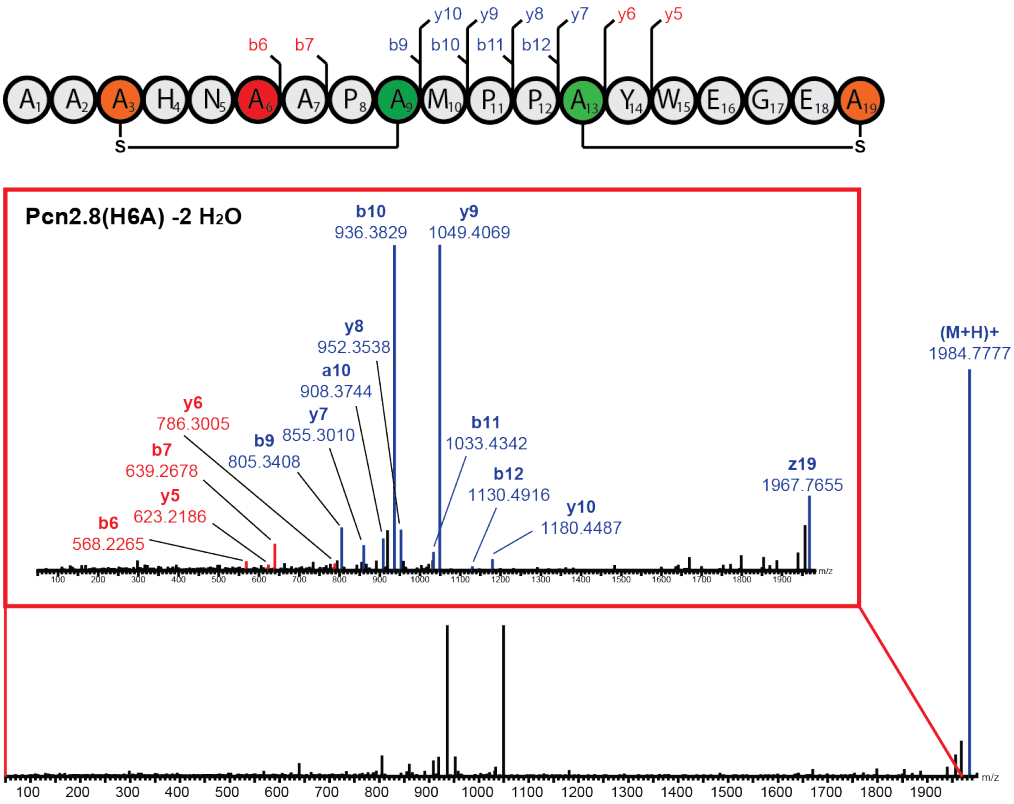


**Figure S42.** MS$^2$ spectra of Pcn2.8(H6A) −2 $H_2O$. The red insert is a magnification of the indicated part of the spectrum shown at the bottom. Identified fragment ions are highlighted: Fragment ions resulting from fragmentation outside of lanthionine rings are colored in blue. Minor fragment ions that likely arise from the presence of trace amounts of non- or partially cyclized peptides are highlighted in red.

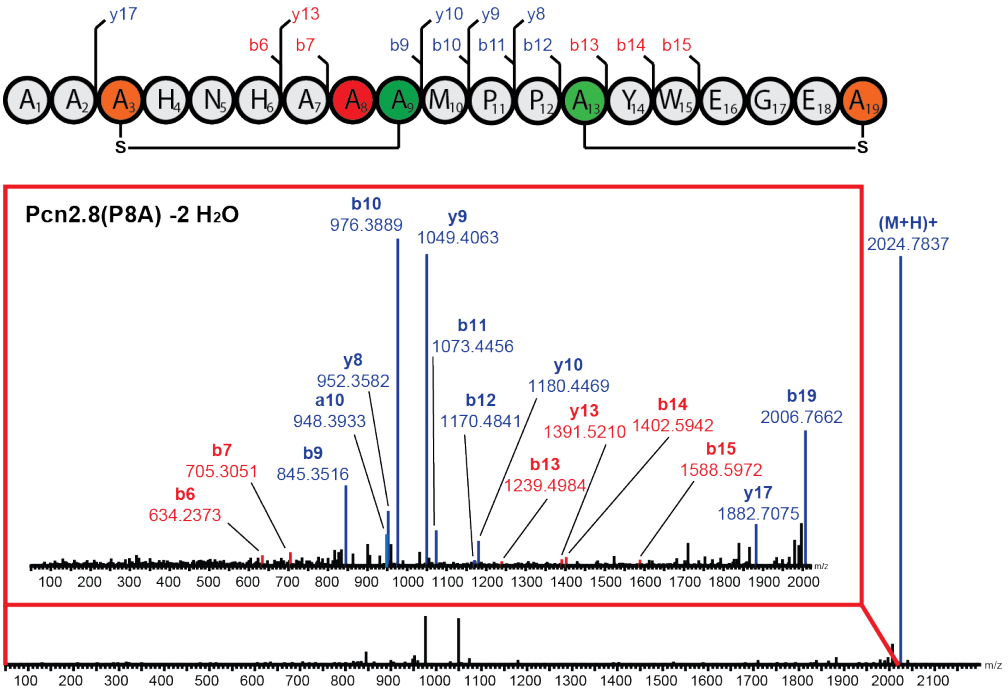


**Figure S43.** MS$^2$ spectra of Pcn2.8(P8A) −2 $H_2O$. The red insert is a magnification of the indicated part of the spectrum shown at the bottom. Identified fragment ions are highlighted: Fragment ions resulting from fragmentation outside of lanthionine rings are colored in blue. Minor fragment ions that likely arise from the presence of trace amounts of non- or partially cyclized peptides are highlighted in red.

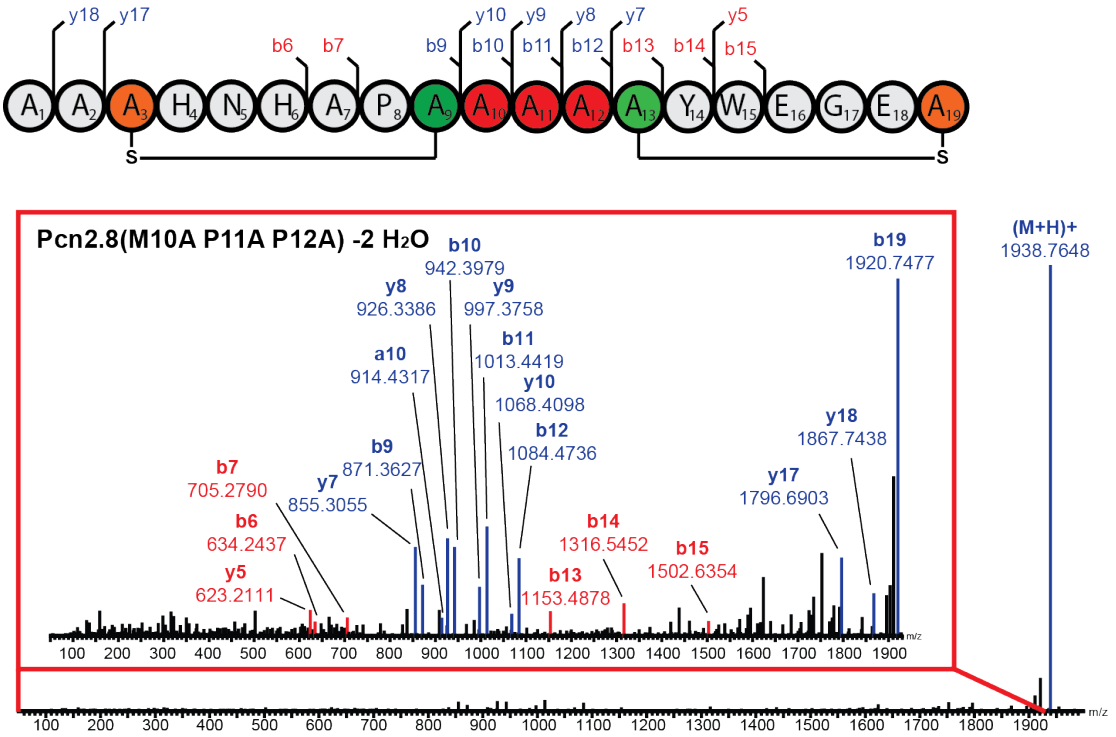


**Figure S44.** MS$^2$ spectra of Pcn2.8(M10A/P11A/P12A) −2 $H_2O$. The red insert is a magnification of the indicated part of the spectrum shown at the bottom. Identified fragment ions are highlighted: Fragment ions resulting from fragmentation outside of lanthionine rings are colored in blue. Minor fragment ions that likely arise from the presence of trace amounts of non- or partially cyclized peptides are highlighted in red.

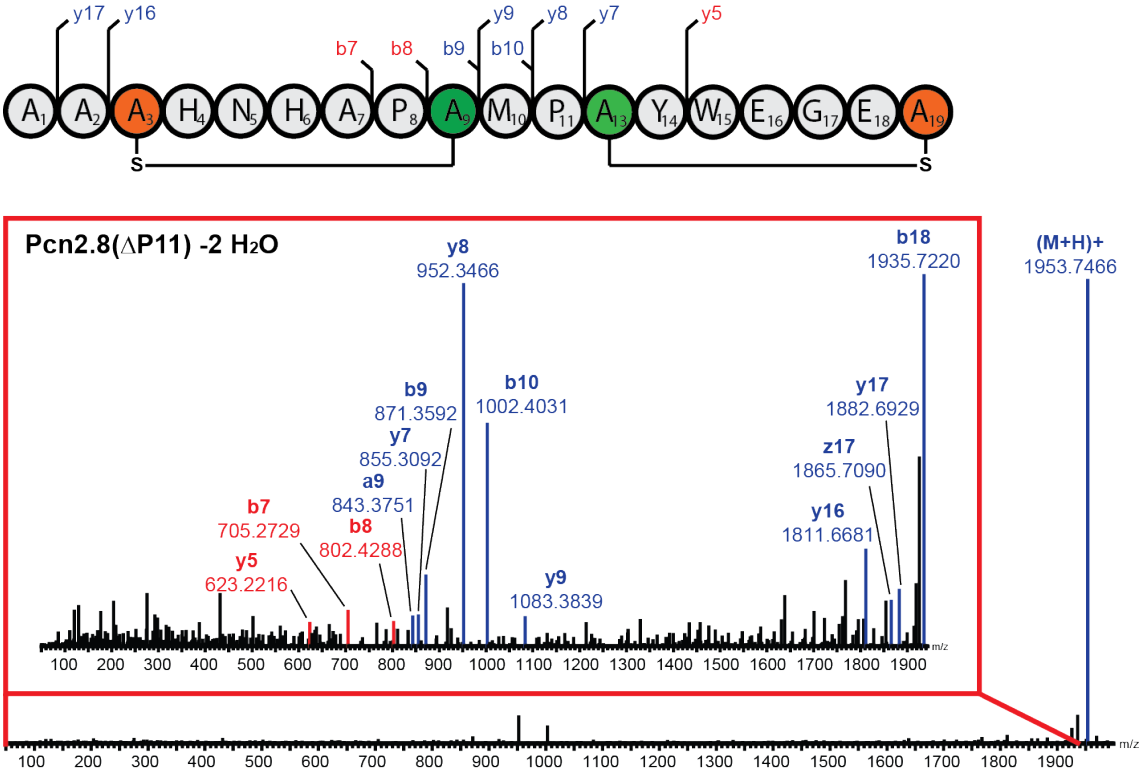


**Figure S45.** MS$^2$ spectra of Pcn2.8(ΔP11) −2 $H_2O$. The red insert is a magnification of the indicated part of the spectrum shown at the bottom. Identified fragment ions are highlighted: Fragment ions resulting from

fragmentation outside of lanthionine rings are colored in blue. Minor fragment ions that likely arise from the presence of trace amounts of non- or partially cyclized peptides are highlighted in red.

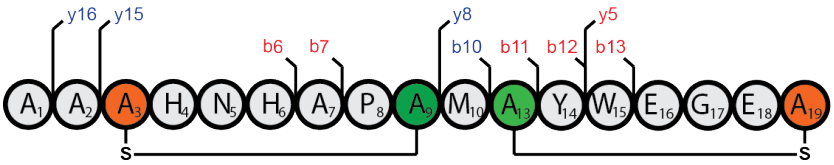


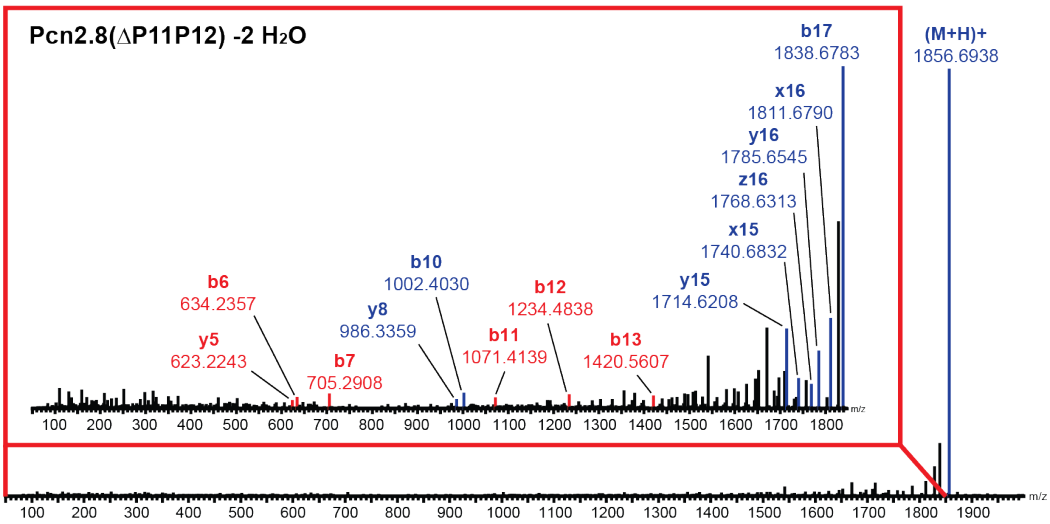


**Figure S46.** MS$^2$ spectra of Pcn2.8(ΔP11P12) −2 $H_2O$. The red insert is a magnification of the indicated part of the spectrum shown at the bottom. Identified fragment ions are highlighted: Fragment ions resulting from fragmentation outside of lanthionine rings are colored in blue. Minor fragment ions that likely arise from the presence of trace amounts of non- or partially cyclized peptides are highlighted in red.

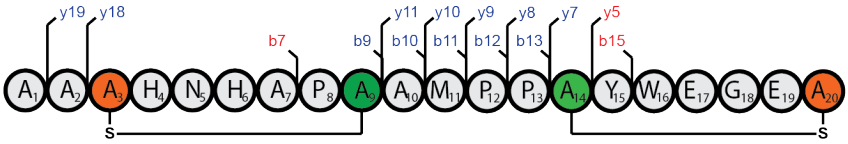


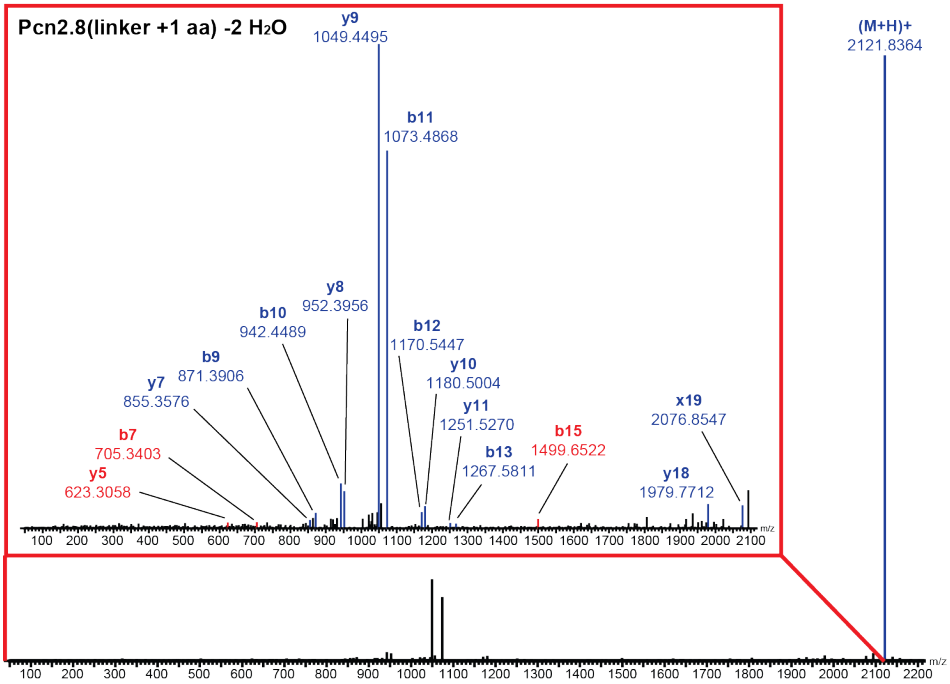

**Figure S47.** $MS^2$ spectra of Pcn2.8(linker +1 aa) −2 $H_2O$. The red insert is a magnification of the indicated part of the spectrum shown at the bottom. Identified fragment ions are highlighted: Fragment ions resulting from fragmentation outside of lanthionine rings are colored in blue. Minor fragment ions that likely arise from the presence of trace amounts of non- or partially cyclized peptides are highlighted in red.

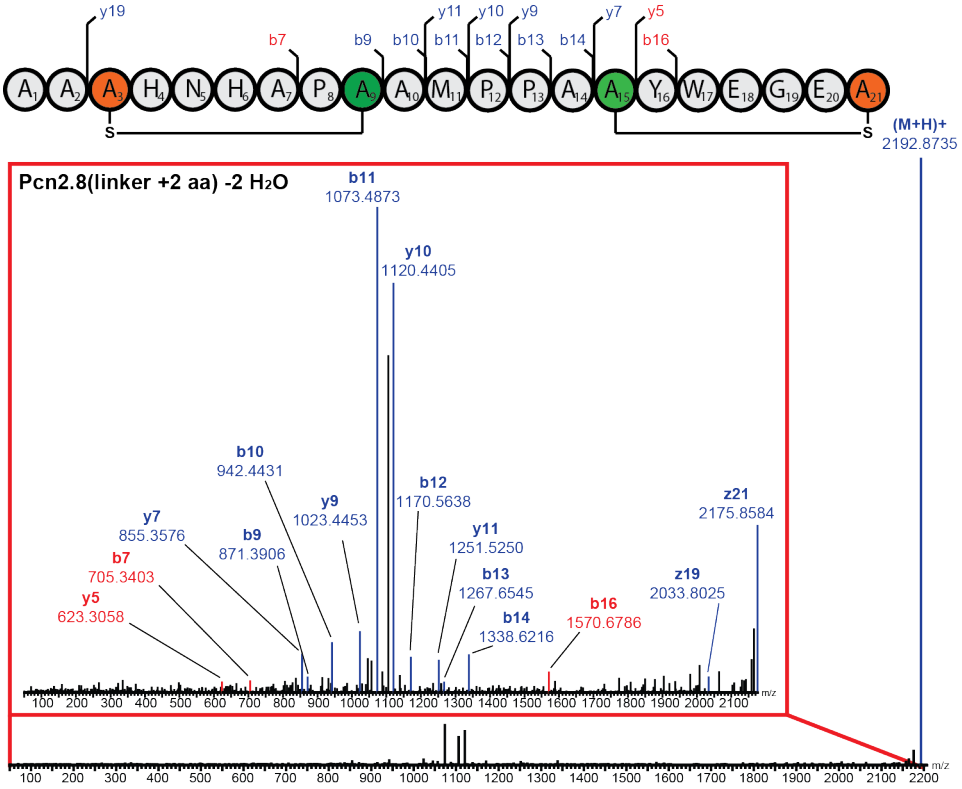


**Figure S48.** $MS^2$ spectra of Pcn2.8(linker +2 aa) −2 $H_2O$. The red insert is a magnification of the indicated part of the spectrum shown at the bottom. Identified fragment ions are highlighted: Fragment ions resulting from fragmentation outside of lanthionine rings are colored in blue. Minor fragment ions that likely arise from the presence of trace amounts of non- or partially cyclized peptides are highlighted in red.

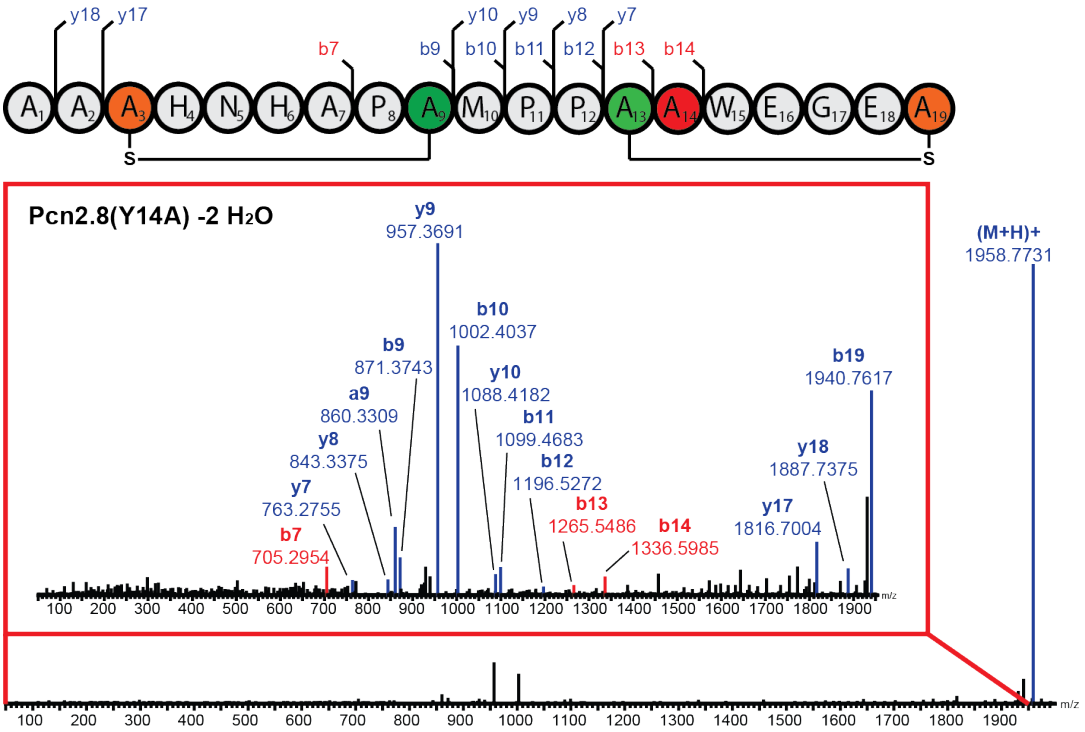


**Figure S49.** MS$^2$ spectra of Pcn2.8(Y14A) −2 $H_2O$. The red insert is a magnification of the indicated part of the spectrum shown at the bottom. Identified fragment ions are highlighted: Fragment ions resulting from fragmentation outside of lanthionine rings are colored in blue. Minor fragment ions that likely arise from the presence of trace amounts of non- or partially cyclized peptides are highlighted in red.

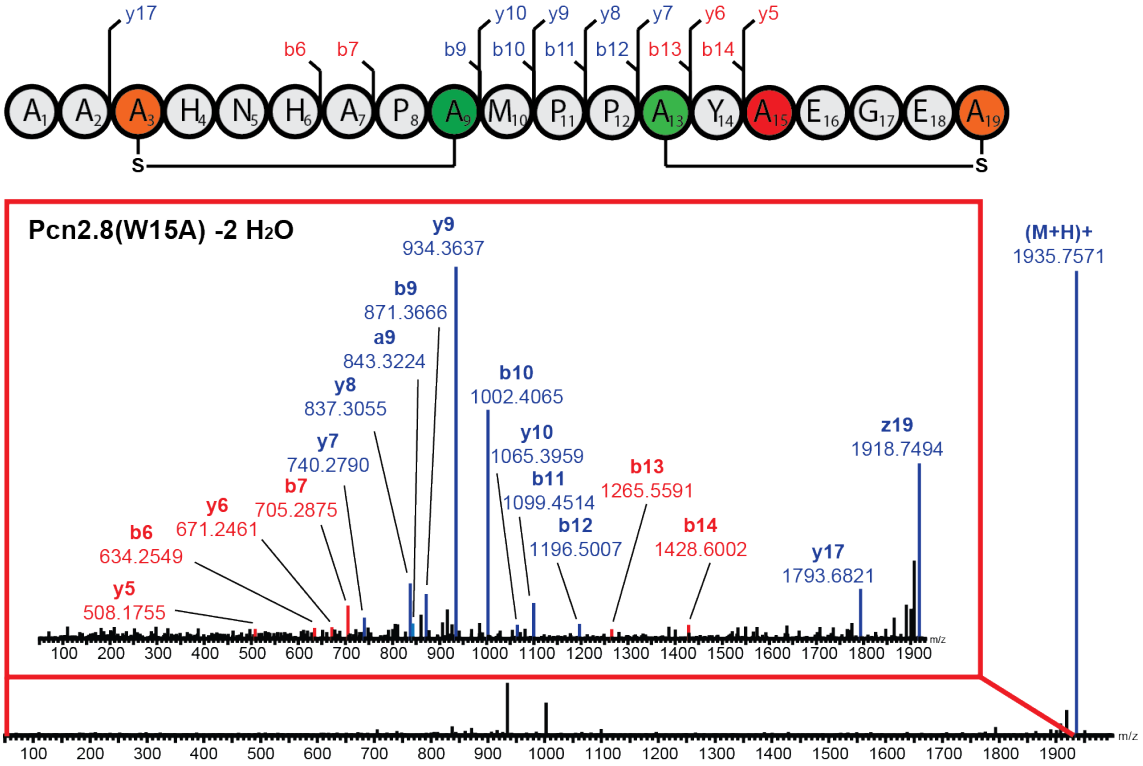


**Figure S50.** MS$^2$ spectra of Pcn2.8(W15A) −2 $H_2O$. The red insert is a magnification of the indicated part of the spectrum shown at the bottom. Identified fragment ions are highlighted: Fragment ions resulting from fragmentation outside of lanthionine rings are colored in blue. Minor fragment ions that likely arise from the presence of trace amounts of non- or partially cyclized peptides are highlighted in red.

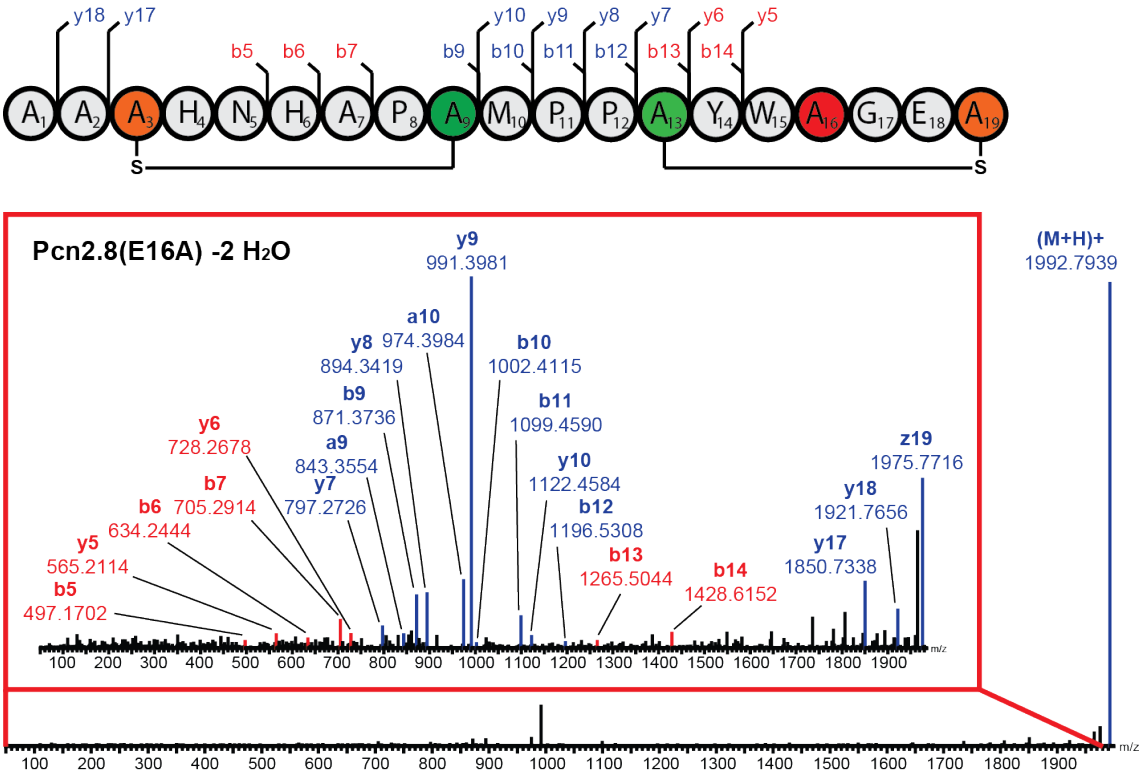


**Figure S51.** MS$^2$ spectra of Pcn2.8(E16A) −2 $H_2O$. The red insert is a magnification of the indicated part of the spectrum shown at the bottom. Identified fragment ions are highlighted: Fragment ions resulting from fragmentation outside of lanthionine rings are colored in blue. Minor fragment ions that likely arise from the presence of trace amounts of non- or partially cyclized peptides are highlighted in red.

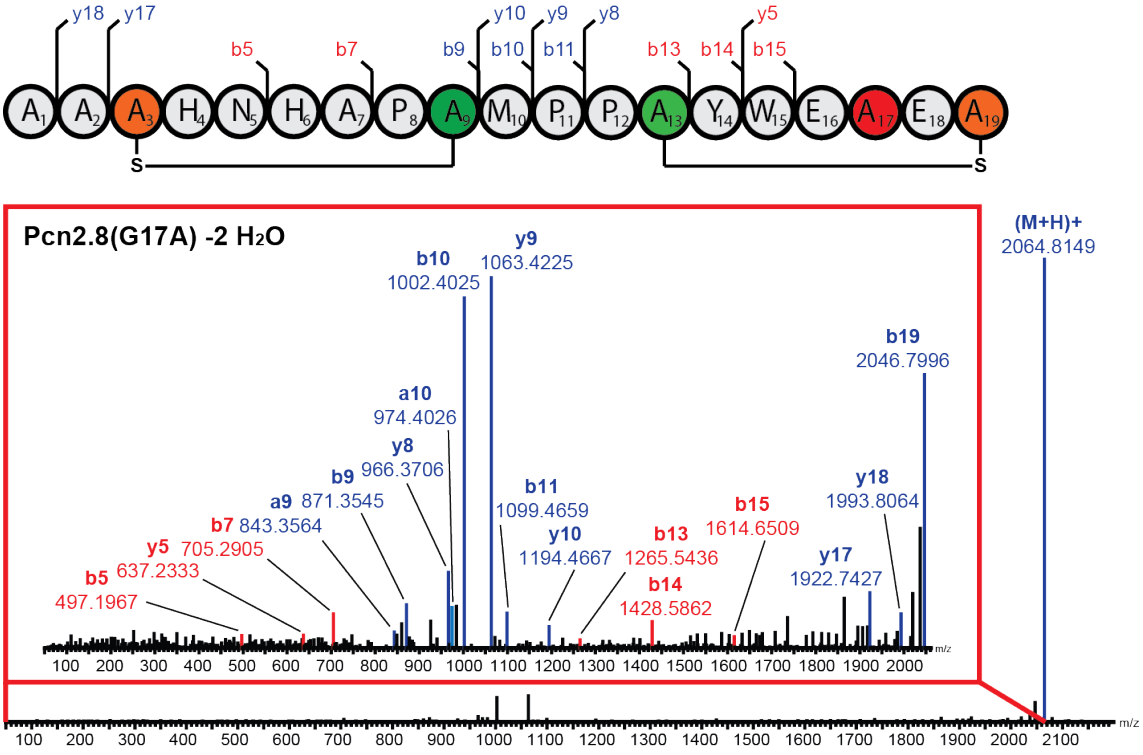


**Figure S52.** MS$^2$ spectra of Pcn2.8(G17A) −2 $H_2O$. The red insert is a magnification of the indicated part of the spectrum shown at the bottom. Identified fragment ions are highlighted: Fragment ions resulting from fragmentation outside of lanthionine rings are colored in blue. Minor fragment ions that likely arise from the presence of trace amounts of non- or partially cyclized peptides are highlighted in red.

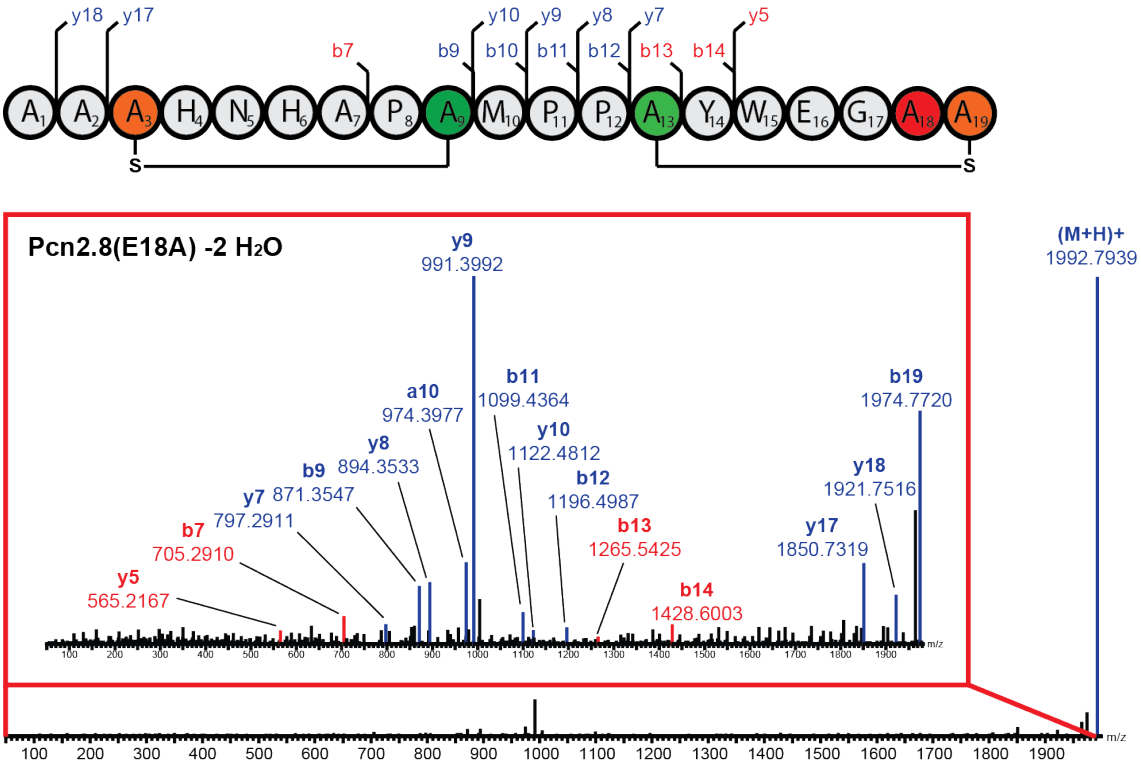


**Figure S53.** MS$^2$ spectra of Pcn2.8(E18A) −2 $H_2O$. The red insert is a magnification of the indicated part of the spectrum shown at the bottom. Identified fragment ions are highlighted: Fragment ions resulting from fragmentation outside of lanthionine rings are colored in blue. Minor fragment ions that likely arise from the presence of trace amounts of non- or partially cyclized peptides are highlighted in red.

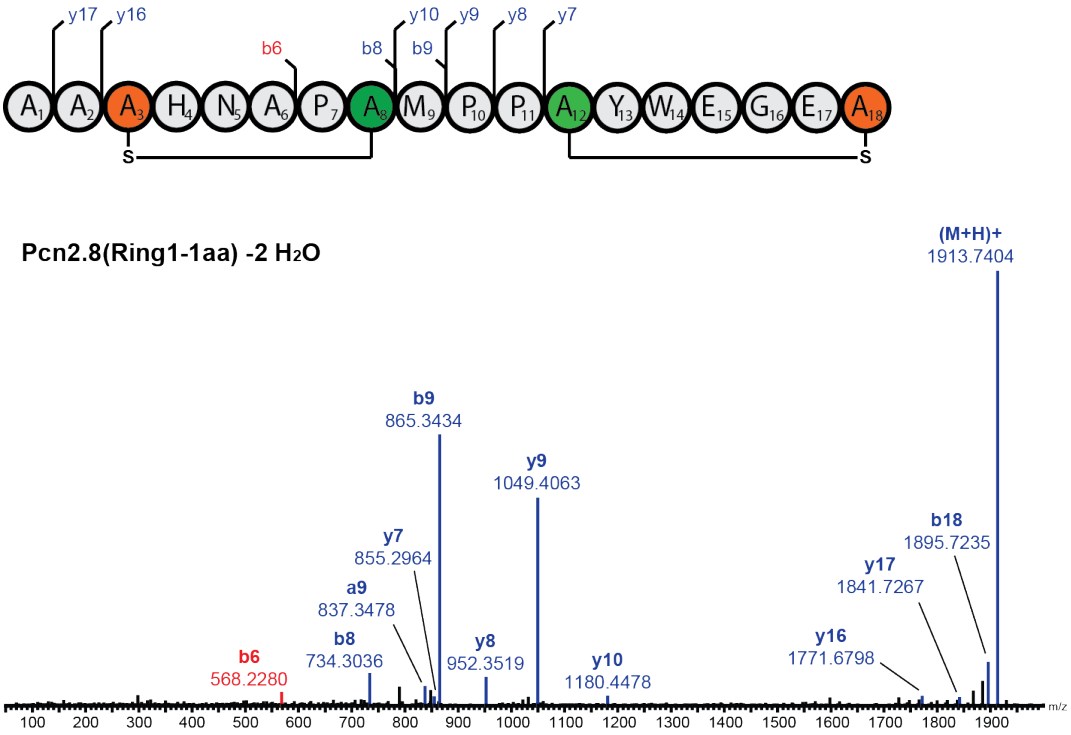


**Figure S54.** MS$^2$ spectra of Pcn2.8(Ring1−1aa) −2 $H_2O$. The red insert is a magnification of the indicated part of the spectrum shown at the bottom. Identified fragment ions are highlighted: Fragment ions resulting from fragmentation outside of lanthionine rings are colored in blue. Minor fragment ions that likely arise from the presence of trace amounts of non- or partially cyclized peptides are highlighted in red.

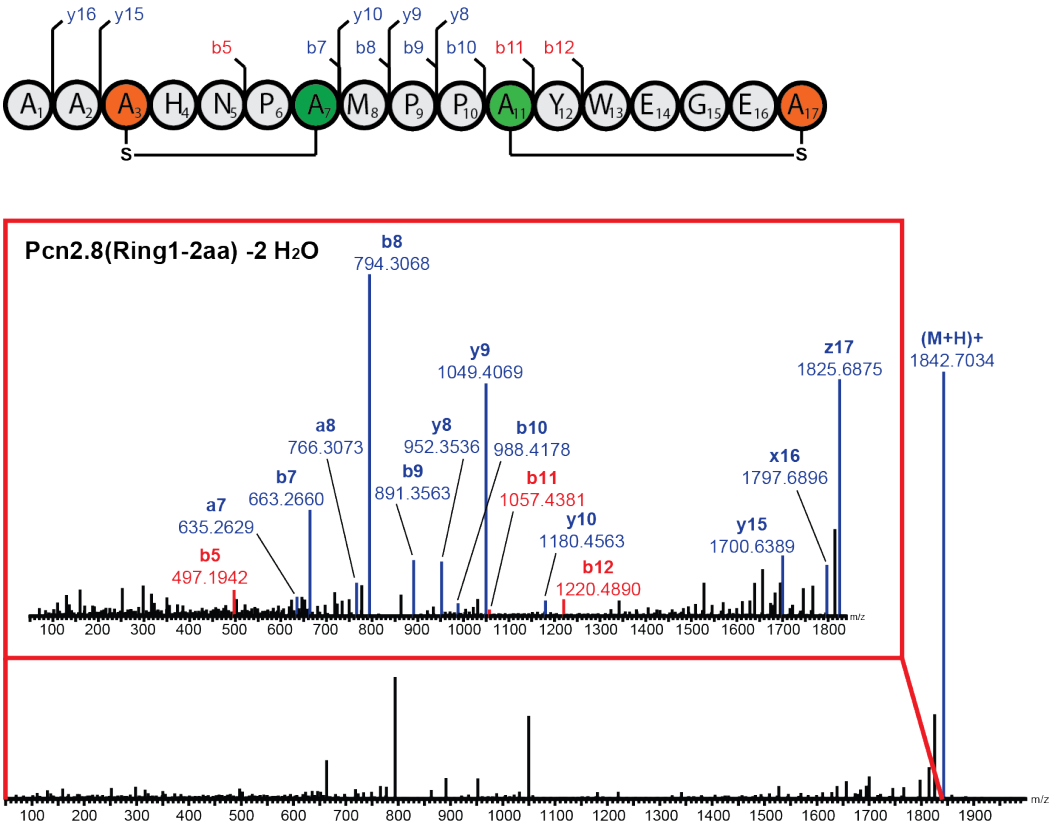


**Figure S55.** MS$^2$ spectra of Pcn2.8(Ring1−2aa) −2 $H_2O$. The red insert is a magnification of the indicated part of the spectrum shown at the bottom. Identified fragment ions are highlighted: Fragment ions resulting from fragmentation outside of lanthionine rings are colored in blue. Minor fragment ions that likely arise from the presence of trace amounts of non- or partially cyclized peptides are highlighted in red.

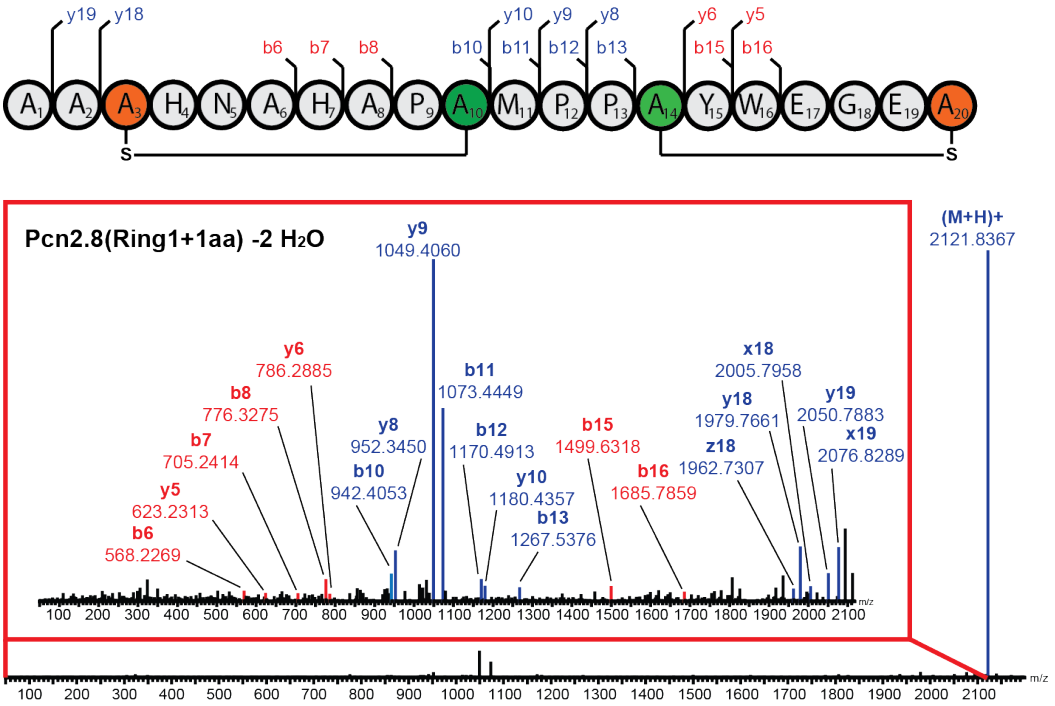


**Figure S56.** MS$^2$ spectra of Pcn2.8(Ring1+1aa) −2 $H_2O$. The red insert is a magnification of the indicated part of the spectrum shown at the bottom. Identified fragment ions are highlighted: Fragment ions resulting from fragmentation outside of lanthionine rings are colored in blue. Minor fragment ions that likely arise from the presence of trace amounts of non- or partially cyclized peptides are highlighted in red.

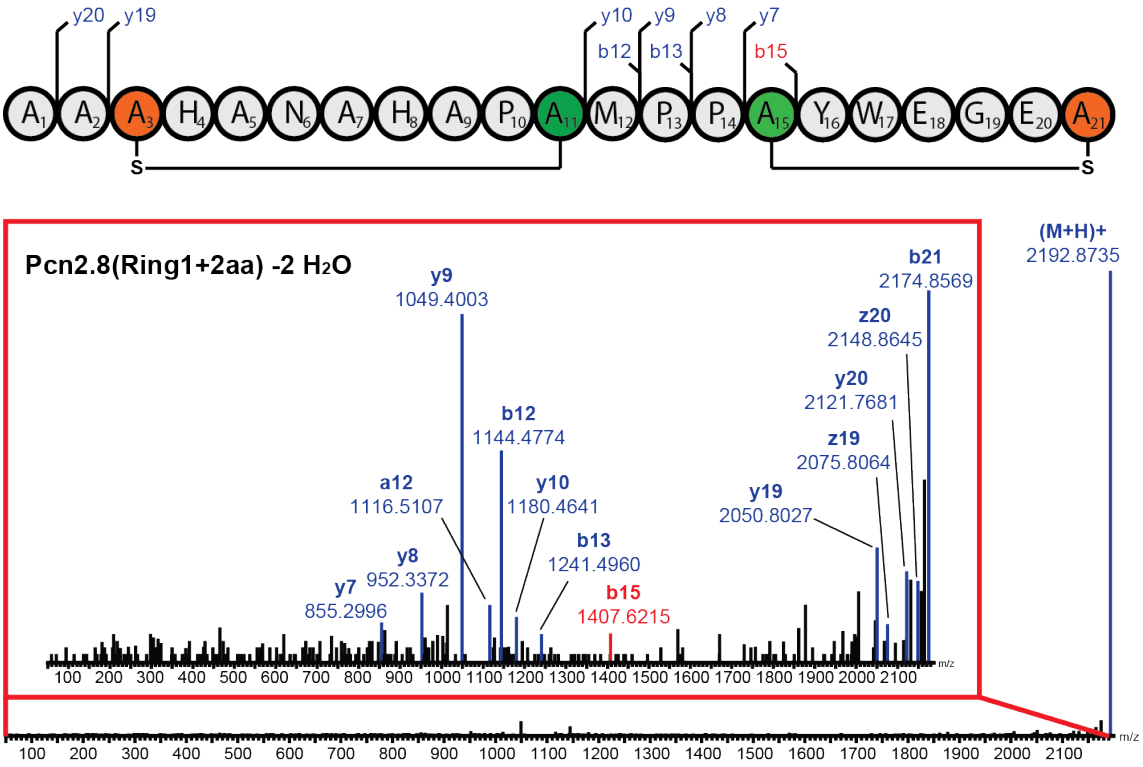


**Figure S57.** $MS^2$ spectra of Pcn2.8(Ring1+2aa) −2 $H_2O$. The red insert is a magnification of the indicated part of the spectrum shown at the bottom. Identified fragment ions are highlighted: Fragment ions resulting from fragmentation outside of lanthionine rings are colored in blue. Minor fragment ions that likely arise from the presence of trace amounts of non- or partially cyclized peptides are highlighted in red.

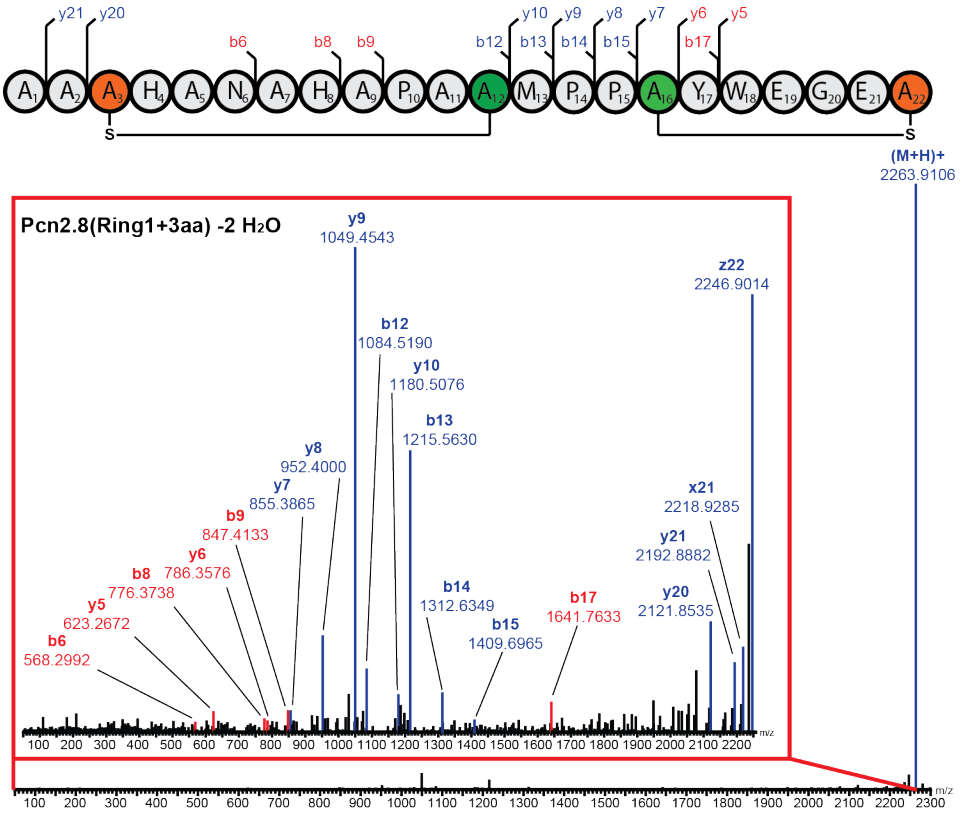


**Figure S58.** MS$^2$ spectra of Pcn2.8(Ring1+3aa) −2 $H_2O$. The red insert is a magnification of the indicated part of the spectrum shown at the bottom. Identified fragment ions are highlighted: Fragment ions resulting from fragmentation outside of lanthionine rings are colored in blue. Minor fragment ions that likely arise from the presence of trace amounts of non- or partially cyclized peptides are highlighted in red.

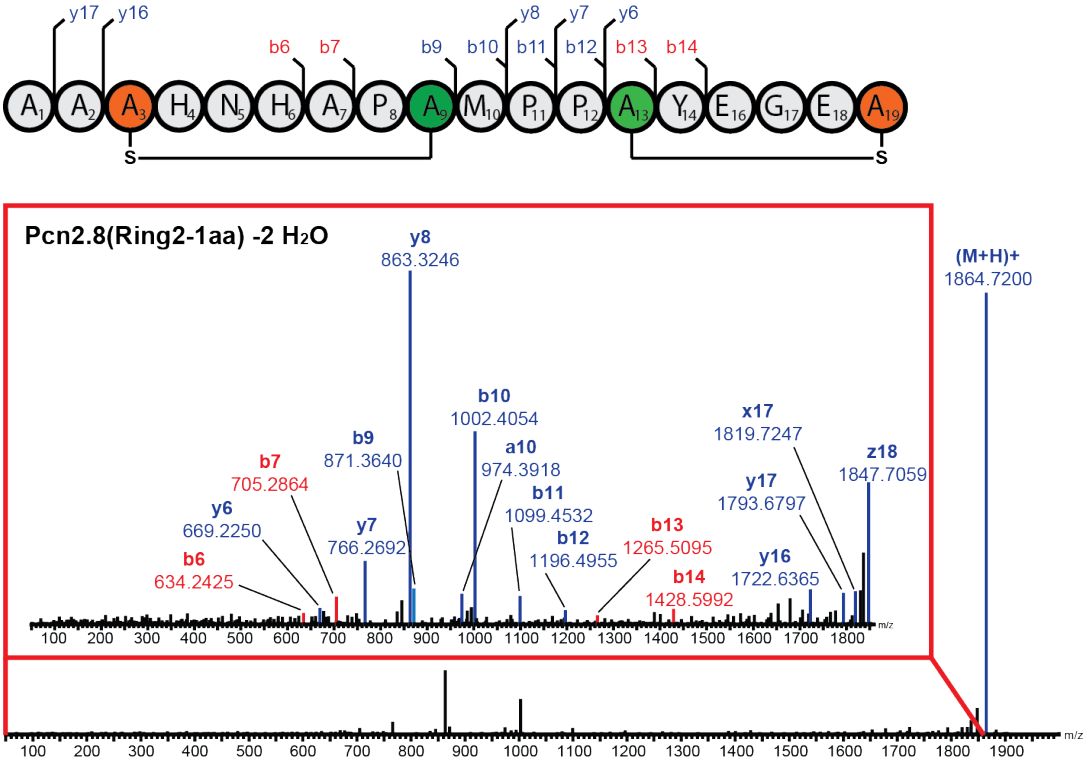


**Figure S59.** MS$^2$ spectra of Pcn2.8(Ring2−1aa) −2 $H_2O$. The red insert is a magnification of the indicated part of the spectrum shown at the bottom. Identified fragment ions are highlighted: Fragment ions resulting from

fragmentation outside of lanthionine rings are colored in blue. Minor fragment ions that likely arise from the presence of trace amounts of non- or partially cyclized peptides are highlighted in red.

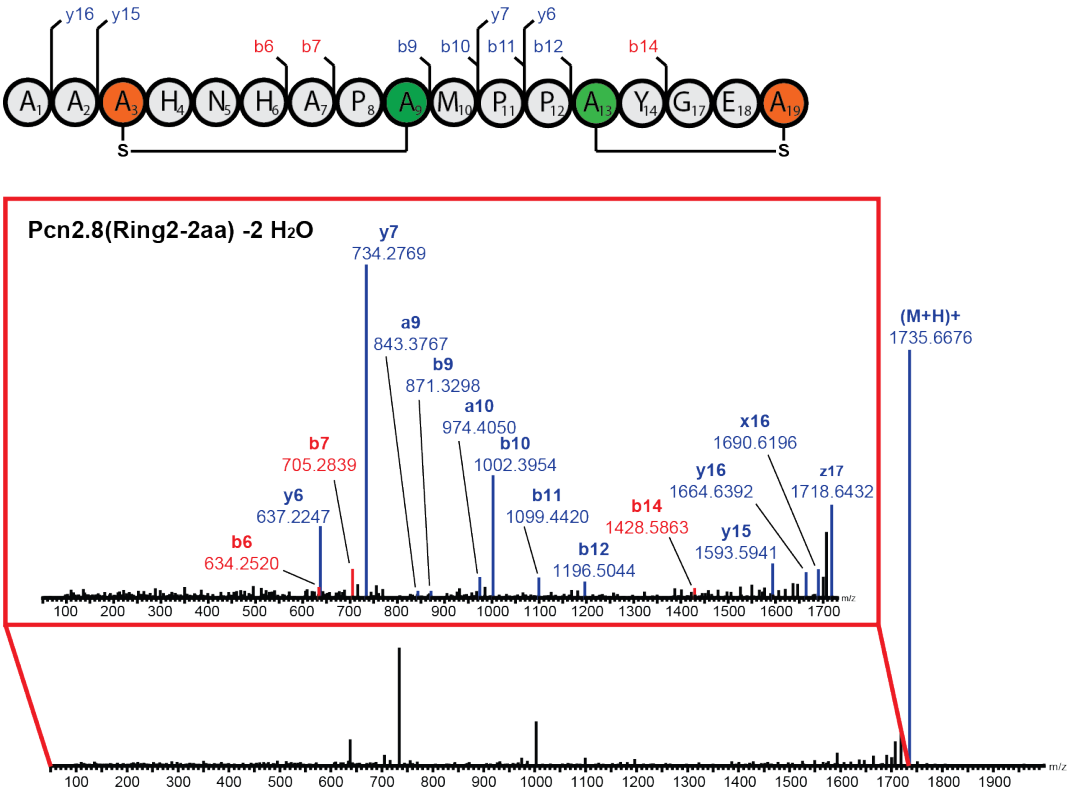


**Figure S60.** MS$^2$ spectra of Pcn2.8(Ring2−2aa) −2 $H_2O$. The red insert is a magnification of the indicated part of the spectrum shown at the bottom. Identified fragment ions are highlighted: Fragment ions resulting from fragmentation outside of lanthionine rings are colored in blue. Minor fragment ions that likely arise from the presence of trace amounts of non- or partially cyclized peptides are highlighted in red.

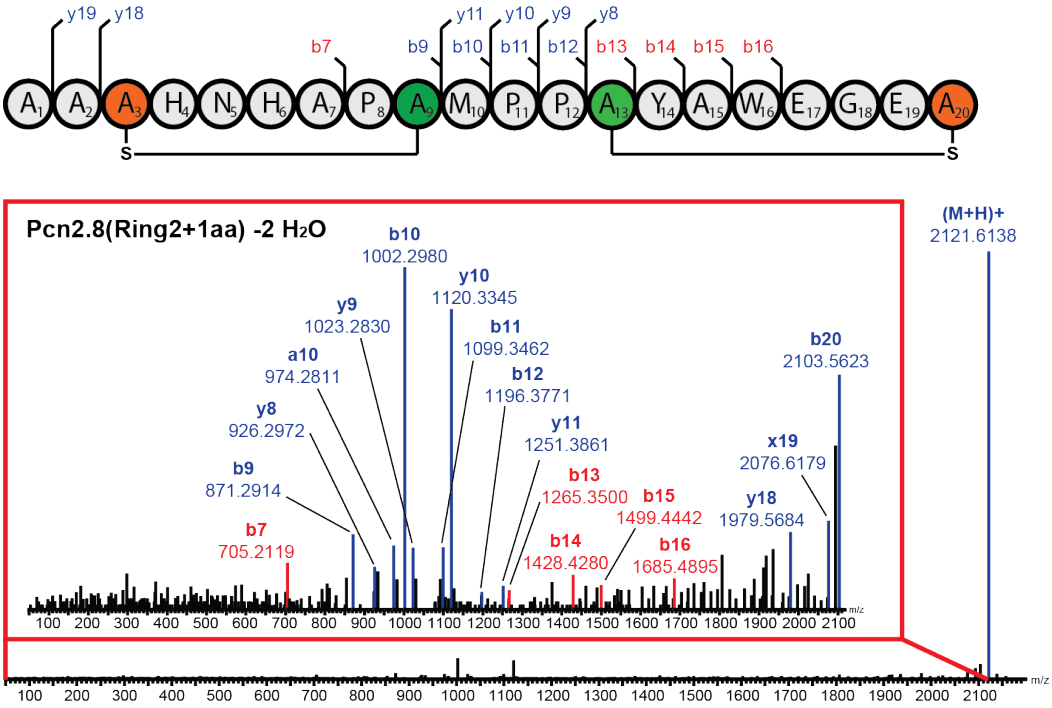


**Figure S61.** MS$^2$ spectra of Pcn2.8(Ring2+1aa) −2 $H_2O$. The red insert is a magnification of the indicated part of the spectrum shown at the bottom. Identified fragment ions are highlighted: Fragment ions resulting from

fragmentation outside of lanthionine rings are colored in blue. Minor fragment ions that likely arise from the presence of trace amounts of non- or partially cyclized peptides are highlighted in red.

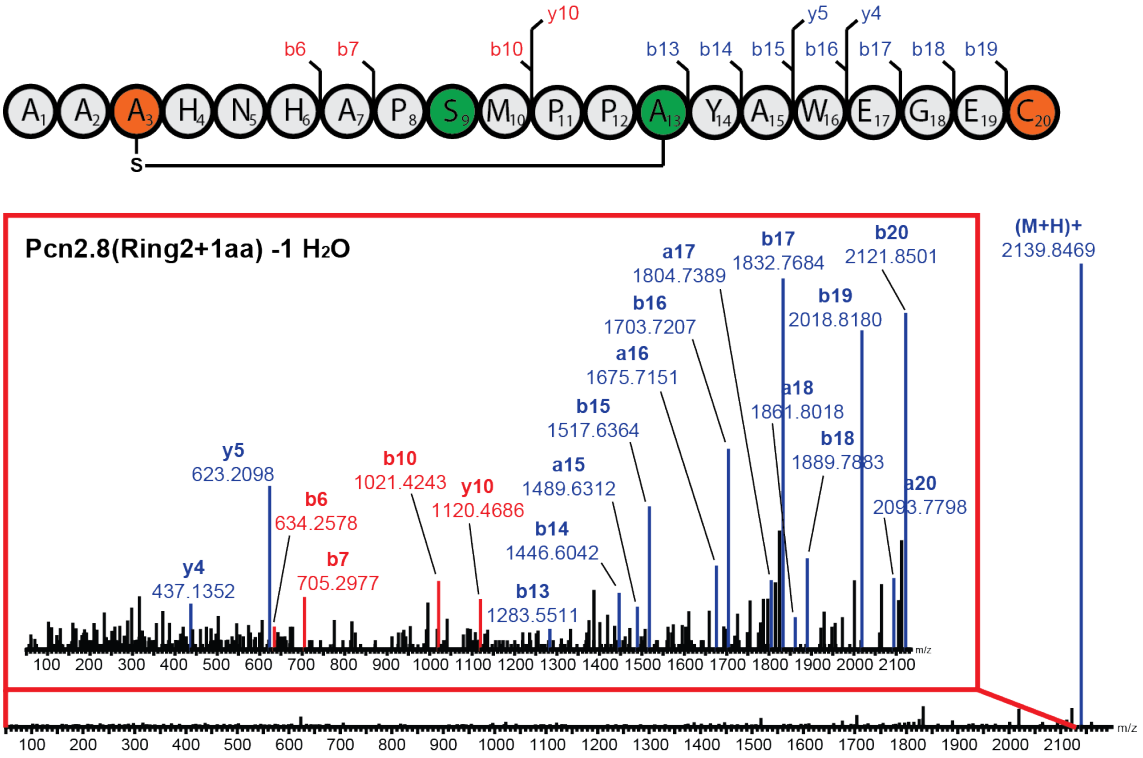


**Figure S62.** $MS^2$ spectra of Pcn2.8(Ring2+1aa) −1 $H_2O$. The red insert is a magnification of the indicated part of the spectrum shown at the bottom. Identified fragment ions are highlighted: Fragment ions resulting from fragmentation outside of lanthionine rings are colored in blue. Minor fragment ions that likely arise from the presence of trace amounts of non- or partially cyclized peptides are highlighted in red.

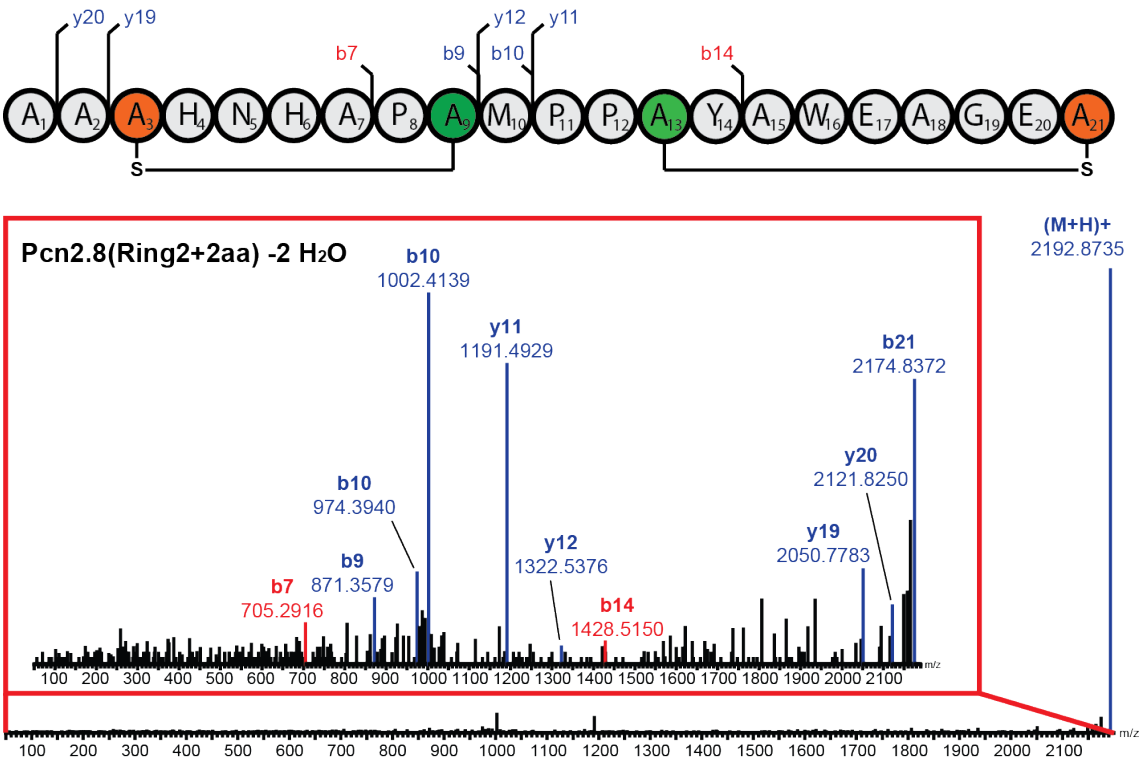

**Figure S63.** $MS^2$ spectra of Pcn2.8(Ring2+2aa) −2 $H_2O$. The red insert is a magnification of the indicated part of the spectrum shown at the bottom. Identified fragment ions are highlighted: Fragment ions resulting from fragmentation outside of lanthionine rings are colored in blue. Minor fragment ions that likely arise from the presence of trace amounts of non- or partially cyclized peptides are highlighted in red.

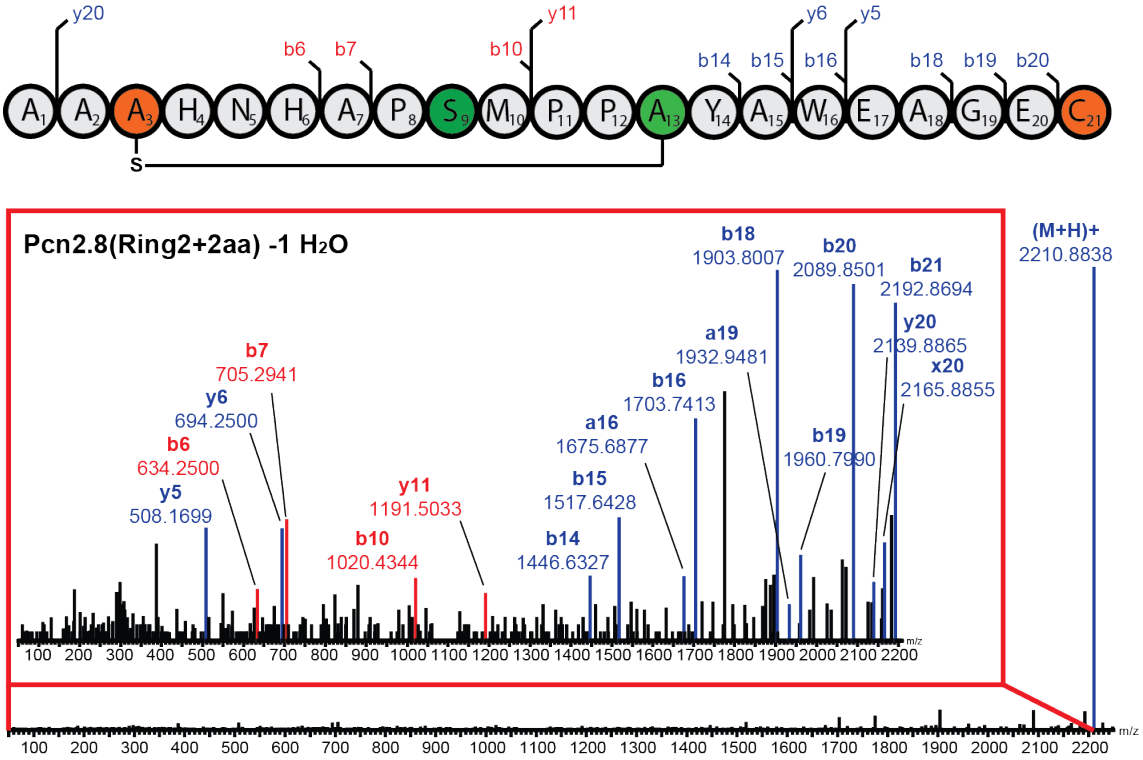


**Figure S64.** $MS^2$ spectra of Pcn2.8(Ring2+2aa) −1 $H_2O$. The red insert is a magnification of the indicated part of the spectrum shown at the bottom. Identified fragment ions are highlighted: Fragment ions resulting from fragmentation outside of lanthionine rings are colored in blue. Minor fragment ions that likely arise from the presence of trace amounts of non- or partially cyclized peptides are highlighted in red.

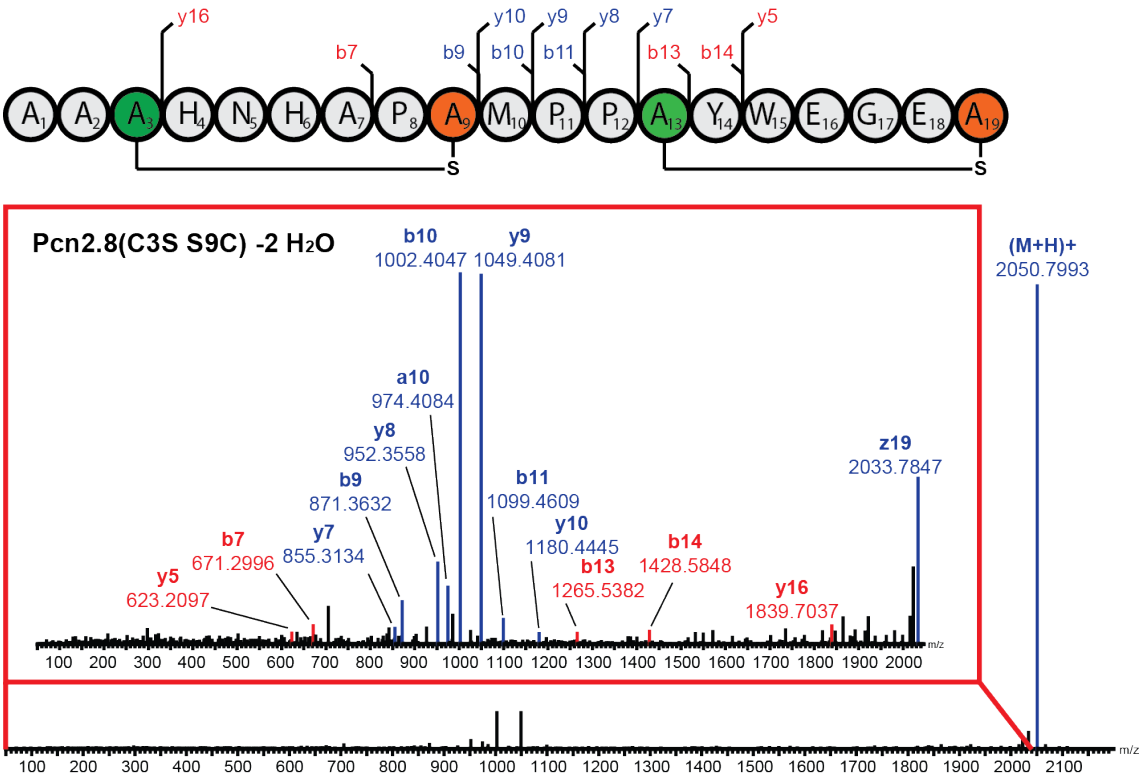

**Figure S65.** $MS^2$ spectra of Pcn2.8(C3S/S9C) −2 $H_2O$. The red insert is a magnification of the indicated part of the spectrum shown at the bottom. Identified fragment ions are highlighted: Fragment ions resulting from fragmentation outside of lanthionine rings are colored in blue. Minor fragment ions that likely arise from the presence of trace amounts of non- or partially cyclized peptides are highlighted in red.

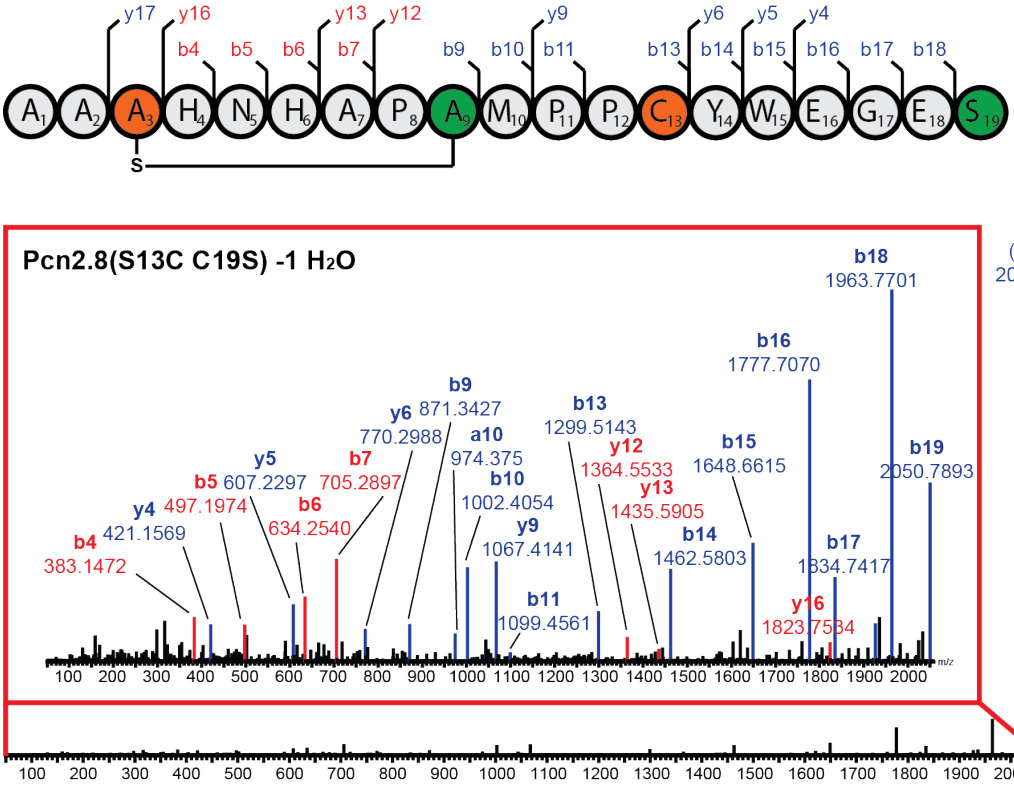


**Figure S66.** $MS^2$ spectra of Pcn2.8(S13C/C19S) −1 $H_2O$. The red insert is a magnification of the indicated part of the spectrum shown at the bottom. Identified fragment ions are highlighted: Fragment ions resulting from fragmentation outside of lanthionine rings are colored in blue. Minor fragment ions that likely arise from the presence of trace amounts of non- or partially cyclized peptides are highlighted in red.

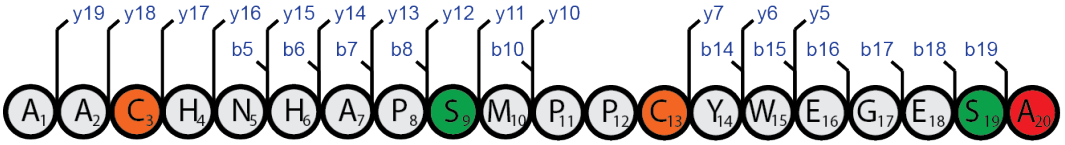

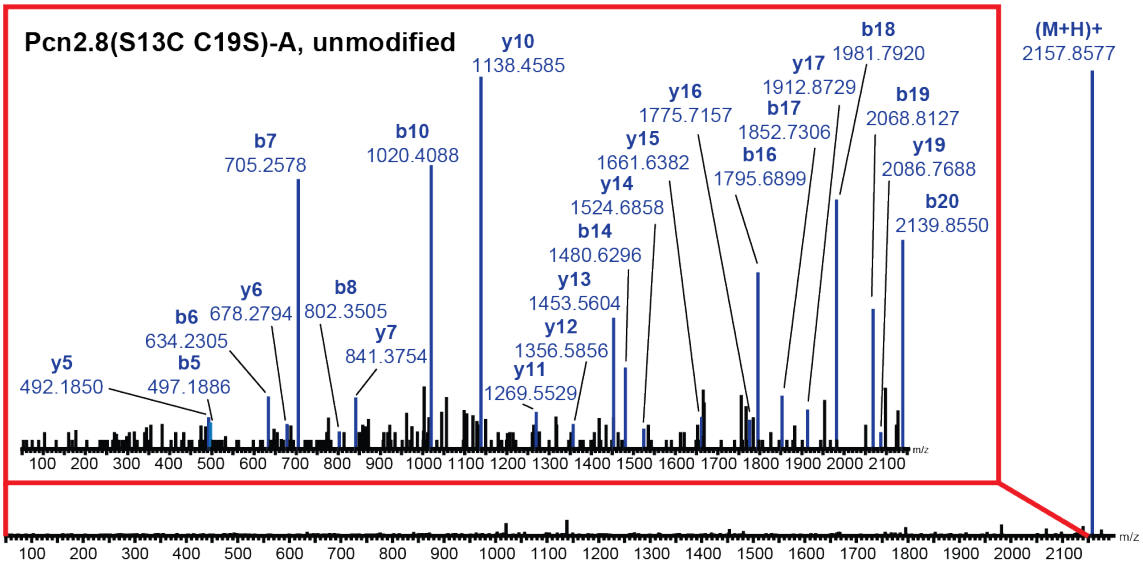

**Figure S67.** MS$^2$ spectra of Pcn2.8(S13C/C19S)-A (unmodified). The red insert is a magnification of the indicated part of the spectrum shown at the bottom. Identified fragment ions are highlighted in blue.

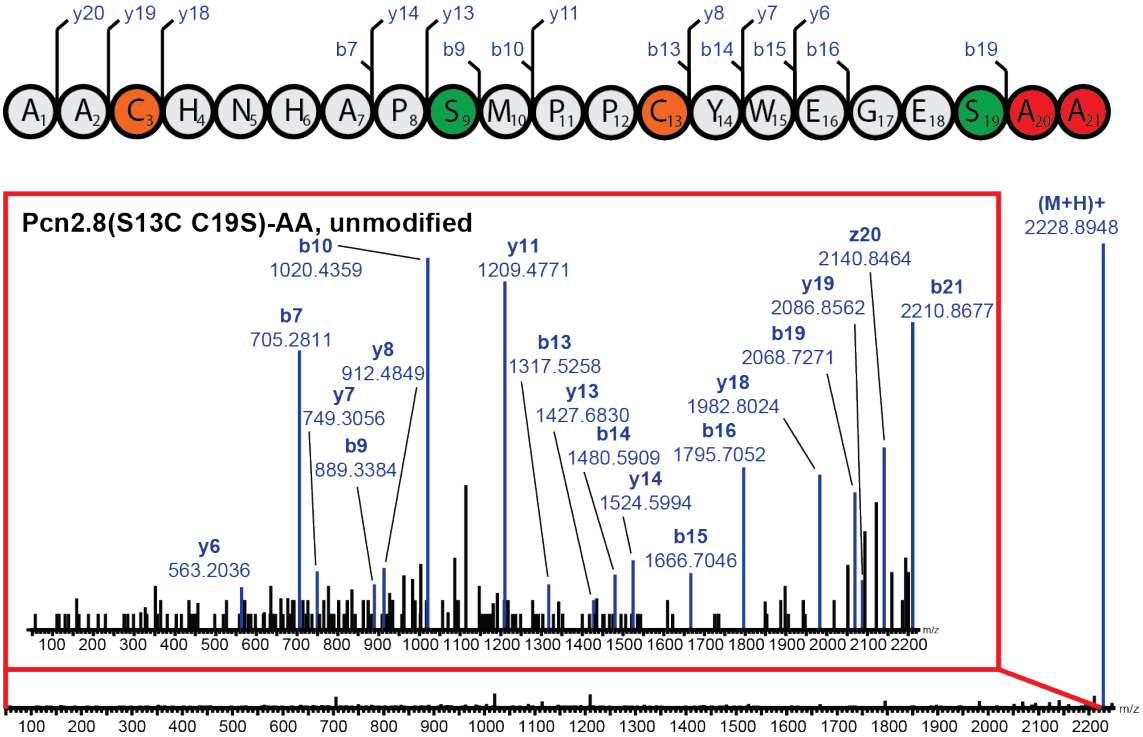


**Figure S68.** MS$^2$ spectra of Pcn2.8(S13C/C19S)-AA (unmodified). The red insert is a magnification of the indicated part of the spectrum shown at the bottom. Identified fragment ions are highlighted in blue.

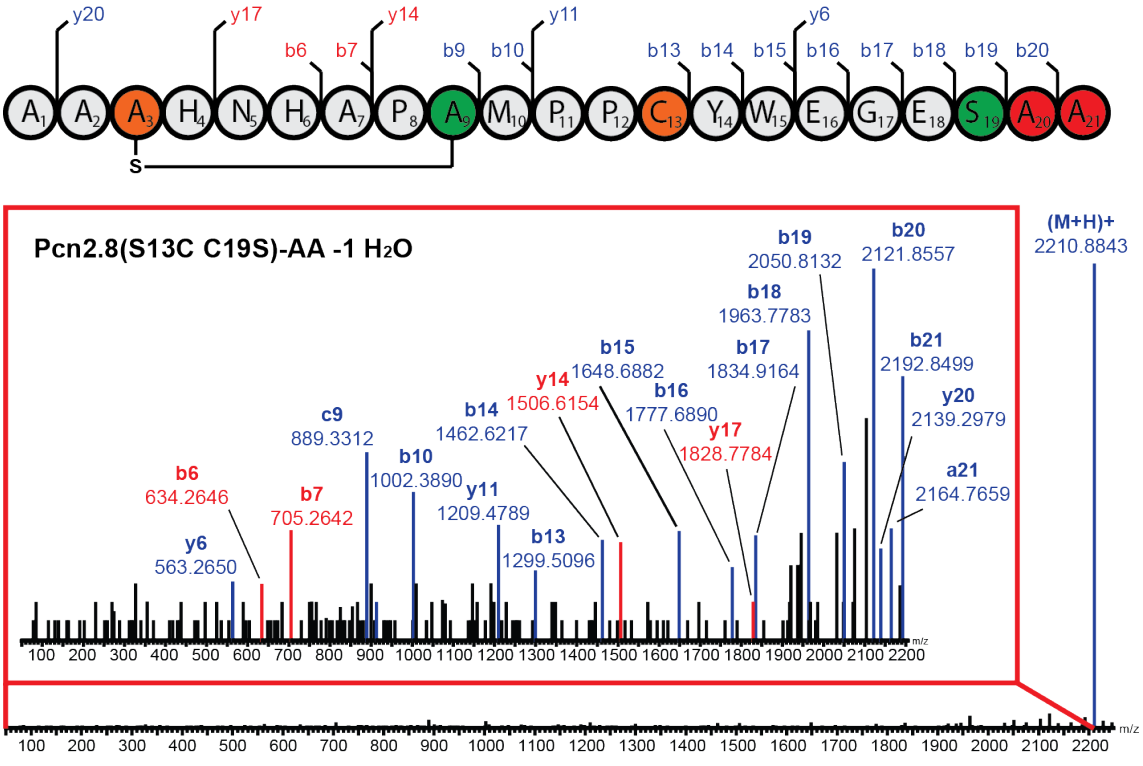


**Figure S69.** MS$^2$ spectra of Pcn2.8(S13C/C19S-AA) −1 $H_2O$. The red insert is a magnification of the indicated part of the spectrum shown at the bottom. Identified fragment ions are highlighted: Fragment ions resulting from

fragmentation outside of lanthionine rings are colored in blue. Minor fragment ions that likely arise from the presence of trace amounts of non- or partially cyclized peptides are highlighted in red.

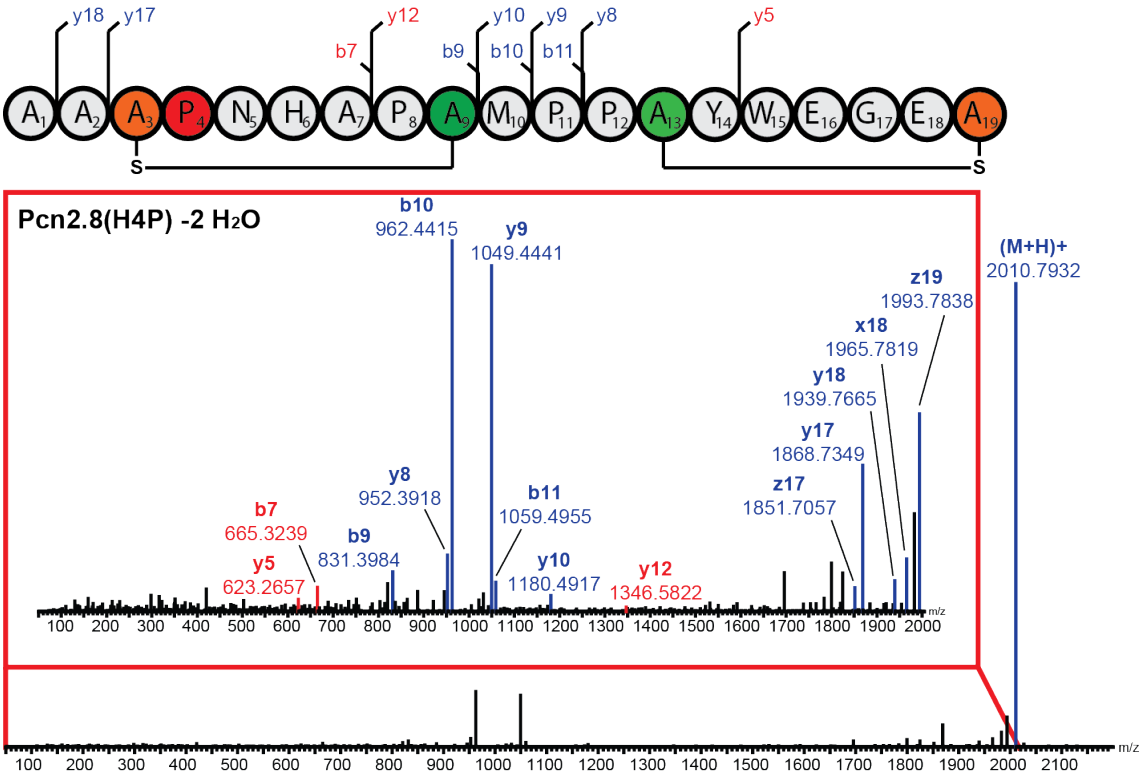


**Figure S70.** MS$^2$ spectra of Pcn2.8(H4P) −2 $H_2O$. The red insert is a magnification of the indicated part of the spectrum shown at the bottom. Identified fragment ions are highlighted: Fragment ions resulting from fragmentation outside of lanthionine rings are colored in blue. Minor fragment ions that likely arise from the presence of trace amounts of non- or partially cyclized peptides are highlighted in red.

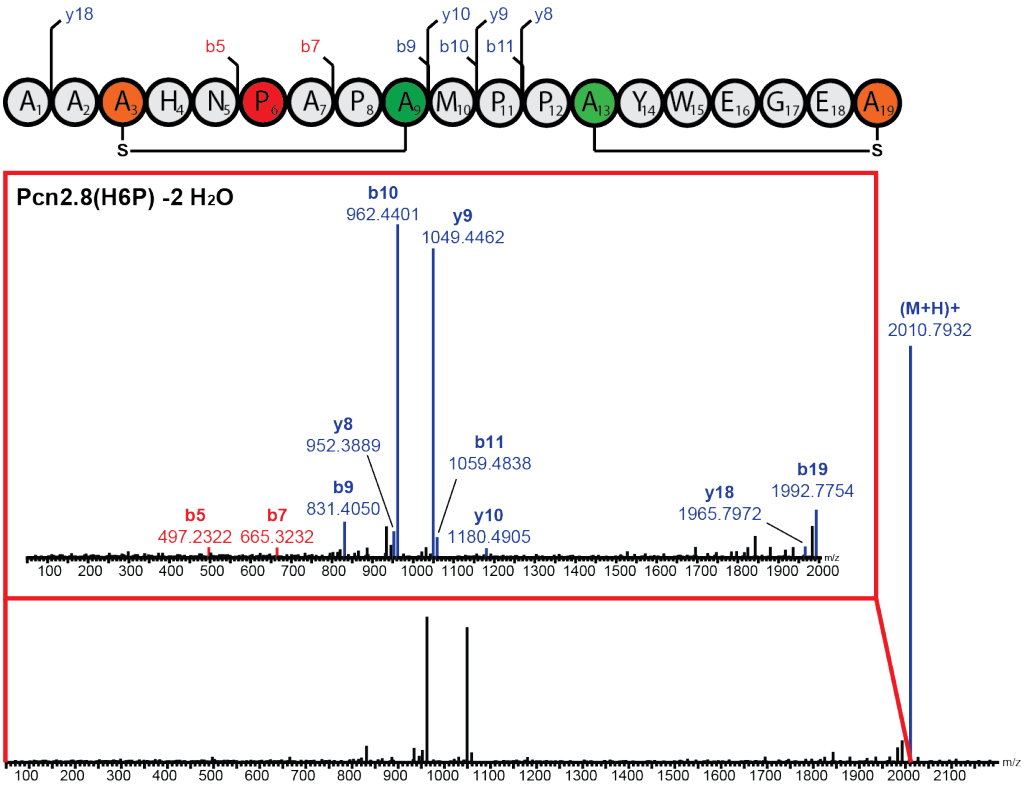

**Figure S71.** $MS^2$ spectra of Pcn2.8(H6P) −2 $H_2O$. The red insert is a magnification of the indicated part of the spectrum shown at the bottom. Identified fragment ions are highlighted: Fragment ions resulting from fragmentation outside of lanthionine rings are colored in blue. Minor fragment ions that likely arise from the presence of trace amounts of non- or partially cyclized peptides are highlighted in red.

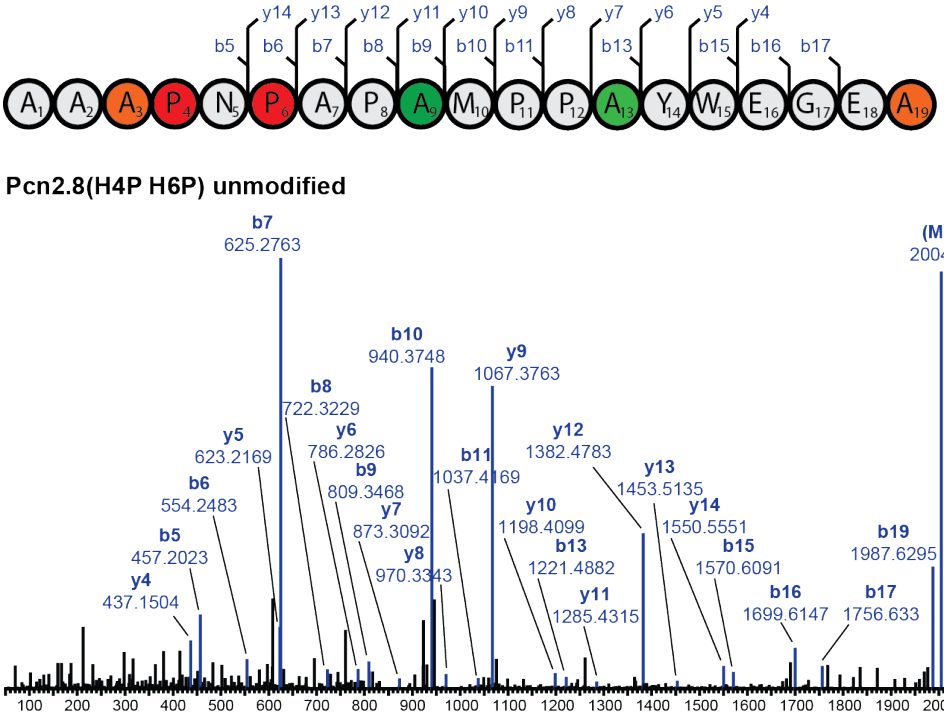


**Figure S72.** $MS^2$ spectra of Pcn2.8(H4P H6P) (unmodified). Identified fragment ions are highlighted in blue.

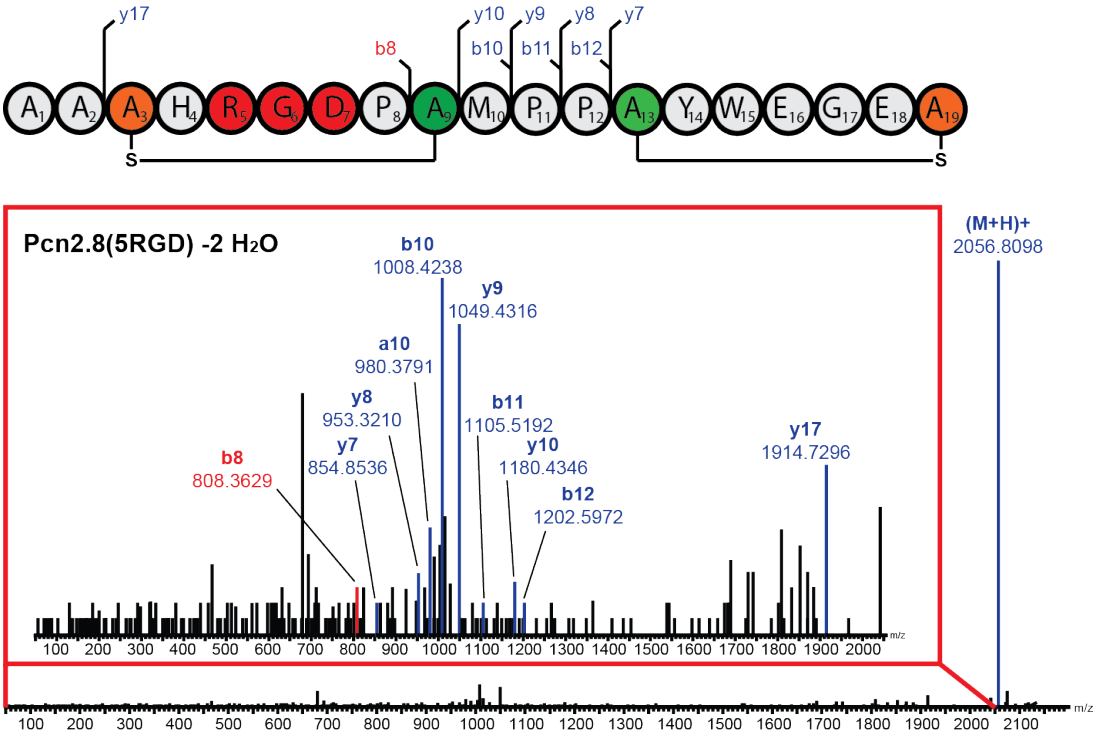


**Figure S73.** $MS^2$ spectra of Pcn2.8(5RGD) −2 $H_2O$. The red insert is a magnification of the indicated part of the spectrum shown at the bottom. Identified fragment ions are highlighted: Fragment ions resulting from fragmentation outside of lanthionine rings are colored in blue. Minor fragment ions that likely arise from the presence of trace amounts of non- or partially cyclized peptides are highlighted in red.

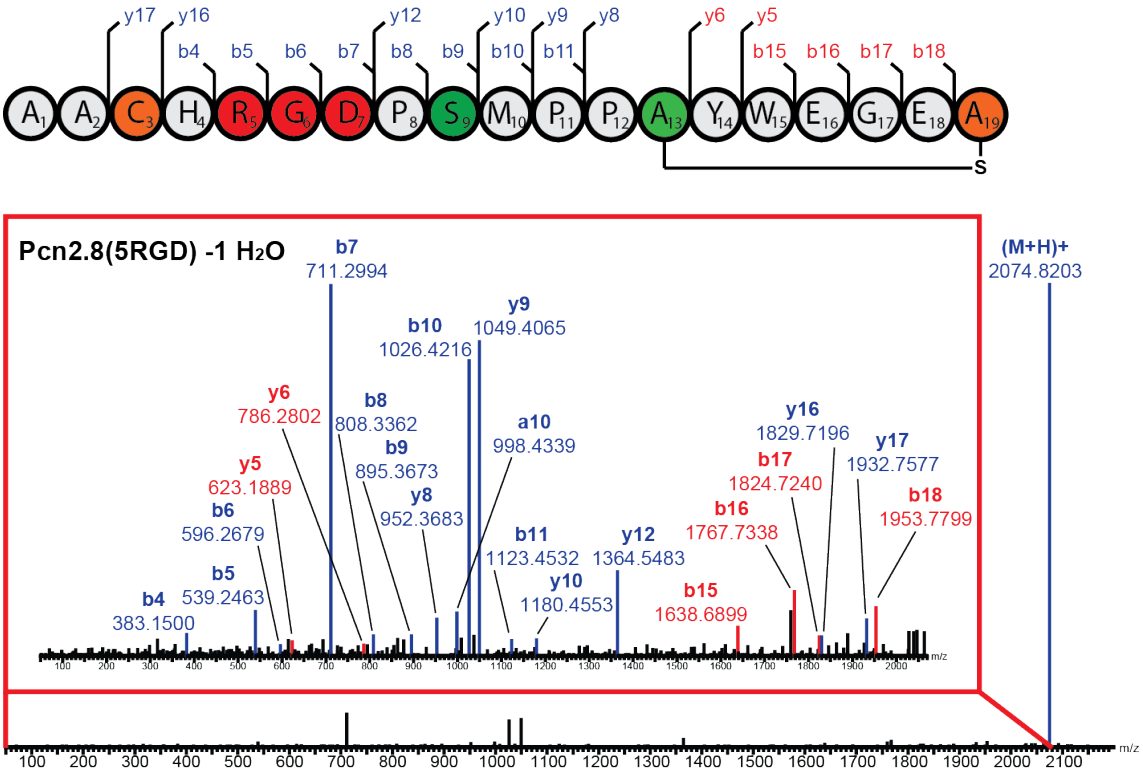


**Figure S74.** MS$^2$ spectra of Pcn2.8(5RGD) −1 $H_2O$. The red insert is a magnification of the indicated part of the spectrum shown at the bottom. Identified fragment ions are highlighted: Fragment ions resulting from fragmentation outside of lanthionine rings are colored in blue. Minor fragment ions that likely arise from the presence of trace amounts of non- or partially cyclized peptides are highlighted in red.

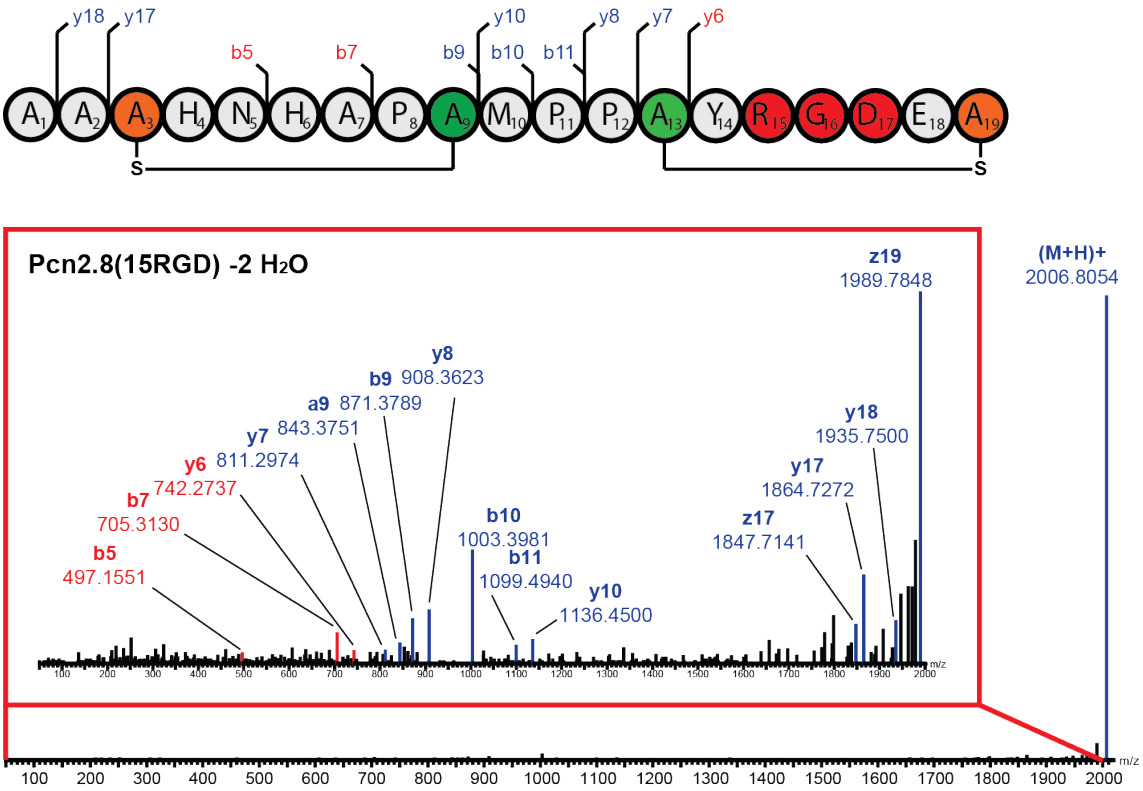


**Figure S75.** MS$^2$ spectra of Pcn2.8(15RGD) −2 $H_2O$. The red insert is a magnification of the indicated part of the spectrum shown at the bottom. Identified fragment ions are highlighted: Fragment ions resulting from

fragmentation outside of lanthionine rings are colored in blue. Minor fragment ions that likely arise from the presence of trace amounts of non- or partially cyclized peptides are highlighted in red.

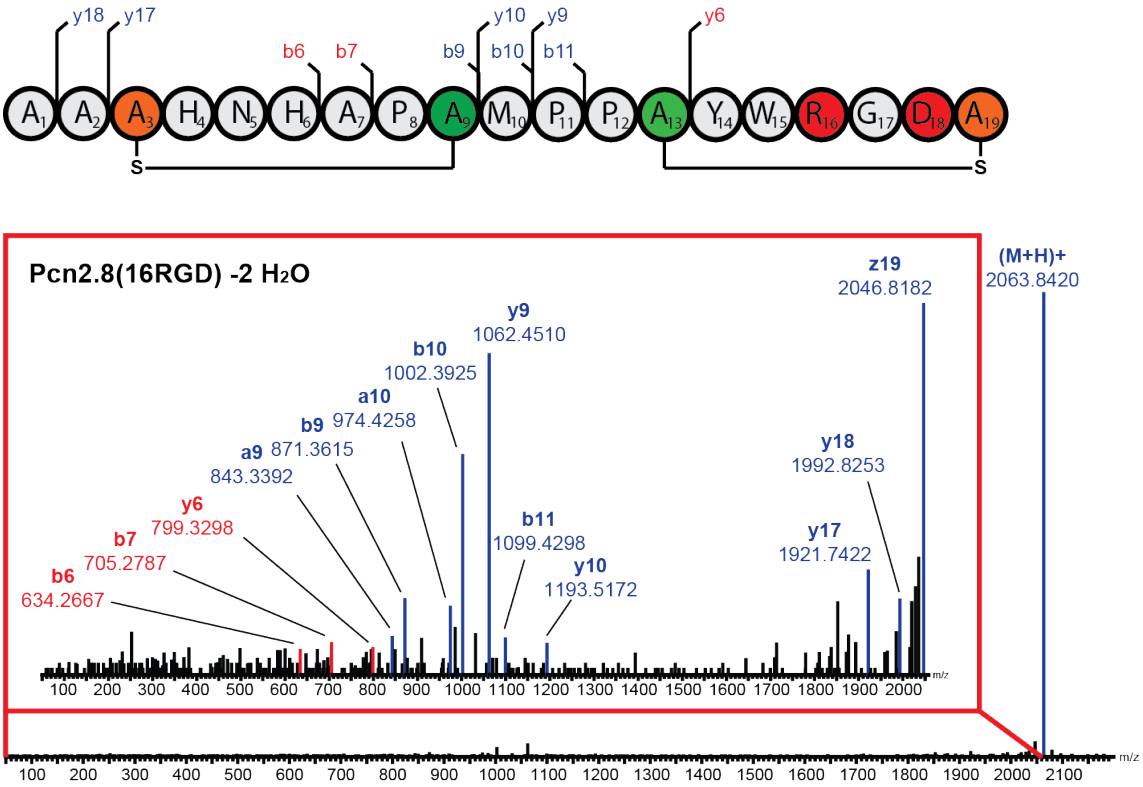


**Figure S76.** $MS^2$ spectra of Pcn2.8(16RGD) −2 $H_2O$. The red insert is a magnification of the indicated part of the spectrum shown at the bottom. Identified fragment ions are highlighted: Fragment ions resulting from fragmentation outside of lanthionine rings are colored in blue. Minor fragment ions that likely arise from the presence of trace amounts of non- or partially cyclized peptides are highlighted in red.

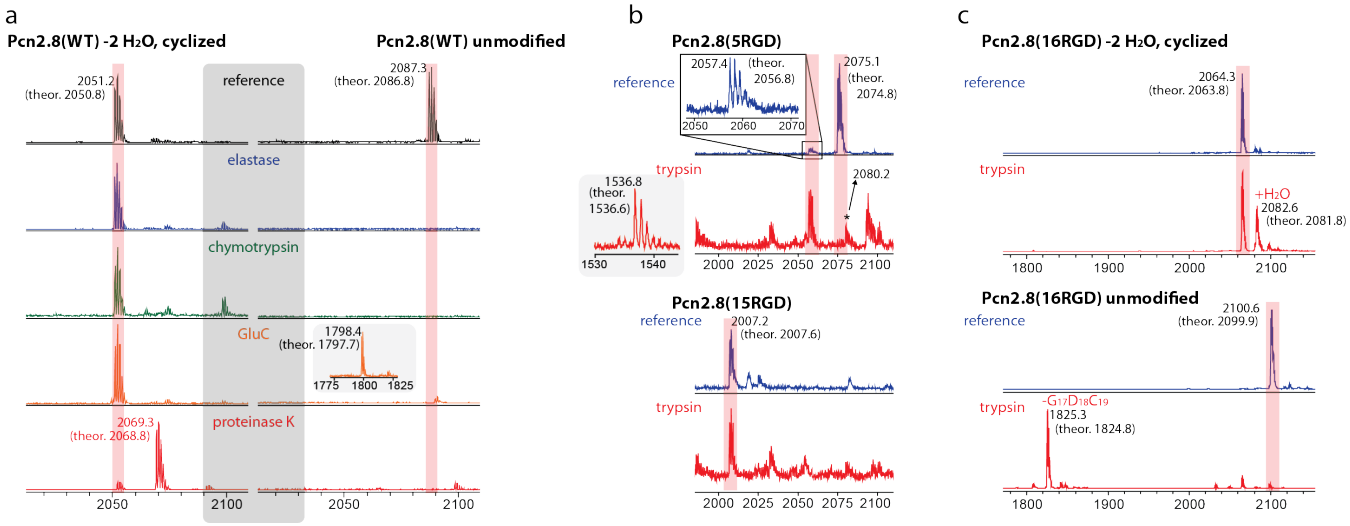


**Figure S77.** a) ProcA2.8(WT) that was twice cyclized (-2 $H_2O$) or unmodified was treated overnight with elastase, chymotrypsin, GluC, and proteinase K. The cyclized peptide was resistant against elastase, chymotrypsin, and GluC, but was cleaved inside a ring once by proteinase K (causing the gain of a water molecule). The linear peptide is readily degraded by every of the tested proteases. The inset shows the observed GluC fragment of linear Pcn2.8(WT). Other protease fragments of the linear peptide were too small to detect. b) Result of overnight trypsin treatment of the Pcn2.8(5RGD) and Pcn2.8(15RGD) core peptides that were obtained from LysC treatment of NiNTA elution fractions. The twice cyclized -2 $H_2O$ species are resistant to trypsin. The once cyclized -1 $H_2O$ species of Pcn2.8(5RGD) that only formed ring 2 is readily degraded (the mass signal of the resulting fragment lacking the first five residues is shown). c) Overnight trypsin treatment of twice cyclized (-2 $H_2O$) and unmodified Pcn2.8(16RGD) core peptide. The linear peptide is readily degraded (causing the loss of the last three amino acids following Arg16). The cyclized peptide shows some resistance against trypsin cleavage, although generation of hydrolyzed peptide is detected as well.

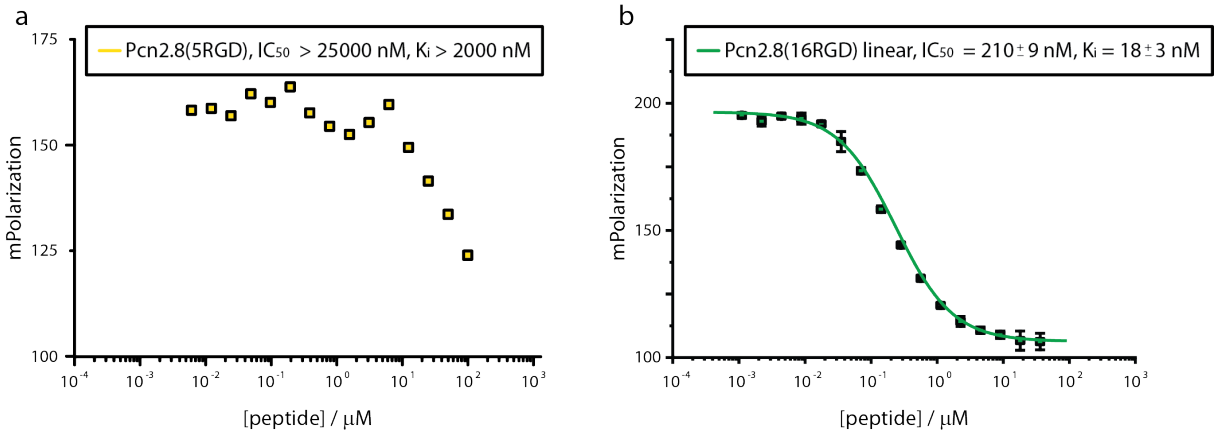


**Figure S78.** a) FP competition experiments with Pcn2.8(5RGD) showing the incomplete binding curve. By comparison with the curves of Pcn2.8(15RGD) and Pcn2.8(16RGD), the values for the $IC_{50}$ and $K_i$ of Pcn2.8(5RGD) are estimated to $IC_{50}$ >25 µM and $K_i$ >2 µM. b) FP competition experiments with linear Pcn2.8(16RGD) core peptide show a ~10-fold higher $K_i$ (18 ± 3 nM) compared to the cyclized Pcn2.8(16RGD) lanthipeptide (Ki = 1.6 ± 0.3 nM).

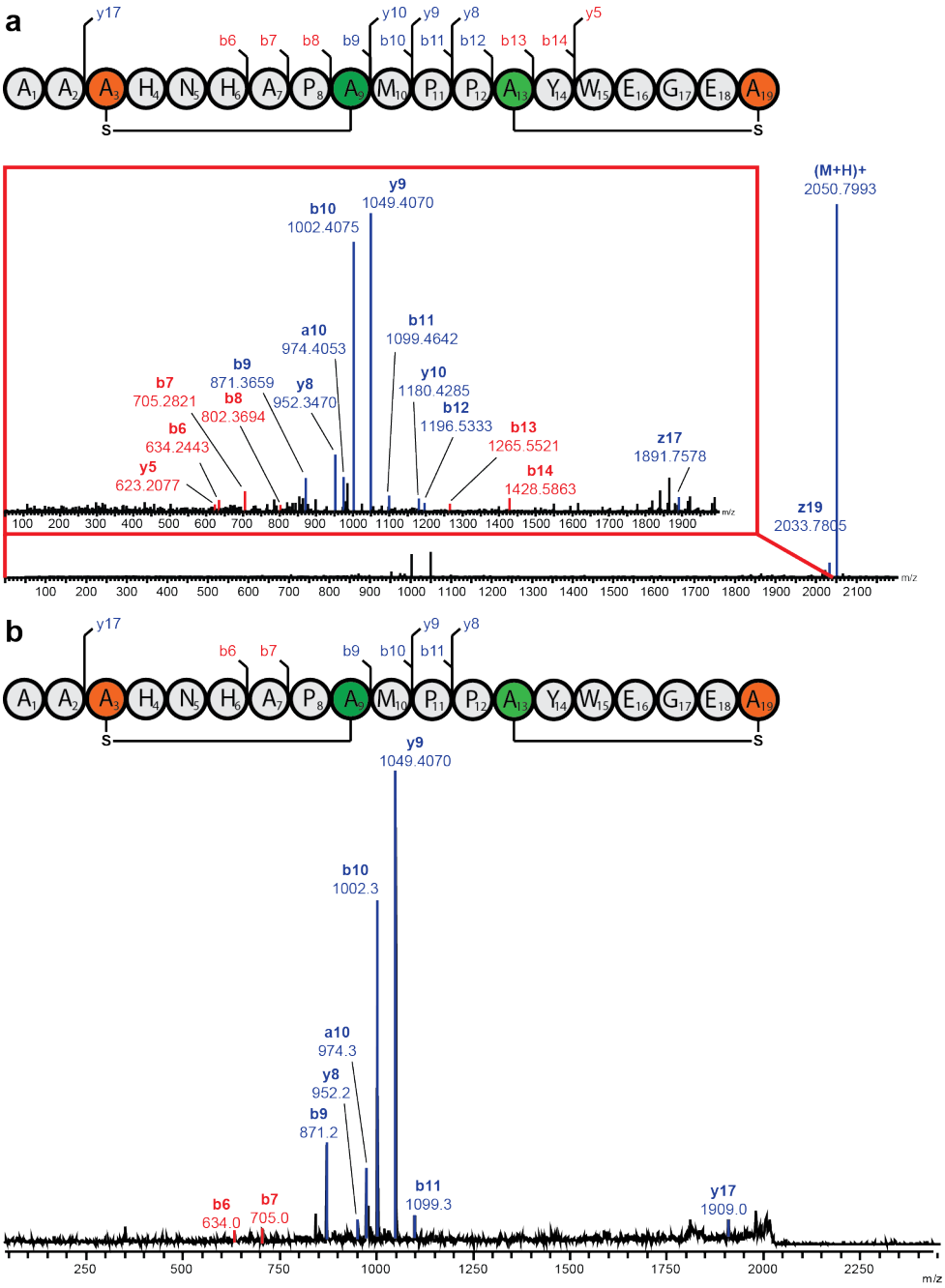


**Figure S79.** Comparison of tandem MS spectra of Pcn2.8(WT) $-2H_2O$ generated via a) collision-induced-dissociation (CID) fragmentation after electron-spray-ionization (ESI) and b) LIFT fragmentation after matrix-assisted laser desorption/ionization (MALDI). A direct comparison shows that both fragmentation techniques yield most peaks needed for identification of the ring topology (b9-b11, y8, y9, y17) as well as some low intensity signals potentially relating to fragmentation of minor peptide species with incomplete cyclization (b6, b7). In general, CID yields more fragment ion peaks and especially low intensity fragment ions are more abundant in the CID than in the LIFT spectra. Thus, CID allows detection of additional fragment ions resulting from fragmentation outside of rings (b12, y10) and potentially fragment ions resulting from fragmentation of non-cyclized side products (b8, b13, b14, y5). These findings are in agreement with the observation that previously reported (Yang, X.; et al. *Nat. Chem. Biol.* **2018**, 14, 375-380.) tandem MS spectra of Pcn2.8 variants generated by LIFT fragmentation only identified the major peaks, but not the lower intensity fragments reported here.